**Trem2 Deficiency Differentially Affects the Phenotype and Transcriptome of Human APOE3 and APOE4 mice: The Role of APOE and TREM2 in Alzheimer's Disease**

by

**Cody Matthew Wolfe**

BS, Grove City College, 2013

MPH, University of Pittsburgh, 2015

Submitted to the Graduate Faculty of the

Environmental and Occupational Health Department

Graduate School of Public Health in partial fulfillment

of the requirements for the degree of

Doctor of Philosophy

University of Pittsburgh

2020

UNIVERSITY OF PITTSBURGH

GRADUATE SCHOOL OF PUBLIC HEALTH

This dissertation was presented

by

**Cody Matthew Wolfe**

It was defended on

August 7, 2020

and approved by

Iliya Lefterov, MD, PhD, Department of Environmental and Occupational Health, Graduate
School of Public Health, University of Pittsburgh

Aaron Barchowsky, PhD, Department of Environmental and Occupational Health, Graduate
School of Public Health, University of Pittsburgh

Nicholas Fitz, PhD, Department of Environmental and Occupational Health, Graduate School of
Public Health, University of Pittsburgh

Bistra Iordanova, PhD, Department of Bioengineering, University of Pittsburgh

**Dissertation Advisor**: Radosveta Koldamova, MD, PhD, Department of Environmental and
Occupational Health, Graduate School of Public Health, University of Pittsburgh

Radosveta Koldamova, MD, PhD

**Trem2 Deficiency Differentially Affects the Phenotype and Transcriptome of Human APOE3 and APOE4 mice: The Role of APOE and TREM2 in Alzheimer's Disease**

Cody Matthew Wolfe, PhD

University of Pittsburgh, 2020

## Abstract

Alzheimer's disease (AD) is the leading cause of dementia worldwide and a significant public health concern impacting not only patients, but their families and caregivers as well. Extracellular deposits of amyloid beta (Aβ) in the brain called amyloid plaques and intracellular tau aggregates called neurofibrillary tangles are morphological hallmarks of the disease. The risk for AD is a complicated interplay between aging, genetic risk factors, and environmental influences. The inheritance of Apolipoprotein E ε4 (*APOE*ε4) and variants of Triggering Receptor Expressed on Myeloid cells 2 (*TREM2*) are major genetic risk factors for AD. Emerging evidence from protein binding assays suggest that APOE and APOE-containing lipoproteins bind to TREM2 in the brain as well as periphery. This raises the possibility of an APOE-TREM2 interaction modulating aspects of AD pathology, potentially in an isoform-specific manner. This dissertation aimed to investigate this interaction using complex AD model mice - a crossbreed of Trem2$^{ko}$ and APP/PSEN1dE9 mice expressing human APOE3 or APOE4 isoform, evaluating cognition, steady-state and dynamic amyloid pathology, glial response, and whole-brain transcriptomics. We found that *Trem2* deletion had the following effects on the phenotype: a) reduced plaque compaction but no effect on steady-state plaque load; b) decreased microglia recruitment to plaques; c) increased plaque growth in correlation with reduced microglia barrier, an effect that is dependent on the

stage of amyloid deposition; d) isoform dependent effect on plaque-associated APOE; e) worsened memory in APP but not in WT littermates. Gene expression analysis identified the Trem2 signature as a cluster of highly interconnected immune response genes commonly downregulated as a result of *Trem2* deletion in all experimental groups, including *Clec7a*, *Itgax*, *Cts7*, *Mpeg1, Csf1r*, *Cx3cr1* and *Spi1*/PU.1. Several of the Trem2 signature genes had higher expression in APP/E4 versus APP/E3 mice, a result validated for *Clec7a* and *Csf1r* by FISH, and for APOE by immunohistochemistry. In contrast, *Tyrobp* and several genes involved in the C1q complement cascade had higher expression levels in APP/E3 versus their APP/E4 counterparts. Collectively, this dissertation provides evidence as to the phenotypic and transcriptomic effects regarding the interplay between human APOE isoform and *Trem2* deletion in association with AD pathology.

# Table of Contents

# List of Tables

# List of Figures

# Preface

I would like to thank my advisors, Dr. Iliya Lefterov and Dr. Radosveta Koldamova as well as Dr. Nick Fitz for providing the opportunity train in their lab for the last few years. I am grateful to the entire Lefterov-Koldamova lab for their contributions to the data presented within this dissertation as well as the friendships generated along the way. Particularly Dr. KyongNyon Nam whose guidance and friendship has alleviated many stressful days. This work would not have been possible without the support of many EOH department faculty members, technicians and administrators whom I have grown close to over the years. I am very grateful to each and every one of them. Many thanks as well to the rest of my dissertation committee members, Dr. Aaron Barchowsky and Dr. Bistra Iordanova, who's incite, and critical assessments were helpful to my progression as a student.

I would like to thank all of my family for their support, particularly my parents, Dan and Dee Wolfe. Their endless support and encouragement taught me to become that man I am today, and to me there is no greater gift than that. They each have passed on the best possible aspects of their personalities all the while teaching me to use the gifts I have been given to continually learn and grow.

I thank my wife, Natalie Wolfe, whose endless love, patience, encouragement, and care has proven to be the most necessary of all. Last, but not least, I thank my children. While unaware of their role, there is no greater balm for a hard day than returning home to the unrelenting joy and happiness that only a child can muster. I dedicate this dissertation to them.

## List of Abbreviations

AD                    Alzheimer's Disease

ABCA1                 Adenosine Triphosphate-Binding Cassette Transporters A1

ABCA7                 Adenosine Triphosphate -Binding Cassette Transporter A7

ABCG1                 Adenosine Triphosphate-Binding Cassette Transporters G1

ADSP                  Alzheimer's Disease Sequencing Project

AICD                  App Intracellular Domain

AKT                   Protein Kinase B

ALS                   Amyotrophic Lateral Sclerosis

APLP1                 App-Like Protein 1

APLP2                 App-Like Protein 2

APOE                  Apolipoprotein E

APOER2                Apoe Receptor 2

APOJ                  Clusterin

APP                   Amyloid Precursor Protein

Arg                   Arginine

ASO                   Anti-Sense Oligonucleotides

Aβ                    β-Amyloid

BBB                   Blood Brain Barrier

BIN1                  Bridging Integrator 1

BSA                   Bovine Serum Albumin

| | |
|---|---|
| CAA | Cerebral amyloid angiopathy |
| CCFC | Contextual And Cued Fear Conditioning |
| CD2AP | Cd2-Associated Protein |
| CD33 | Sialic Acid-Binding Ig-Like Lectin 3 |
| CFS | Cerebral Spinal Fluid |
| CLU | Clusterin |
| CNS | Central Nervous System |
| CR1 | Complement Receptor 1 |
| CS | Conditioned Stimulus |
| Cys | Cysteine |
| DAM | Disease-Associated Microglia |
| DAVID | Database for Annotation, Visualization And Integrated Discovery |
| EOAD | Early-Onset Ad |
| FTD | Frontotemporal Dementia |
| GWAS | Genome-Wide Association Studies |
| HDL | High-Density Lipoproteins |
| i.p. | Intraperitoneally |
| IP3 | Inositol Trisphosphate |
| ITAMs | Immunoreceptor Tyrosine-Based Activation Motifs |
| LDL | Low-Density Lipoprotein |
| LDLR | Low-Density Lipoprotein Receptor |
| LOAD | Late Onset Ad |
| LPS | Lipopolysaccharide |

**Abbreviations Continued**

| | |
|---|---|
| LRP1 | Ldlr-Related Receptor 1 |
| MCI | Mild Cognitive Impairment |
| ME | Module Eigengene |
| MS4A family | Membrane Spanning 4-Domains A |
| NIA-AA | National Institute of Aging, and the Alzheimer's Association |
| NHD | Nasu–Hakola Disease |
| NOR | Novel Object Recognition |
| PBS | Phosphate Buffered Saline |
| PET | Positron Emission Tomography |
| PI3K | Phosphoinositide 3-Kinase |
| PICALM | Phosphatidylinositol-Binding Clathrin Assembly Protein |
| PIP3 | Phosphatidylinositol-3,4,5-Trisphosphate |
| PLCγ | Phospholipase Cγ |
| PSEN1 | Presenilin 1 |
| PSEN2 | Presenilin 2 |
| R47H | Arginine to Histidine At Position 47 |
| ROI | Regions of Interest |
| SFKs | Src Family Kinases |
| smFISH | Single Molecule Fluorescence In Situ Hybridization |
| SORL1 | Sortilin Related Receptor 1 |
| sTREM2 | Soluble Trem2 |
| SYK | Spleen Tyrosine Kinase |
| ThioS | Thioflavin S |

**Abbreviations Continued**

| | |
|---|---|
| TR | Thiazine Red |
| TREM2 | Triggering Receptor Expressed on Myeloid Cells 2 |
| TYROBP | Tyro Protein Tyrosine Kinase Binding Protein |
| US | Unconditioned Stimulus |
| VLDLR | Very-Low-Density Lipoprotein Receptor |
| WES | Whole-Exome Sequencing |
| WGCNA | Weighted Gene Co-Expression Network Analysis |
| WGS | Whole-Genome Sequencing |
| X04 | Methoxy-X04 |
| X34 | Methoxy-X34 |

## 1.0 Introduction

### 1.1 Alzheimer's Disease

### 1.1.1 History

In the 19th century, individuals with dementia began to be regarded as medical patients, and senile dementia was first recognized as a disease (Knopman et al., 2019). The concurrent rise in medical awareness has led to the division of the term dementia into multiple differing neuropathological conditions. The term Alzheimer's Disease (AD) was first introduced in 1910 in a clinical psychiatry textbook based on the seminal case published in 1906 by Alois Alzheimer. AD is now characterized by the extracellular accumulation of amyloid $\beta$ (A$\beta$) plaques and intracellular hyperphosphorylated tau tangles that ultimately lead to impaired cognitive abilities and irreversible memory loss (Crous-Bou et al., 2017). The term AD became synonymous with dementia around the late 1960s until the late 1980s, an attitude which partially persists to this day. This vernacular arose from the clinical model in which AD comprised all forms of dementia that could not be tied to another clinically observable cause, even though a definitive diagnosis of AD can only occur postmortem.

AD is associated with the onset of progressive memory deterioration, and functional deficits with death as the unavoidable outcome. The disease lifespan includes an estimated 10-year preclinical stage, 4-year prodromal stage, and 6-year dementia stage (Vermunt et al., 2019). Evidence points to pathological changes including the buildup of oligomeric A$\beta$ and Tau accumulation occurring in the years before the manifestation of clinical symptoms, making the use

and validation of biomarkers that measure pathology and brain atrophy a growing necessity. Until around 2010, the diagnosis of AD relied heavily on reporting symptoms that fit within the known cognitive domains, but the reclassification system put into place in 2011 by the National Institute of Aging and the Alzheimer's Association (NIA-AA) now includes the preclinical mild cognitive impairment (MCI) stage as a part of the AD diagnosis. The most recent diagnostic criteria must now include the preclinical phase in which biomarker evidence of AD-related pathology exists without any AD-related symptoms (Dubois et al., 2014; Dubois et al., 2016; Sperling et al., 2011). Recent studies have shown the ability to use cerebrospinal spinal fluid (CSF) and positron emission tomography (PET) imaging as reliable biomarkers for cerebral Aβ and tau deposition in cognitively normal older adults and those with mild AD (Brier et al., 2016). Evidence suggests that AD-related cognitive changes may result from the complex interplay between tau and amyloid proteins; the earlier and more accurate *in vivo* imaging of these proteins will have a dramatic impact on AD research and treatment.

**1.1.2 APP Processing**

Classically, the Aβ hypothesis has been driven by the observation that genetic mutations in the *APP* gene or the presenilin genes *PSEN1* and *PSEN2* result in the deposition of Aβ faster than it can be cleared (Selkoe and Hardy, 2016). The human *APP* gene is located on chromosome 21q21.3 and contains 18 exons comprised of approximately 240 kilobases and is a member of the APP protein family along with two other homologous proteins called APP-like protein 1 and 2 (APLP1, APLP2) (Tanzi et al., 1987). APP undergoes both amyloidogenic and non-amyloidogenic processing. Under non-amyloidogenic processing, APP on the cell surface is cleaved by α-secretase in the AV domain, producing sAPP, which gets released into the extracellular environment and

prevents the generation of Aβ (Sisodia, 1992). The cleavage by α-secretase leaves behind a membrane-bound C-terminal fragment called C83. Subsequent cleavage of C83 by γ-secretase produces a 3kDa p3 fragment that is released through the secretory pathway or via exocytosis. Furthermore, γ-secretase cleavage also creates an APP intracellular domain (AICD) fragment that is short and very unstable (Passer et al., 2000). Only 16 amino acids differ between the fragments generated by non-amyloidogenic α-secretase cleavage and amyloidogenic β-cleavage; however, only amyloidogenic processing ultimately leads to Aβ related AD pathology (Yuksel and Tacal, 2019).

During amylogenic processing, APP is first cleaved by β-secretase, generating sAPP and leaving a portion of the protein bound to the membrane to be further cleaved by γ-secretase. Due to the imprecise nature of γ-secretase cleavage, multiple species of Aβ exist; peptides terminating at position 40 (Aβ1-40) are the most common, and the second most common terminus is at position 42 (Aβ1-42) (Schmidt et al., 2009). Aβ1-42 and longer Aβ peptides are more hydrophobic, fibrillogenic, and highly self-aggregating- they go on to form amyloid deposits more readily than Aβ1-40 (Caughey and Lansbury, 2003). Familial AD studies suggested that the ratio between the two most prevalent peptides, Aβ1-42 and Aβ1-40, can be used as a marker for AD progression (Borchelt et al., 1996). Preliminary evidence suggests that measuring the Aβ1-42/Aβ1-40 ratio along with other AD biomarkers in the CSF can improve diagnostic performance, but a sufficiently strong body of evidence does not yet exist for Aβ1-42/Aβ1-40 ratio to be used as a single source biomarker (Hansson et al., 2019). Misfolded Aβ monomers are rich in β-sheet conformations, leading to both soluble and insoluble forms of oligomeric deposits. If Aβ monomers are not cleared, they develop into oligomers, which continue to aggregate into protofibrils, then into fibrils that ultimately collect to form amyloid plaques (Ni et al., 2011). Cognitive deficits have been identified preceding the appearance amyloid deposition or insoluble amyloid fibrils, implicating

Aβ oligomers in AD pathology before the existence of amyloid plaques (Hsia et al., 1999; Mucke et al., 2000). Additionally, amyloid can build up in the cerebrovasculature causing cerebral amyloid angiopathy (CAA) which increases the risk for intracerebral hemorrhage and cognitive impairments (Tanaka et al., 2020). Amyloid pathology is also implicated in the loss of synaptic integrity and. Is suggested to precede neuronal loss which is a hallmark of AD (Jellinger, 2020). Cognitive deficits have been shown to reflect decreases in synaptic density in the hippocampus of human AD patients (Masliah et al., 2001).

### 1.1.3 Functional Genomics and AD

The majority of AD cases develop without an identifiable single source genetic variant as a causative agent. This does not, however, discount the possibility that a multitude of gene variants as well as environmental factors modulate AD risk. With the rise in high throughput sequencing, the genotyping and sequencing of hundreds of thousands of human samples to screen for genetic variants has become possible. The availability of these samples gave rise to genome-wide association studies (GWAS), which report the loci which are enriched in a disease population above expected based on control samples. Many initial AD GWAS were undertaken (Harold et al., 2009; Jun et al., 2010; Naj et al., 2011) and ultimately aggregated into a meta-analysis study, resulting in the identification of many AD-related risk genes (Lambert et al., 2013). As the availability and technology of sequencing improved, the widespread use of whole-exome sequencing (WES) and whole-genome sequencing (WGS) has allowed for the identification of rare variants associated with AD. Analysis of GWAS and other gene expression data has led to the identification of three major groups of genes enriched in AD cases: those involved in endocytosis, lipid metabolism, and immune response.

Endocytosis is a process by which matter is brought into a cell; the failure to efficiently accomplish this can lead to the buildup of proteins, as observed in AD. The most notable endocytosis-related AD risk genes that have been identified are sortilin-related receptor 1 (*SORL1*), bridging integrator 1 (*BIN1*), CD2-associated protein (*CD2AP*), and phosphatidylinositol-binding clathrin assembly (*PICALM*). The brain contains thousands of lipid species that play a vital role in cell signaling, making the regulation of lipid metabolism and homeostasis vital to a healthy system. The gene with the highest risk factor for AD, Apolipoprotein E (*APOE*), falls into this category, further emphasizing the importance of lipid metabolism. Additionally, ATP-binding cassette transporter A7 (*ABCA7*) and Clusterin (*CLU*) are AD risk genes associated with lipid metabolism. Furthermore, increasing evidence suggests that alterations in immune response play a role in AD progression: genes such as Complement receptor 1 (*CR1*), Membrane Spanning 4-Domains A (MS4A family), Sialic Acid-Binding Ig-Like Lectin 3 (*CD33*), and Triggering receptor 2 on myeloid cells (*TREM2*) are all implicated as AD risk factors. This dissertation focuses on the interplay between the AD risk-modifying variants of two of these genes: *APOE* and *TREM2*.

### 1.1.4 APOE and TREM2

In humans, the inheritance of one *APOEε4* allele increases the risk of late-onset AD (LOAD) by 3–4-fold, while two copies of the allele increase the risk 9–15-fold (Neu et al., 2017). Aβ pathology is distinctly associated with APOE variants, as carriers of the *APOEε4* allele exhibit earlier disease onset and increased levels of amyloid plaques (Corder et al., 1993; Cosentino et al., 2008; Schmechel et al., 1993). Levels of insoluble Aβ1-40 and Aβ-42 levels are increased if APOE4 is expressed in the brain during the early stages of amyloid deposition (Liu et al., 2017).

However, this effect is not observed in mice expressing APOE3, nor is it seen when the expression of APOE4 is increased after the initial seeding stage, indicating that APOE4 has the greatest impact during the earliest phases of amyloid accumulation. APOE and APOE receptors likely modulate aspects of Aβ efflux, with APOE being shown to promote clearance of Aβ across the blood brain barrier and by activating microglial phagocytosis and migration in an isoform-dependent manner (APOE3 > APOE4), implicating microglial dysfunction as a player in APOE-associated AD risk (Jiang et al., 2008a; Lee et al., 2012).

TREM2 is a cell surface receptor on myeloid cells that interacts with the protein tyrosine kinase binding protein (TYROBP). TREM2 binds Lipopolysaccharides (LPS) (Daws et al., 2003), phospholipids (Wang et al., 2015), HDL (Yeh et al., 2016), LDL, APOE (Atagi et al., 2015; Bailey et al., 2015; Yeh et al., 2016), CLU (Yeh et al., 2016), apoptotic neurons (Hsieh et al., 2009), and Aβ (Zhao et al., 2018b) all of which activate signaling pathways. TREM2 activation initiates a multitude of signaling pathways that promote microglial chemotaxis, phagocytosis, cell survival, and proliferation, making it critical for normal immune function (Kleinberger et al., 2014; Mazaheri et al., 2017; Poliani et al., 2015; Ulland et al., 2017; Wang et al., 2015). In humans, the rare *TREM2* variant R47H (arginine to histidine at position 47) is associated with AD; the inheritance of this allele increases the risk of developing AD by approximately 4-fold, likely due to the universal reduction in binding (Guerreiro et al., 2013a; Jonsson et al., 2013; Lessard et al., 2018; Sudom et al., 2018). *Trem2* haploinsufficiency and complete deficiency in mouse models of AD are consistently associated with a reduced microglial barrier around amyloid deposits, reduced plaque compaction, and increased dystrophic neurites surrounding plaques (Jay et al., 2017; Jay et al., 2015; Wang et al., 2015; Wang et al., 2016; Yuan et al., 2016). APOE binds to TREM2 (Atagi et al., 2015; Bailey et al., 2015; Yeh et al., 2016), providing a molecular pathway for an APOE-TREM2 interaction to modulate AD pathogenesis.

**1.1.5 Microglia and AD**

The identification of many genes associated with the immune response has piqued interest in the role of microglia in the pathogenies of AD. In AD, microglia are important in the phagocytosis of debris, clearance of Aβ, the release of pro-inflammatory cytokines, and the development of a plaque-associated barrier (Hansen et al., 2018). Microglia are the resident macrophages in the brain and account for approximately 10% of all cells present in the central nervous system (CNS) (Colonna and Butovsky, 2017). Microglia are highly dynamic cells that interact with most other cell types in the brain and are constantly surveilling their surroundings. Quiescent microglia have small cellular bodies surrounded by extensive processes that survey their environment (Li et al., 2013). The morphological alterations in microglia upon activation are one of the first observable changes. Upon activation, microglia develop larger, amoeboid cell bodies with shorter, thicker processes directed towards the target area (Boche et al., 2013). Reactive microglia phagocytize debris and secrete inflammatory factors. Changes in morphology occur in conjunction with transcriptional changes; upon activation, microglia significantly reduce expression of *TMEM119*, and *P2RY12* and increase their expression of *CLEC7A*, IBA1, F4/80, and other phagocytic markers (Gyoneva and Ransohoff, 2015).

Previous studies that focused on microglia polarization utilized either the M1 or M2 phenotype as a key determinant of inflammation (Boche et al., 2013). The M1 phenotype is considered pro-inflammatory, as it is characterized by the production and release of cytokines that can contribute to neuronal injury (Hu et al., 2015). Alternatively, the M2 phenotype is associated with protection and anti-inflammatory signaling due to the release of neurotrophic factors that promote repair. This classification was determined *in vitro* by stimulating the cells with a single cytokine and then measuring the response of a small number of genes (Martinez et al., 2006).

However, *in vivo*, microglia encounter a complex array of signals including cytokines, chemokines, and other molecules. Additionally, the polarization states *in vivo* are not particularly distinct and have a high degree of functional overlap. Thus, the original classification is oversimplified to reliably reflect microglial activation states; the classification criteria have shifted following the advent of single-cell sequencing.

Advances in next-generation sequencing technologies and single-cell gene expression profiling have allowed for the identification of subsets of cells, such as microglia, that have different activation profiles (Keren-Shaul et al., 2017; Krasemann et al., 2017). Recently, Keren-Shaul et al. identified a subset of microglia named "disease-associated microglia" (DAM) that accumulate during AD and other neurodegenerative diseases (Keren-Shaul et al., 2017). DAM are characterized by the upregulation of genes such as *Clec7a*, *Itgax*, *Trem2*, and *Apoe*, which are involved in lysosomal, phagocytic, and lipid metabolism pathways (Deczkowska et al., 2018). Importantly, a significant downregulation of the so-called "homeostatic microglial" genes was detected contemporaneously with the upregulation of DAM genes (Keren-Shaul et al., 2017). Furthermore, genetic ablation of *Trem2* suppressed mouse *Apoe* expression and restored homeostatic microglial function in AD mouse models (Krasemann et al., 2017).

## 1.2 Public Health Significance

AD is the most common cause of dementia, and the intracellular buildup of hyperphosphorylated tau and extracellular buildup of Aβ ultimately leads to impaired cognitive abilities and irreversible memory loss (Crous-Bou et al., 2017). Currently, AD is the fourth-leading cause of death in adults worldwide after heart disease, cancer, and stroke (Larson et al., 2013). The

current number of people worldwide who are suffering from AD is estimated to be 24.3 million and has been predicted to rise to 42 million in 2020 and 81 million by 2040 (Larson et al., 2013). In the United States, over 80% of all AD cases are in patients > 75 years old (Fig. 1A), a number which is only likely to increase as the average lifespan increases and the population ages. Additionally, females also have a disproportionately higher estimated lifetime risk compared to males (Fig. 1B); this cannot be accounted for solely by the longer average life expectancy seen in women but is most likely also related to differences in hormones and lifestyle. The annual death rate per 100,000 people has more than doubled in the last 20 years and unfortunately, AD is one of the only major causes of death in which the percentage change in the last 20 years has increased instead of decreased, ultimately costing the United States hundreds of billions of dollars (Fig. 1C-E).
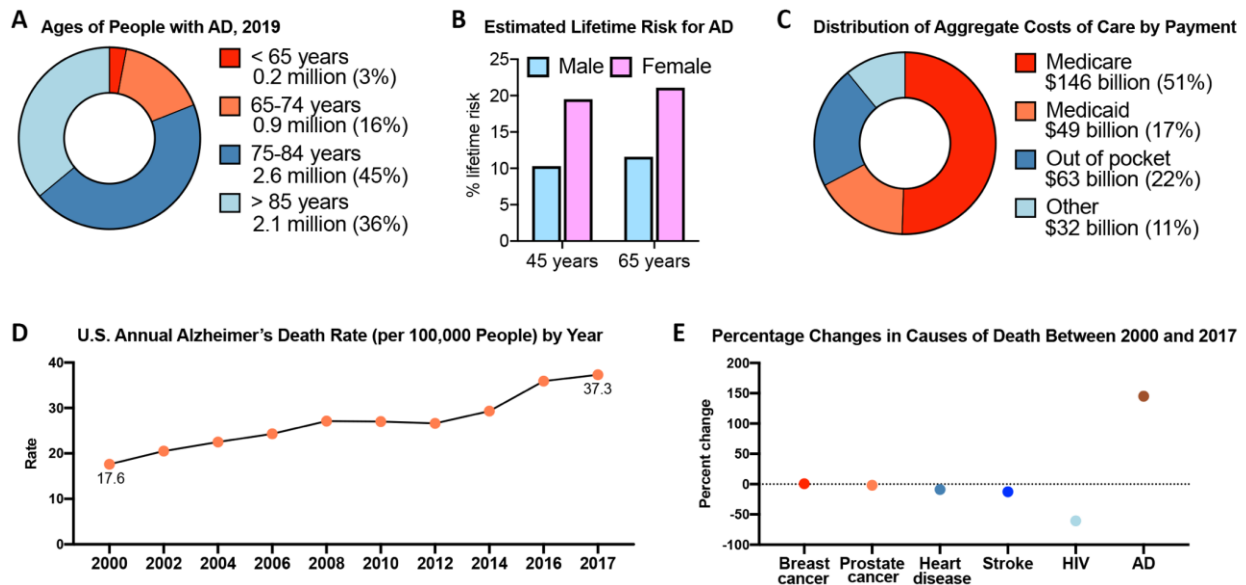


**Figure 1. AD statistics in the United Stated in 2019.**
Statistics generated for the 2019 Alzheimer's facts and figures report (Association, 2019). (A) Ages of People with Alzheimer's Dementia, 2019. (B) Estimated Lifetime Risk for Alzheimer's Dementia, by Sex, at Ages 45 and 65. (C) Distribution of Aggregate Costs of Care by Payment Source for Americans Age 65 and Older with Alzheimer's or Other Dementias, 2019. "Other" payment sources include private insurance, health maintenance organizations, other managed care organizations, and uncompensated care. (D) U.S. Annual Alzheimer's Death Rate (per 100,000 People) by Year. (E) Percentage Changes in Selected Causes of Death (All Ages) Between 2000 and 2017.

Over 100 drugs have been tested since the late 1990s, but only four have been authorized for use in humans, and they only help manage the symptoms of the disease while doing nothing alter the disease progression (Alzheimer's, 2018). There are currently two types of drugs available: cholinesterase inhibitors, which prevent acetylcholinesterase from breaking down acetylcholine, which is crucial for cellular communication and memory maintenance. The other drug class used is NMDA receptors which block the effects of glutamate, which is released in excessive amounts in AD patients and damages neuronal cells (Alzheimer's, 2018). Interestingly, data generated from studies of twins estimate the hereditability of AD to be around 58%, which suggests that both genetic and non-genetic factors modulate disease progression (Gatz et al., 2006). Efforts to identify more of these factors and how they work to modulate AD pathology will ultimately lead to changes in clinical identification and treatment opportunities for patients suffering from AD. The APOE$\varepsilon$4 variant and *TREM2* deficiency via the R47H mutation are two major genetic risk factors for LOAD, and yet surprisingly little is known about how either of these genes modulates plaque growth. Even less about the interplay between APOE4 and TREM2 regarding the effects on the phenotype and transcriptional regulation. The data presented here works to address this problem by developing a better understanding of the pathological implications of *TREM2* deficiency and the expression of human APOE3 and APOE4.

# 2.0 Materials and Methods

## 2.1 Key Resources Table

**Table 1 Key Resources Table.**

| REAGENT or RESOURCE | SOURCE | IDENTIFIER |
|---|---|---|
| **Antibodies** | | |
| Anti-OC | Millipore | Cat No. AB2286, RRID: AB_1977024 |
| Horse anti-rabbit Dylight 594 | Vector Labs | Cat No. Di-1094, RRID:AB_2336414 |
| Normal goat serum | Vector Labs | Cat No. S-1000-20 |
| 6E10 biotinylated antibody | Biolegend | Cat No. 803009, RRID:AB_2564656 |
| Anti-IBA1 antibody | Wako | Cat No. 019-19741, RRID:AB_839504 |
| Anti-GFAP antibody | Agilent | Cat No. Z033429-2 |
| Normal Donkey Serum | Jackson Lab | Cat No.017-000-121, RRID:AB_2337258 |
| Donkey anti-rabbit Alexa 594 | Invitrogen | Cat No. R37119, RRID:AB_2556547 |
| Donkey anti-rabbit Alexa 488 | Invitrogen | Cat No. A-21206, RRID:AB_141708 |
| Anti-APOE antibody | Invitrogen | Cat No. PA527088, RRID:AB_2544564 |
| Goat anti-rabbit Dylight 488 | Vector Labs | Cat No. Di-1488, RRID:AB_2336402 |
| **Chemicals, Peptides, and Recombinant Proteins** | | |
| Methoxy-X34 (X34) 1,4-bis (3-carboxy-4-hydroxyphenylethenyl)-benzene | W. Klunk | N/A |
| Methoxy-X04 (X04) 1,4-bis(4′-hydroxystyryl)-2-methoxybenzene | W. Klunk | N/A |
| Thioflavin S (ThioS) | Sigma Aldrich | Cat No. 1326-12-1 |
| Thiazine Red (TR) | Sigma Aldrich | Cat No. 1121-911 |
| **Critical Commercial Assays** | | |
| Vector ABC kit | Vector Labs | Cat No. PK-7200 |
| DAB substrate kit | Vector Labs | Cat No. SK-4100 |

**Table 1 Continued**

| | | |
|---|---|---|
| Multiplex Fluorescent Reagent kit v2 | Advanced Cell Diagnostics | Cat No: 323100 |
| **Deposited Data** | | |
| Raw and analyzed data | This paper | GEO: GSE144125 |
| **Experimental Models: Organisms/Strains** | | |
| Mouse APP/PS1dE9: APP(B6.Cg-Tg (APPswe, PSEN1dE9)85Dbo/J) | The Jackson Laboratory | RRID:MMRRC_042050-JAX |
| Mouse Trem2[ko]: (*Trem2*[em2ADiuj]/J) | The Jackson Laboratory | 027197-JAX |
| Mouse APOE3^{+/+}: (*B6.129P2-Apoe*[tm3(APOE*3)Mae] *N8)* | Taconic Bioscience | 1548 |
| Mouse APOE4^{+/+}: (*B6.129P2-Apoe*[tm3(APOE*4)Mae] *N8)* | Taconic Bioscience | 1549 |
| **Software and Algorithms** | | |
| ANY-maze | Stoelting Co., USA | http://www.anymaze.co.uk/ |
| Subread/featureCounts (v1.5.3) | (Liao et al., 2013) | https://sourceforge.net/projects/subread/files/subread-1.5.3/ |
| Rsubread (v1.34.2) | (Liao et al., 2019) | https://bioconductor.org/packages/release/bioc/html/Rsubread.html |
| DEseq2 (1.24.0) | (Love et al., 2014) | https://bioconductor.org/packages/release/bioc/html/DESeq2.html |
| EdgeR (v3.26.5) | (Robinson et al., 2009) | https://bioconductor.org/packages/release/bioc/html/edgeR.html |
| WGCNA (v1.68) | (Langfelder and Horvath, 2008) | https://cran.r-project.org/web/packages/WGCNA/index.html |
| R (v3.6.0) | The R Foundation | https://www.r-project.org/ |
| Database for Annotation, Visualization and Integrated Discovery (DAVID v6.8) | (Huang et al., 2009) | https://david.ncifcrf.gov |
| Cytoscape (v3.7.1) | National Resource for Network Biology | https://cytoscape.org/ |

**Table 1 Continued**

| Prism (v8.2.0) | GraphPad | https://www.graphpad.com/scientific-software/prism/ |
|---|---|---|
| NIS Elements software AR | Nikon Instruments Inc | https://www.microscope.healthcare.nikon.com/products/software/nis-elements |
| Imaris (v9.3.1) | Bitplane | https://imaris.oxinst.com/packages |
| Adobe Photoshop CC (v20.0.5) | Adobe | https://www.adobe.com/products/photoshop.html |
| **Other** | | |
| FISHprobe: Mm-*Clec7a* | Advanced Cell Diagnostics | Cat No. 532061 |
| FISHprobe: Mm-*Csf1r* | Advanced Cell Diagnostics | Cat No. 428191 |
| FISHprobe: Mm-Tmem119 | Advanced Cell Diagnostics | Cat No. 472901 |
| FISHprobe: Mm-Apoe | Advanced Cell Diagnostics | Cat No. 313271 |

## 2.2 Experimental Model and Subject Details

### 2.2.1 Animals

Mouse strains. This study adhered to the guidelines outlined in the Guide for the Care and Use of Laboratory Animals from the United States Department of Health and Human Services and was approved by the University of Pittsburgh Institutional Animal Care and Use Committee. APP/PS1dE9 (B6.Cg-Tg (APPswe, PSEN1dE9)85Dbo/J) and *Trem2*$^{em2ADiuj}$/J mice were purchased from The Jackson Laboratory (USA) and human *APOE3 (B6.129P2-Apoe*$^{tm3(APOE*3)Mae}$ *N8)* and *APOE4 (B6.129P2-Apoe*$^{tm3(APOE*4)Mae}$ *N8)* targeted replacement mice from Taconic (USA) (Sullivan et al., 1997). APP/PS1dE9 mice express mutant familial variants of human amyloid precursor protein (APP) with Swedish mutation, and human presenilin 1 carrying the exon-9-

deleted variant (PSEN1dE9). All purchased mice were on a C57BL/6 genetic background and crossbred for at least 10 generations in our laboratory.

Breeding. APP/PS1dE9 mice were bred to human APOE3$^{+/+}$ or APOE4$^{+/+}$ targeted replacement mice (Fitz et al., 2012; Nam et al., 2018) to generate APP/PS1dE9/APOE3$^{+/+}$ (referred to as APP/E3, APP/PS1dE9/APOE4$^{+/+}$ (APP/E4), APOE3$^{+/+}$ (E3), APOE4$^{+/+}$ (E4) mice expressing human *APOE* isoforms and wild-type *Trem2*. Trem2$^{-/-}$ mice were bred to human APP/PS1dE9/APOE3$^{+/+}$ or APP/PS1dE9/APOE4$^{+/+}$ targeted replacement mice to generate APP/PS1dE9/APOE3$^{+/+}$/Trem2$^{-/-}$ (referred to as APP/E3/Trem2$^{ko}$), APP/PS1dE9/APOE4$^{+/+}$/Trem2$^{-/-}$ (APP/E4/Trem2$^{ko}$), APOE3$^{+/+}$/Trem2$^{-/-}$ (E3/Trem2$^{ko}$); and APOE4$^{+/+}$/Trem2$^{-/-}$ (E4/Trem2$^{ko}$) mice. All *APOE3* or *APOE4* mice were littermates and fed normal mouse chow diet ad libitum. Mice had water accessible at all times and were kept on a 12-hour light-dark cycle. Male and female mice from each genotype were used for this study at an average age of 6.5 months.

<center>**2.3 Method Details**</center>

**2.3.1 Behavioral Testing**

Novel Object Recognition. Novel object recognition (NOR) was performed as previously described (Carter et al., 2017) with minor modifications. The NOR task assesses recognition memory and is based on the spontaneous tendency of mice to explore a novel object over a familiar one. Mice were placed in individual containers before any testing then returned to their housing cages after the daily testing was completed. Each mouse was handled for 3 min. for three

successive days before testing to reduce anxiety. The NOR task was performed over three consecutive days, each pertaining to a unique phase. On Day 1, habituation phase, each animal was allowed to freely explore an open arena (40 cm X 40 cm X 30 cm tall white plastic box) for two 5 min. trials with a 5 min. inter-trial interval. On Day 2, familiarization phase, each animal was returned to the same arena for two 5 min. trials separated by a 5 min. intertrial interval with two identical objects (tower of LEGO® bricks 8 cm X 3.2 cm, built using white, blue, yellow, red, and green bricks) located in opposite diagonal corners of the arena. After a 24-hour retention period, the testing phase was initiated on Day 3. The animal was returned into the arena with two objects in the same positions as the previous day, but one object was replaced with a novel object (metal bolt and nut of similar size). Mice were allowed to explore for one 10 min. interval. The exploration of both objects was recorded and scored with ANY-maze software (Stoelting Co., USA). The exploration by the software was defined as the mouse sniffing, climbing on, or interacting while facing an object within 3 cm. Mice were consistently placed into the middle of the arena facing the posterior wall to prevent any object preference. The arena and objects were cleaned with 70% ethanol between animals to prevent any olfactory cues. Animals that failed to have a total exploration time of 10 sec for the objects during the novel phase were excluded from the analysis. The total distance traveled by each mouse was recorded during the habituation phase to assess locomotor activity. The percent exploration was determined by dividing the time exploring the novel object by the total time exploring both objects. This calculated value provides an indicator of recognition memory, with less time spent exploring the novel object signifying memory deficits.

Contextual and Cued Fear Conditioning. Contextual and Cued Fear Conditioning (CCFC) was performed as previously described (Carter et al., 2017). CCFC provides a measure of memory

in relation to receiving a mild foot shock to a particular environment (context) or stimulus (cue). CCFC testing was initiated 24 hours following completion of NOR and was performed for three consecutive days. On Day 1, training phase, mice were placed in a conditioning chamber (Stoelting Co., USA) for 5.5 min. The first 2 min. was silent, allowing the mouse to acclimate to the chamber. This was followed by a 30 sec tone (2,800 Hz; Intensity 85 dB, conditioned stimulus (CS)) ending in a 2 sec foot shock (0.7 mA, unconditioned stimulus (US)) through the floor of the conditioning chamber. The process was repeated one more time (learning phase) and ended by 30 sec of reacclimation. On Day 2, contextual phase, mice were placed in the same conditioning chamber for 5 min. with no tone or shock administered, to measure contextual fear conditioning. For the final day, the gray walls of the chamber were covered with black and white striped walls to introduce a novel environment for assessing cued fear conditioning. Mice were placed in the conditioning chamber for 5 min. After the first 2 min. of silence (novel phase), the tone was administered for 3 min. (cued phase). Testing was performed at the same time of the day to ensure 24-hours between phases. The chamber was cleaned with 70% ethanol between each animal. Freezing time was defined as the absence of movement except for respiration and recorded using ANY-maze software. Animals that had below 30 sec total freezing time during the contextual phase were excluded from the analysis. Freezing time was calculated as percent freezing of the total time in the chamber during each phase of testing. Since freezing behavior is a fear characteristic in rodents, memory deficits were defined as diminished freezing when reintroduced to the context or cue from the training phase.

### 2.3.2 Animal Tissue Processing

Two days post behavior, mice were anesthetized by intraperitoneal injection using Avertin (250mg/kg of body weight). Blood was collected from the right ventricle through a cardiac puncture, followed by transcardial perfusion through the left ventricle with 20 mL of cold 0.1 M phosphate buffered saline (PBS), pH 7.4. The brain was removed and divided into hemispheres. One hemisphere was dissected into the cerebellum, subcortical, hippocampus and cortex regions and flash frozen on dry ice. A separate section of the anterior cortex was removed for whole-brain RNA-seq. The other hemisphere was drop fixed in 4% phosphate-buffered paraformaldehyde at 4°C for 48 hours and stored in 30% sucrose until sectioning (Nam et al., 2018). Hemibrains were mounted in O.C.T. and cut in the coronal plane at 30 µm sections using a frozen cryotome (Thermo Scientific, USA). Six serial sections were collected with each section 450 µm apart, starting approximately 150 µm caudal to the first appearance of the dentate gyrus; covering an area in the brain from bregma −1.25 mm and ending at bregma −3.95 mm. Sections were stored in glycol-based cryoprotectant at -20°C until histological staining (Nam et al., 2018).

### 2.3.3 Chemicals

Methoxy-X34 (X34) 1,4-bis (3-carboxy-4-hydroxyphenylethenyl)-benzene, was provided by William E Klunk, MD, Ph.D., (University of Pittsburgh). For *in vivo* labeling of dense plaques, we used Methoxy-X04 (X04) 1,4-bis(4′-hydroxystyryl)-2-methoxybenzene, synthesized in W. Klunk's lab (University of Pittsburgh). X04 readily crosses the blood-brain barrier (Klunk et al., 2002) and remains bound to plaques for at least 90 days (Condello et al., 2011b). One mg/mL X04

stock solution was made by dissolving X04 in a vehicle consisting of 4% DMSO and 7.7% Cremophore EL in PBS.

### 2.3.4 Histological Staining

For the OC-X34 dual stain, free-floating sections were washed followed by 30 min incubation in 50mM sodium citrate buffer at 80°C for antigen retrieval. Sections were then washed, blocked with 5% normal horse serum made in 0.1% triton-X 100 PBS for 1 hour and finally incubated in anti-OC (1:1000, Millipore) primary antibody overnight at 4°C. The following morning, the sections were washed, incubated in horse anti-rabbit Dylight 594 (Di-1094 Vector Labs) for 2 hours, and washed before mounting on positively charged glass slides. The slides were treated with 100 µM X34 followed by two 5 min destaining steps in 50% ethanol and coverslipped. Fluorescent images were taken using a Nikon Eclipse 90i microscope at 10X magnification. OC-X34 images were analyzed using Nikon NIS elements software and thresholding for the detection of plaques. The ratio between X34 positive (compact plaque) and OC positive areas (protofibular Aβ) was used to determine plaque compaction. Plaques with increased OC / X34 ratio are less compact than plaques with a ratio closer to one. We also assessed the area of OC not associated with X34 positive plaques (non-core bound OC) as a percentage of total detectable OC area (total OC).

A second series of brain tissue was used for 6E10 immunostaining as previously described (Nam et al., 2018) with some modifications. Antigen retrieval was performed on free-floating sections using 70% formic acid, followed by quenching of endogenous peroxidases with 0.3% hydrogen peroxide. The tissue was incubated in 3% normal goat serum (Vector, USA) then blocked for endogenous avidin and biotin. Sections were incubated in 6E10 biotinylated antibody

(1:1000 Biolegend, USA) for 2 hours and subsequently developed using the Vector ABC kit and DAB substrate kit (Vector, USA). Sections were mounted onto superfrost plus slides (Fisher Scientific, USA) and coverslipped. Bright-field images were taken using a Nikon Eclipse 90i microscope at 4X magnification. Thioflavin S (ThioS) staining was performed on an third series of brain sections. Sections were mounted onto slides, washed in PBS, and stained with 0.02% ThioS (Sigma, USA) in PBS for 10 min. Next, sections were differentiated in 50% ethanol for 2 min. After a final wash in PBS, slides were coverslipped. Fluorescent images were taken using a Nikon Eclipse 90i microscope at 4X magnification.

To quantify plaque pathology, two separate regions of interest (ROI) were drawn around the cortex and hippocampus for each section and an image intensity threshold was established to detect the stained plaques compared to the background using NIS Elements software (Nikon Instruments Inc., USA). OC, X34, 6E10, and ThioS staining values were represented as the area of staining normalized to ROI area or percentage of area covered by 6E10 or ThioS stain.

A fourth series of brain sections were immunostained with anti-IBA1 antibody (WAKO, USA) and anti-GFAP antibody (Agilent, USA). Free-floating sections were washed, then antigen retrieval performed in sodium citrate buffer at 80°C for 60 min, blocked in Normal Donkey Serum (Jackson Lab, USA) for 1 hour, and finally incubated in IBA1 antibody (1:1000) overnight at 4°C. Sections were washed and transferred into secondary donkey anti-rabbit Alexa 594 (Invitrogen, USA) for 1 hour, before being washed and transferred to GFAP antibody (1:1000) overnight at 4°C. Again, sections were washed and transferred into secondary donkey anti-rabbit Alexa 488 (Invitrogen, USA) for 1 hour, before being washed and mounted onto slides. Slides were stained with X34 as documented for ThioS, followed by DAPI staining, and coverslipped. Fluorescent images of individual plaques were taken using a Nikon Eclipse 90i microscope at 20X

magnification. Plaques were chosen with an average area of 300 µm$^2$. The number of IBA1 positive microglia and GFAP positive astrocytes were counted in circular radiating regions of interest with a diameter of 10, 20, 40, and 60 µm from the edge of the X34 positive plaque.

A fifth series of brain sections were immunostained with anti-APOE antibody (Invitrogen, USA) and Thiazine Red (TR, Sigma Aldrich). Free-floating sections were washed, blocked in Normal Donkey Serum (Jackson Lab, USA) for 1 hour, and incubated in APOE antibody (1:100) overnight at 4°C. Sections were transferred into secondary donkey anti-rabbit Alexa 488 (Invitrogen, USA) for 1 hour, before being washed and mounted onto slides. Mounted slides were stained with 2µM TR in PBS for 15 min. After a final wash, slides were dried and coverslipped. Fluorescent images of plaques were taken using a Nikon Eclipse 90i microscope at 10X magnification. Staining was defined by threshold analysis using NIS Elements software, and the area of APOE staining associated with TR positive plaque area was assessed.

A sixth series of brain sections were immunostained with anti-LAMP1 antibody (Abcam, USA) and X34. Free-floating sections were washed, blocked in Normal Goat Serum (Jackson Lab, USA) for 1 hour, and incubated in LAMP1 antibody (1:500) overnight at 4°C. Sections were transferred into secondary goat anti-rat Cy5 (Vector, USA) for 2 hours, before being washed and mounted onto slides. Mounted slides were stained with X34 as above. Fluorescent images of plaques were taken using a Nikon Eclipse 90i microscope at 10X magnification. Staining was defined by threshold analysis using NIS Elements software, and the area of LAMP1 staining associated with X34 positive plaques was assessed. For all plaque specific imaging, plaques were selected so they were at least 50 µm from the edge of the tissue, and at least 50 µm away from other plaques, with an even representation of all plaque sizes and composition across all groups to account for any bias introduced by differences in plaque stage, composition, or size.

**2.3.5 *In vivo* Plaque Labeling**

X04 was administered intraperitoneally (i.p.) at a concentration of 10 mg/kg to mice at either 3.5 or 5.5 months of age and sacrificed after 30 days for the collection of brain tissue for *in vivo* labeling of dense core amyloid plaques. Tissues used for the X04-TR-IBA1 triple stain allowed for the assessment of plaque growth dynamics and microglia plaque barrier. Free-floating sections were washed, incubated in 0.5 uM TR in PBS for 20 min followed by a final PBS wash. Sections were then incubated in 50mM sodium citrate buffer for 30 min at 80°C to perform antigen retrieval, washed, incubated in 5% normal goat serum made in 0.1% triton-X 100 PBS for 1 hour, and finally incubated in anti-IBA1 (1:1000, Wako) primary overnight at 4°C. The following morning the sections were washed, incubated in goat anti-rabbit Dylight 488 (Di-1488 Vector Labs) for 2 hours, and washed before mounting on positively charged glass slides. X04-TR-IBA1 triple stained tissues were imaged on all three channels using an Olympus FV1000 confocal microscope at 60x, with 1.5 μm step size. For confocal imaging, plaques were selected if they were at least 50 μm from the edge of the tissue, and at least 50 μm away from other plaques, with an even representation of all plaque sizes and composition across all groups.

To assess the size of β-amyloid plaques at each age group (4.5 and 6.5 months), we analyzed plaque volume using Imaris on an independent set of APP/E3, APP/E3/Trem2$^{ko}$, APP/E4 and APP/E4/Trem2$^{ko}$ mice that were injected at 5.5 months of age and sacrificed 48 hours later to extract quantitative data from the high-resolution three-dimensional confocal images. In the 48 hour controls, plaques of all sizes and compositions were intentionally imaged in order to account variance when thresholding near detection limits. Greater than 94% of all the plaques imaged in the experimental groups fall within the minimum and maximum range of TR plaque volume analyzed in the 48hr control group. Additionally, when comparing the TR volume to X04 volume

21

in the 48 hour control plaques we saw a very high correlation ($R^2 = 0.9579$) and no departure from the linear regression line in either the extremely small, or extremely large plaques (see Fig. 8). Briefly, images were loaded into the Imaris (v9.3.1) environment and voxels less than 500 intensity were removed from all channels to reduce background noise. Surfaces were then generated for the X04 and TR channels and the volume of each surface created was analyzed. Surfaces were created to assess IBA1 coverage and, using the "surface-surface contact area" XTension, the percent of IBA1 / TR surface contact was calculated. A 1 voxel shell is generated surrounding the TR labeled amyloid plaque and any time IBA1 signal is colocalized with the TR shell it is counted as surface contact. The sum of the colocalized voxels divided by the total surface area of TR generated the percent surface contact. The surface area contacted by microglia is subtracted from the total surface area giving the exposed surface area of each plaque (surface area not covered by microglia). The change in plaque volume was calculated by subtracting the volume of the plaque at the time of sacrifice (TR) from the volume of the plaque at the time of *in vivo* labeling (X04). In the 48-hour control mice, we found no significant difference in the volume of X04 and TR labeling, an average growth volume (TR-X04) near 0 and an average fold change near 1 (TR/X04).

**2.3.6 Tissue Homogenization for ELISA**

The frozen cortices were homogenized according to previously published work (Fitz et al., 2010). Individual cortices were weighed and transferred into a glass Dounce containing the appropriate amount of tissue homogenization buffer (1M TRIS base, 0.5M EDTA, and 0.2M EGTA) and protease inhibitor (Sigma-Aldrich, USA). Cortices were homogenized in 1 mL of tissue homogenization buffer and protease inhibitor per each 100 mg of tissue. Once homogenized, the tissue was spun in a centrifuge at *16,000 rcf f*or 1 hour. The supernatant was kept for future

use for the determination of soluble Aβ. 70% formic acid was then added to the pellet and sonicated for two fifteen sec intervals before being spun again at *16,000 rcf* for 1 hour. The resulting supernatant was kept and used for the determination of insoluble Aβ.

**2.3.7 Aβ ELISA**

Aβ ELISA was performed according to previously published work (Fitz et al., 2010) with modifications. The wells of MaxiSorp plates (Nunc) were coated by adding 100 µl/well of 6E10 antibody (Biolegend, USA) diluted to 5 µg/ml in Coating buffer (0.1M $NaHCO_3$, 0.1M $Na_2 CO_3$, pH 9.6) and incubated overnight at 4°C while rocking. The next day, wells were washed with PBS and 200 µL/well of Block Ace Solution (1% Block Ace (Bio Rad, USA) in PBS, 0.05% $NaN_3$) was added. Plates were incubated for 4 hours at room temperature with rocking to block non-specific binding. Once the Block Ace Solution was removed 50 µl/well of Buffer EC (20mM sodium phosphate, 2mM EDTA, 400mM NaCl, 0.2% BSA, 0.05% CHAPS, 0.4% Block Ace, 0.05% $NaN_3$, pH 7.0) was added to the wells to prevent drying while adding samples. 100 µL of standards and samples were added to each well, and high-range samples were diluted with Buffer EC where necessary. For the insoluble Aβ fraction, samples were also neutralized with FA neutralization solution (1M TRIS base, 0.5M $Na_2HPO_4$, 0.05% $NaN_3$) before dilution. For standards, ranging from 0-0.8pM, equal parts of 8 pM stocks of Aβ40 and Aβ42 were used. Once standards and samples were loaded, the plates were incubated overnight at 4˚C with rocking. Plates were washed and 100 µL detection antibody HJ5.1 (1:3300, a gift from John Cirito) diluted in 0.05%-PBSTween was added to each well and incubated for 90 min. at room temperature with rocking. After washing, 100 µL HRP40 secondary (1:16000, Fisher Scientific, USA) diluted in 1% BSA-PBSTween, was added to each well and incubated for 90 min. at room temperature with

rocking. Wells were washed and 100 µL of prepared TMB Substrate/$H_2O_2$ Solution (Thermo Sci-1854050) was added. Absorbance was read at 650 nm on a plate reader (Molecular Devices, USA). All samples were run on the same day in duplicates. The concentration of total Aβ in pM was interpolated using linear regression on GraphPad Prism 7.0 and multiplied by the dilution factor for each sample.

Bradford Assay. Protein concentrations were determined according to previously published work (Fitz et al., 2014). The Bradford assay was used to determine the protein concentration of all samples. Bovine Serum Albumin (BSA, Fisher Scientific, USA) standards ranging from 0-100 µg/ml were used. A 40% Bio-Rad Protein Assay Dye Reagent (Bio-Rad, USA) was prepared with a 1:1 volume of diluted samples and absorbance was read at 595 nm. Total Protein (µg/ml) was interpolated using linear regression on GraphPad Prism 7.0 and multiplied by the dilution factor for each sample. To normalize the data, total protein concentration from the Bradford assay (µg/ml) was divided by the pM concentration of total Aβ for each sample from ELISA.

**2.3.8 Fluorescence *in situ* Hybridization (FISH)**

In a separate cohort, mice were perfused, and tissue fixed and sectioned as documented above. RNAscope experiments were performed using the Multiplex Fluorescent Reagent kit v2 (Advanced Cell Diagnostics, USA) following the manufacturer's recommendations with minor adjustments. Six freshly sectioned tissues per animal were mounted onto superfrost plus slides (Fisher Scientific, USA) within a 0.75" x 0.75" square, and baked at 60°C for 60 min. Slides were incubated in X-34 for 10 min. before being dehydrated using a series of ethanol dilution steps, then submerged in target retrieval reagent at 100°C for 10 min. Protease digestion was performed at 40°C for 30 min. using Protease III, and probe hybridization was carried out at 40°C for 2 hours.

24

We used probe sets available from ACD for Mm-*Clec7a*, Mm-*Csf1r*, and Mm-*Tmem119*. Following the amplification steps, the sections were counterstained with DAPI and coverslipped. Imaging was carried out using a Nikon Eclipse 90i microscope at 20X magnification with imaging of individual plaques and analyzed using NIS Elements software (Nikon Instruments Inc., USA). One circular ROI that extends 50 µm from the center of the X-34 positive plaque was drawn, and a threshold established for each probe to determine the area of puncta coverage. Four ROI's of the same area were randomly selected from areas away from the plaque on the same image and averaged to determine the area of puncta coverage greater than 50 µm from plaque center. *Apoe* FISH analysis was performed on *Tmem119*-positive microglia within the same 50 µm ROI. The nuclei and surrounding area of cells with positive *Tmem119* signal were outlined and identified as microglia. The intensity of *Apoe* FISH signal was normalized to the number of *Tmem119* positive cells.

**2.3.9 mRNA-seq Data**

RNA was isolated from the frontal cortex and purified using RNeasy mini kit (Qiagen, Germany). RNA quality was assessed using 2100 Bioanalyzer (Agilent Technologies, USA) and only samples with RIN > 8 were used for library construction. Library generation was performed by Novogene Co. Ltd. and sequenced using an Illumina HiSeq 2500 instrument. Following initial processing and quality control, the sequencing data was aligned to the mouse genome mm10 using Subread/featureCounts (v1.5.3; https://sourceforge.net/projects/subread/files/subread-1.5.3/) with an average read depth of 50 million successfully aligned reads. Statistical analysis was carried out using Rsubread (v1.34.2; https://bioconductor.org/packages/release/bioc/html/Rsubread.html), DEseq2 (1.24.0; https://bioconductor.org/packages/release/bioc/html/DESeq2.html), EdgeR

(v3.26.5; https://bioconductor.org/packages/release/bioc/html/edgeR.html), and WGCNA (v1.68; https://cran.r-project.org/web/packages/WGCNA/index.html) all in the R environment (v3.6.0; https://www.r-project.org/). For network analysis using WGCNA, samples were clustered by gene expression profile which enabled the detection of outliers that were removed from the downstream analysis. Modules were generated automatically using a soft thresholding power, $\beta = 10$, a minimum module size of 44 genes and a minimum module merge cut height of 0.25. To account for bias introduced by sequencing batch, we implemented empirical Bayes-moderated linear regression which removes variation in the data due to unwanted covariates while preserving variation due to retained covariates. Networks were built using the top 5 genes identified as hub genes from any given module (gene significance $> 0.2$, and module membership $> 0.8$). Following hub gene selection, all other connections generated from the top 5 genes were visualized using Cytoscape (v3.7.1). Functional annotation clustering was performed using the Database for Annotation, Visualization and Integrated Discovery (DAVID v6.8, https://david.ncifcrf.gov). All GO terms are considered significant if p<0.05 following multiplicity correction using the Benjamini-Hochberg method to control the FDR.

## 2.4 Quantification and Statistical Analysis

Sample sizes (n) indicated in the figure legends. No outliers were removed from the analysis. All researchers were blinded to experimental groups during the analysis. All results are reported as means $\pm$ SEM. Data was analyzed by two-way ANOVA with APOE isoform and *Trem2* status as main factors followed by Sidak multiple comparison test. Histology and FISHwas analyzed by one-way ANOVA followed by Tukey's multiple comparison test. Unless otherwise

indicated, all statistical analyses were performed in GraphPad Prism (v 8.2.0), or in R (v 3.6.0) and significance was determined as $p<0.05$. Number of experiments and statistical information are stated in the corresponding figure legends. In figures, asterisks denote statistical significance marked by * $p<0.05$; ** $p<0.01$; *** $p<0.001$.

## 2.5 Data and Code Availability

The RNA-seq expression data has been deposited in the GEO database under the accession number: GSE144125.

**3.0 The Role of APOE and TREM2 in Alzheimer's Disease – Current Understanding and Perspectives**

The data presented in this chapter is open access published in *Int. J. Mol. Sci.* 2019, *20*, 81

Cody M Wolfe[1], Nicholas F Fitz[1], Kyong Nyon Nam[1], Iliya Lefterov[1]*, Radosveta Koldamova[1]*

[1] Department of Environmental & Occupational Health, University of Pittsburgh, Pittsburgh, PA, USA 15261

**3.1 Abstract**

Alzheimer's disease (AD) is the leading cause of dementia worldwide. The extracellular deposits of Amyloid beta (Aβ) in brain – called amyloid plaques, and neurofibrillary tangles – intracellular tau aggregates, are morphological hallmarks of the disease. The risk for AD is a complicated interplay between aging, genetic risk factors, and environmental influences. One of Apolipoprotein E (*APOE*) alleles – *APOEε4*, is the major genetic risk factor for Late Onset AD (LOAD). APOE is the primary cholesterol carrier in brain, and plays an essential role in lipid trafficking, cholesterol homeostasis, and synaptic stability. Recent GWAS studies have identified other candidate LOAD risk loci, as well. One of those is the triggering receptor expressed on myeloid cells 2 (*TREM2*), in brain expressed primarily by microglia. While the function of TREM2 is not fully understood, it promotes microglia survival, proliferation, and phagocytosis, making it important for cell viability and normal immune functions in brain. Emerging evidence from protein binding assays suggests that APOE binds to TREM2 and APOE-containing lipoproteins in brain as well as periphery and are putative ligands for TREM2, thus raising the possibility of an APOE-

TREM2 interaction modulating different aspects of AD pathology, potentially in an isoform specific manner. This review is focusing on the interplay between APOE isoforms and TREM2 in association with AD pathology.

## 3.2 Introduction

AD is the leading cause of dementia worldwide and accounts for 60-80% of all cases (Crous-Bou et al., 2017). AD is characterized by senile plaques made of β-amyloid peptide (Aβ) and neurofibrillary tangles of hyperphosphorylated tau protein. There are two types of AD: familial, early-onset AD, and LOAD, with LOAD accounting for approximately 95% of all AD cases (Guerreiro et al., 2012; Tanzi, 2012). Familial AD accounts for a small percentage of all cases and occurs exclusively through gene mutations in amyloid precursor protein (APP), or presenilins (PSEN1, PSEN2) that increase the production of Aβ (Guerreiro et al., 2012; Tanzi, 2012), or the ratio between longer (Aβ42) and shorter Aβ peptides. These mutations follow a pattern of Mendelian inheritance and result in symptom manifestation before the age of 65 (Campion et al., 1999). In contrast, LOAD has no known causative gene mutations, however, genome-wide association studies (GWAS), and whole exome sequencing have identified over 30 AD risk loci (Pimenova et al., 2018). Over half of those have been implicated in innate immune response including APOE and TREM2 (Guerreiro et al., 2013a; Jonsson et al., 2013; Karch et al., 2014; Shi and Holtzman, 2018).

In humans, the *APOE* gene resides on chromosome 19 and has three alleles with different allele frequencies: *APOEε2*, 5–10 %; *APOEε3*, 65–70 %; and *APOEε4*, 15–20 % (Bu, 2009). APOE is a 299 amino acid protein, is a major cholesterol carrier in the circulation and the only

cholesterol transporter in brain (Liu et al., 2013). In mouse models for AD, the human isoforms APOE2 and APOE3 have the ability to bind and clear Aβ more efficiently compared to APOE4 (Castellano et al., 2011). The physiological role of APOE in lipid trafficking is crucial as lipids play an essential role in immune regulation through cell signaling, membrane fluidity, and serve as ligands for a number of immune receptors (Mahoney-Sanchez et al., 2016). TREM2 is a cell surface receptor on myeloid cells and through its interaction with protein tyrosine kinase binding protein (TYROBP), TREM2 activation initiates a multitude of pathways that promote cell survival (Ulland et al., 2017; Wang et al., 2015), proliferation (Poliani et al., 2015), chemotaxis, and phagocytosis (Hsieh et al., 2009; Kleinberger et al., 2014; Mazaheri et al., 2017; Poliani et al., 2015; Takahashi et al., 2005; Wang et al., 2015; Zheng et al., 2017), making it vital for normal immune function. The most common *TREM2* variant, R47H (arginine to histidine at position 47), impairs ligand binding and increases the risk of developing AD by approximately 4-fold (Guerreiro et al., 2013a; Jonsson et al., 2013). TREM2 has the ability to recognize a variety of ligands many of them on the surface of apoptotic cells, phospholipids, glycolipids, and lipoproteins including low-density lipoprotein (LDL) and high-density lipoproteins (HDL), Clusterin (APOJ) and APOE (Atagi et al., 2015; Bailey et al., 2015; Yeh et al., 2016). Emerging evidence suggests that TREM2 can bind to and is a putative receptor for APOE (Atagi et al., 2015; Bailey et al., 2015; Yeh et al., 2016), thus raising the possibility of an APOE-TREM2 interaction modulating AD pathogenesis. This review focuses on the interplay between APOE isoform and TREM2 and their association with AD.

## 3.3 APOE

### 3.3.1 APOE Structure and Isoforms
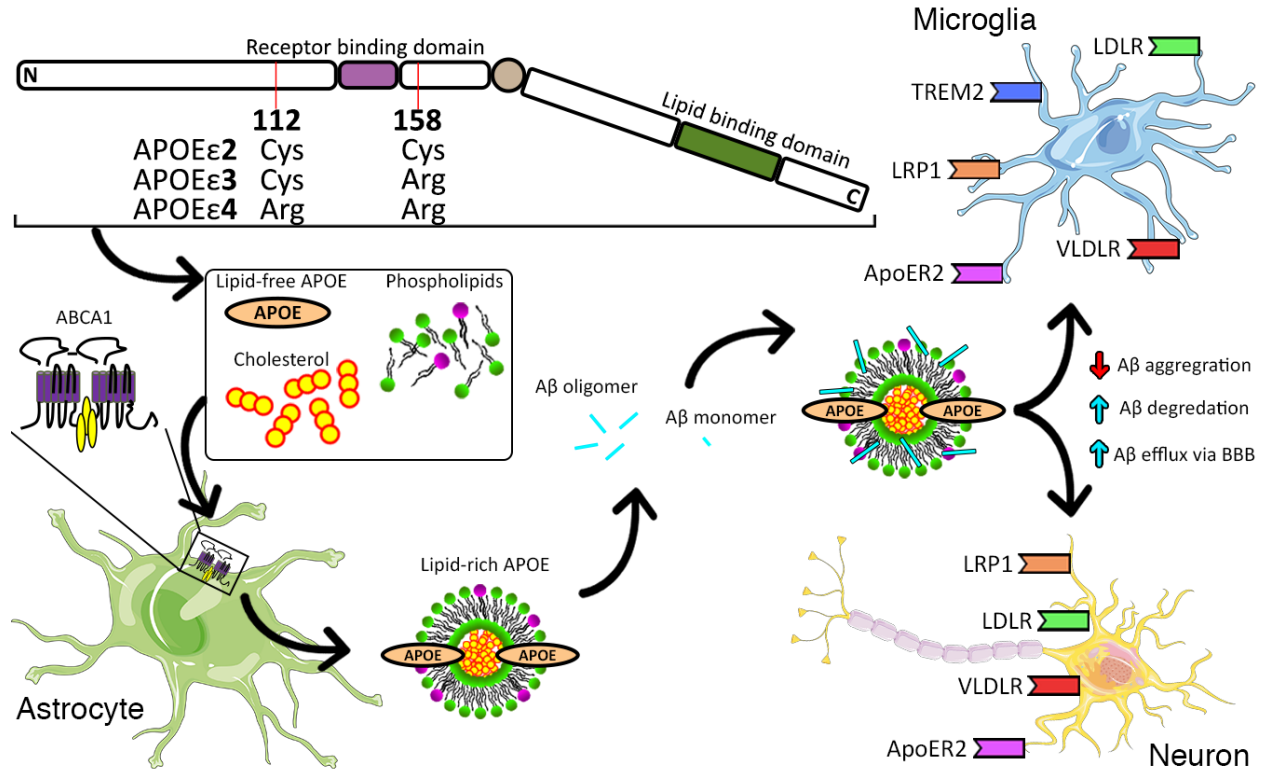


**Figure 2. Role of APOE in AD.**
In humans, there are three APOE isoforms: APOEε2, APOEε3, and APOEε4. In the brain, APOE is secreted mainly by astrocytes and its lipidation is mediated by ABCA1. ABCA1 transports cholesterol and phospholipids to naïve APOE forming discoidal HDL particles. Lipid-rich APOE particles can interact with Aβ monomers and oligomers and bind to the LDL receptor family including LRP1, LDLR, VLDLR, and ApoER2 on both neurons and microglia, while also interacting with TREM2 only in microglia.

In brain, APOE is secreted by glia, mainly astrocytes, and is lipidated by adenosine triphosphate-binding cassette transporters A1 (ABCA1) and G1 (ABCG1) (Fig. 2). ABCA1 transports cholesterol and phospholipids to lipid-free APOE, thus forming discoidal HDL particles (reviewed in (Koldamova et al., 2010, 2014)). The discoidal HDL particles are composed of 100 to 200 lipid molecules that are surrounded by two apolipoprotein molecules (Nagata et al., 2013). Once sufficient cholesterol and phospholipids are available to ABCA1 it undergoes a conformation

change and forms a dimer. The lipidated dimers interact with actin filaments on the plasma membrane, thereby immobilizing them until lipid-free apolipoprotein directly binds to the ABCA1 dimer. Upon binding, the apolipoprotein accepts the lipids presented by ABCA1 and forms a discoidal HDL particle leaving the ABCA1 dimer to dissociate back to a monomer and begin the process again (Nagata et al., 2013). In brain, APOE is primarily synthesized de novo and there is a limited exchange between APOE circulating in the blood and brain (Lane-Donovan et al., 2016; Zhang and Liu, 2015). In humans, APOE isoforms differ at either position 112 or 158 (Fig. 2). APOE2 has cysteine (Cys) residues at both positions 112 and 158, APOE3 has a Cys residue at 112 and an arginine (Arg) residue at 158, and APOE4 has Arg residues at both positions (Weisgraber et al., 1981). All other mammals investigated so far have a single APOE isoform with Arg at the residue equivalent to human APOE 112 (Mahley et al., 2009).

APOE has two functional domains: an N-terminal domain, residues 136-150, and a C-terminal lipid binding domain, residues 244-272 (Bu, 2009; Liu et al., 2013)). The N-terminal domain forms a four-helix bundle (Wilson et al., 1991) and the amino acid differences between isoforms alter the protein structure, thus leading to differential lipid and receptor binding. With a Cys residue at position 112, both APOE2 and APOE3 have the ability to form disulfide-linked hetero- and homodimers, while Arg at position 112 of APOE4 significantly impedes the binding (Weisgraber and Shinto, 1991). The structural variation between isoforms due to amino acid Cys/Arg at position 158 impacts the receptor-binding domain of APOE and thus, the binding affinity to APOE receptors. The variation at position 112 plays a role in domain-domain interaction and affects lipid binding properties of APOE (Weisgraber, 1990), thus explaining the binding preference of APOE4 for very low-density lipoproteins (VLDL) and APOE3 to HDL (Dong and

Weisgraber, 1996). Therefore, the stability and functional role of APOE is largely dependent on its ability to interact with lipids and its receptor binding properties.

**3.3.2 APOE Receptors**

APOE predominantly binds to receptors of LDL receptor family, which includes low-density lipoprotein receptor (LDLR), LDLR-related receptor 1 (LRP1), very-low-density lipoprotein receptor (VLDLR), and APOE receptor 2 (APOER2) (Kanekiyo and Bu, 2014; Lane-Donovan et al., 2014; Shinohara et al., 2017) (Fig. 2). The members of the LDL receptor family share structural properties consisting of a short intracellular domain, a transmembrane domain, and a large extracellular domain with a varying number of complement-type repeats which allow them to interact with APOE (Lane-Donovan et al., 2014). The first identified key member of this family of receptors was LDLR, which is the main receptor for LDL and VLDL. LDLR preferentially binds to lipidated APOE particles, and its deficiency leads to severe hypercholesterolemia and premature atherosclerosis (Jeon and Blacklow, 2005). LRP1 binds to APOE aggregates and is essential for early development, as the deletion of the *Lrp1* gene in mice results in embryonic lethality (Herz et al., 1992), while brain-specific knockdown of *Lrp1* inhibits synaptic transmission and motor function (May et al., 2004). LDLR and LRP1 are the main APOE receptors in brain and deletion of *Ldlr* increases APOE levels (Fryer et al., 2005; Liu et al., 2007). Both APOER2 and VLDLR are almost exclusively expressed in the brain, are structurally very similar to each other, bind to lipid-free APOE, and are dependent on the extracellular ligand Reelin (Trommsdorff et al., 1999). In mice deletion of both *Apoer2* and *Vldlr* leads to defective lamination of the cerebellum, cortex, and hippocampus, as well as a reduction in cerebellum volume and impaired motor function (Trommsdorff et al., 1999).

Activation of APOE receptors by Reelin initiates a signaling cascade through the initiation of Src family kinases (SFKs). The activation includes PI3 kinase and Protein kinase B (Akt), which result in reduced phosphorylation of the microtubule stabilizing protein tau, and regulation of microtubule dynamics (Hiesberger et al., 1999; Zhang et al., 2007). As noted above, due to the amino acid substitution of Arg with Cys at 158 leading to conformational differences, APOE2 exhibits a severely decreased binding affinity to LDLR (1-2% of APOE3) (Kowal et al., 1990), a significantly decreased affinity to bind LRP1 (40% of APOE3) (Kowal et al., 1990), but similar affinity to VLDLR (Ruiz et al., 2005). The receptors from the LDL receptor family have distinct physiological roles due in part to their affinity to ligands, signaling potency, cellular localization, expression pattern, and endocytosis rate (Shinohara et al., 2017).

### 3.3.3 APOE Function in the CNS

The human brain accounts for approximately 2% of the weight of the body but contains over 20% of its total cholesterol (Bjorkhem and Meaney, 2004). In brain, cholesterol is necessary for the formation and maintenance of synapses, and APOE plays a major role in cholesterol homeostasis. The blood brain barrier (BBB) prevents the exchange between brain and plasma cholesterol and lipids transported by HDL, LDL and VLDL (Zhang and Liu, 2015). APOE as the major lipid carrier in the brain and has an important role in the transport of cholesterol and other lipids from astrocytes to neurons, where they are needed to maintain synaptic plasticity (Mauch et al., 2001). The important role of APOE in synaptic integrity and plasticity, as well as dendritic complexity, has been demonstrated by experiments in APOE knockout mice (Fitz et al., 2015; Lane-Donovan et al., 2016).

Disruptions in synaptic function, decreased synaptic density and alterations in autophagy are a pathological feature of neurological disorders, including AD (Azarnia Tehran et al., 2018; Koffie et al., 2011; Nixon, 2017; Sheng et al., 2012). There is increasing evidence that APOE isoforms differentially impact synaptic integrity and plasticity (Ji et al., 2003; Love et al., 2006; Yong et al., 2014; Zhu et al., 2012). In mice and humans, APOE4 correlates inversely with dendritic spine density (Ji et al., 2003; Mounier et al., 2015), and synaptic proteins PSD-95, synaptophysin, and syntaxin 1 are altered in an APOE isoform-specific manner (APOE4 < APOE3 < APOE2) (Love et al., 2006). It has been shown that in targeted replacement mice expressing human APOE, APOE4 isoform has a differential effect on neuronal signaling in young and aged mice indicated by the expression level of proteins in NMDAR-dependent ERK/CREB pathway, reduced expression of APOE receptor LRP1 and lower NR2A phosphorylation (Yong et al., 2014). Other studies demonstrated that in APOE4 expressing mice dendritic spine density and complexity, as well as glutamate receptor function, and synaptic plasticity are impaired (Chen et al., 2010; Dumanis et al., 2009). Meta-analyses addressing the differential effect of APOE isoforms in cognitively healthy adults over the age of 60 suggest that *APOEε4* carriers exhibit impaired episodic memory, executive function, and global cognition, with no impact on primary memory, verbal ability, or attention (Small et al., 2004; Wisdom et al., 2011). Studies utilizing the same cognitive tests and similar in size patient cohorts are rare thus making the findings inconsistent between groups (O'Donoghue et al., 2018). Whether or not memory and cognitive impairments in humans, carriers of *APOEε4* allele, are associated with a disturbed neuronal signaling and the level of NR2A phosphorylation, as in APOE4 expressing mice, is not known.

### 3.4.1 TREM2 Structure and Expression
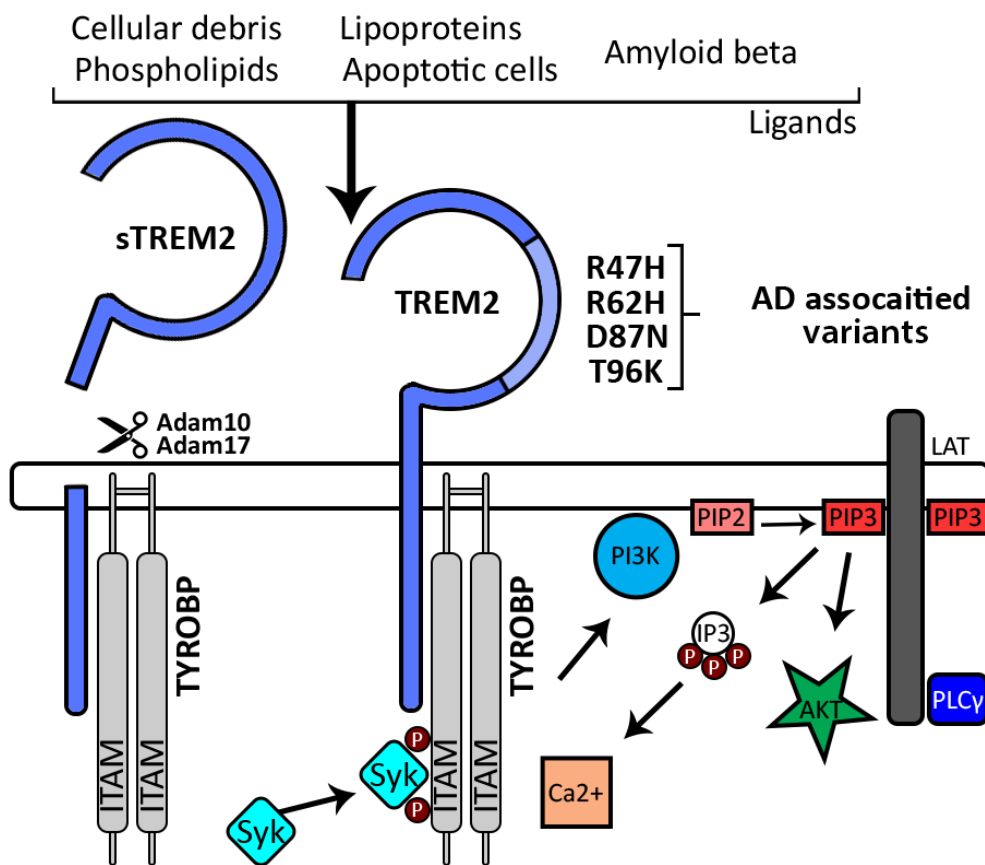


**Figure 3. TREM2 activation and downstream signaling.**
sTREM2 is generated by ADAM 10 or ADAM17 mediated proteolytic cleavage. Ligand activated TREM2 interacts with immune receptor tyrosine-based activation motifs (ITAMs) on TYROBP which leads to TYROBP phosphorylation and recruitment of spleen tyrosine kinase (SYK). TYROBP/SYK mediated activation of phosphoinositide 3-kinase (PI3K) – AKT pathway and phosphorylation of LAT (linker for activation of T-cells family member 1), recruits other signaling adaptors including phospholipase Cγ (PLCγ). PLCγ degrades phosphatidylinositol-3,4,5-trisphosphate (PIP3) into inositol trisphosphate (IP3), inducing an efflux of Ca2+. The ability of TREM2 to bind ligands is influenced by genetic variations, some of which are associated with AD and located adjacent to or within an electrostatically basic patch (light blue).

TREM2 is a transmembrane receptor of the immunoglobulin superfamily expressed on the

plasma membrane of myeloid cells and microglia and is active in the innate immune response

(Colonna and Wang, 2016). TREM2 protein consists of an extracellular Ig-like domain, a

transmembrane domain, and a small cytoplasmic tail. In the CNS, TREM2 expression is strongest in the basal ganglia, corpus callosum, spinal cord, and medulla oblongata (Paloneva et al., 2002). Human TREM2 is located on chromosome 6p21.1 in the TREM gene cluster near other TREM and TREM-like genes: TREML1, TREM2, TREML2, TREML3, TREML4, and TREM1 (Guerreiro et al., 2013b; Klesney-Tait et al., 2006). Many of these genes are conserved in mice and humans with only Trem3 and Trem6 unique to mice and TREML3 to humans. Both TREM2 and TREM1 interact with TYROBP to initiate pathways involved in cell activation and phagocytosis (Klesney-Tait et al., 2006; Poliani et al., 2015). TREMs proteins are implicated in the clearance of extracellular debris (Painter et al., 2015).

The proteolytic cleavage of TREM2 ectodomain generates soluble TREM2 (sTREM2) (Wunderlich et al., 2013) (Fig. 3). sTREM2 has the ability to passes the Brain - cerebral spinal fluid (CSF) barrier and can be detected in CSF (Liu et al., 2018).

### 3.4.2 TREM2 Function

TREM2 binds Lipopolysaccharides (LPS) (Daws et al., 2003), phospholipids (Wang et al., 2015), HDL (Yeh et al., 2016), LDL, APOE (Atagi et al., 2015; Bailey et al., 2015; Yeh et al., 2016), CLU (Yeh et al., 2016), apoptotic neurons (Hsieh et al., 2009), and Aβ (Zhao et al., 2018b) all of which activate signaling pathways (Fig. 3). TREM2 conveys intracellular signals through TYROBP, an adaptor protein that contains functional docking sites known as ITAMs. Upon TREM2 activation through ligand binding, the ITAMs on TYROBP are phosphorylated and recruit SYK. SYK activates the PI3K–AKT pathway and also phosphorylates the adaptor LAT (linker for activation of T-cells family member 1), which recruits other signaling adaptors including PLCγ.

PLCγ degrades PIP3 into IP3, which creates an efflux of Ca2+ (Colonna and Wang, 2016; Peng et al., 2010; Wang et al., 2015) (Fig. 3).

Unlike the signaling cascade triggered by ligand activated TREM2 (Fig. 3), the biological role of sTREM2 is not well understood. It has been proposed, however, that it either acts as a decoy receptor opposing full-length TREM2 (Zhong et al., 2017) or has another still unidentified function. In cell culture, at least, sTREM2 promoted survival of bone marrow-derived macrophages (BMDM) (Wu et al., 2015), yet failed to rescue phagocytosis in TREM2-deficient BMDM cells (Xiang et al., 2016).

A well-established function of TREM2 is the regulation of cell proliferation. Knockdown of TREM2 in primary microglia leads to a reduction in cell number (Zheng et al., 2016) and *TREM2* deficiency inhibits myeloid cell population growth in response to traumatic brain injury (Saber et al., 2017) and aging (Poliani et al., 2015). Expression of *TREM2*, even at a normal level, may also impact the proliferation of endothelial cells. Recently, Carbajosa et al. investigated the impact of *TREM2* deficiency, in brain of young and aged mice using RNA-seq, and found a disruption of gene networks related to endothelial cells that is more apparent in younger than in older mice. They suggested that the absence of TREM2 in microglia influences endothelial gene expression, which may link immune response and brain vascular disease as an underlying factor in AD pathogenesis (Carbajosa et al., 2018). Microglia survival in the context of *TREM2* expression has been also linked to CSF-1-CSF-1R pathway, which is primarily active in conditions of reactive microgliosis (Chitu and Stanley, 2006) and affects Aβ clearance (Mitrasinovic et al., 2003). Since it has been demonstrated that, that TREM2 signaling, via TYROBOP, synergizes with CSF-1R signaling to promote survival of macrophages (Otero et al., 2009), a similar mechanism can be involved in microglial survival as well. A recent study by Wang et al.

demonstrating that TREM2-deficient microglia exhibited reduced survival at low CSF-1 concentrations support the role of CSF-1R signaling in microglia survival (Wang et al., 2015). In conjunction with decreased survival, TREM2-deficient microglia demonstrate a reduced chemotactic capacity. Migration of microglia towards injected apoptotic neurons as well as towards sites of laser-induced damage was also reduced in *Trem2*-/- mice (Mazaheri et al., 2017).

### 3.4.3 TREM2 Variants and Neurodegeneration

Rare biallelic mutations that result in loss of function of TREM2 cause Nasu–Hakola disease (Paloneva et al., 2002) (NHD) and in some cases Fronto temporal dementia (FTD)(Cuyvers et al., 2014; Guerreiro et al., 2013b). NHD is manifested with bone cysts and early onset of neurodegeneration. Brain pathology is comprised of axonal degeneration, white matter loss, cortical atrophy, increased microglia density, and astrogliosis (Klunemann et al., 2005; Sasaki et al., 2015; Satoh et al., 2011). The variants associated with NHD and FTD can be a result of coding mutations in the transmembrane domain (D134G, K186N) (Paloneva et al., 2002), ectodomain (Y38C, T66M) (Giraldo et al., 2013; Guerreiro et al., 2013b; Le Ber et al., 2014), early stop codons (Paloneva et al., 2003; Soragna et al., 2003), or mutations in a splice site (Chouery et al., 2008; Numasawa et al., 2011). Considering the role of TREM2 in microglial function, variants in *TREM2* can be part of functional networks involved in multiple neurodegenerative disorders. Numerous studies have evaluated the effect of TREM2 on risk for AD (discussed in section 4.2), frontotemporal dementia (FTD) (Thelen et al., 2014), amyotrophic lateral sclerosis (ALS) (Cady et al., 2014; Chen et al., 2015a; Rayaprolu et al., 2013), Lewy body dementia (Walton et al., 2016), posterior cortical atrophy (Carrasquillo et al., 2016), Creutzfeldt-Jakob disease (Slattery et al., 2014), progressive supranuclear palsy (Rayaprolu et al., 2013), Parkinson's disease (Rayaprolu et

al., 2013), ischemic stroke (Rayaprolu et al., 2013), and multiple system atrophy (Chen et al., 2015b).

TREM2 R47H variant was identified as a risk factor for AD independently by 2 groups that Analyzed European and North American (Guerreiro et al., 2013a) and Icelandic cohorts (Jonsson et al., 2013). Later in the same year, Cruchaga et al. demonstrated that TREM2-R47H variant is associated with a higher level of tau and phospho-tau in CSF (Cruchaga et al., 2013). The initial findings for TREM2- R47H variant were confirmed by other groups (Hooli et al., 2015; Lill et al., 2015). Sims et al reported, in addition, a significant association of TREM2-R47H and -R62H variants with LOAD and showed that even after removing these variants from the analysis the association remained significant suggesting the presence of other *TREM2* risk variants (Sims et al., 2017). TREM2 pW191X and pL211P variants were recently identified associated with LOAD in African American cohort but the variants shown to confer AD risk in Caucasians were extremely rare (Jin et al., 2015). Similarly, Yu et al. reported several new *TREM2* variants in Han Chinese population, however, none of them was significantly associated with AD risk and TREM2 R47H variant was not detected in this population (Yu et al., 2014).

In addition to TREM2, another gene in the same cluster - *TREML2* was also examined for association with LOAD. In a meta-analysis study of 36,306 human CSF samples, the missense variant rs3747742 of TREML2 seemed to confer a protective effect against AD (Benitez et al., 2014). A complete list of so far identified TREM2 variants - can be found on the ALZ forum website https://www.alzforum.org/.

Recently, Kober et al. demonstrated that NHD variants impact protein stability and decrease TREM2 cell surface expression, while AD variants impact TREM2 ligand binding (Kober et al., 2016) (Fig. 3). When mapping the electrostatic surface of TREM2, Kober et al.

identified a large basic patch that was not present in other members of the TREM family (Kelker et al., 2004) indicating a unique role for this domain in TREM2 function. Many of the AD-related mutations can be found near or within this basic region of TREM2. Both R47H and R62H decrease the size of the basic patch and reduce binding properties resulting in a loss of function, while T96K increases the size corresponding to a gain of function (Kober et al., 2016).

## 3.5 APOE, TREM2, and AD

### 3.5.1 APOE and AD

Studies in mice have suggested that a relationship between APOE isoform and Aβ metabolism was involved in AD pathogenesis. Considering APOE as an Aβ binding protein (Strittmatter et al., 1993), many of the early *in vitro* studies tested Aβ binding to APOE and other apolipoproteins (Ghiso et al., 1993; Koldamova et al., 2001; LaDu et al., 1994; Manelli et al., 2004; Wisniewski et al., 1993). While the binding was repeatedly confirmed, none of those studies provided any indication that the risk for AD was dependent on differences in APOE-Aβ binding.

APOEε4 is the major genetic risk factor for LOAD (Corder et al., 1993; Schmechel et al., 1993). Inheritance of a single copy of APOEε4 increased AD risk by ~3 fold, and the inheritance of two copies increases risk by ~12 fold (Holtzman et al., 2011). Compared to AD patients who are not *APOEε4* carriers, AD patients who carry at least one *APOEε4* allele exhibit an earlier disease onset, faster disease progression, and increased brain atrophy (Agosta et al., 2009; Corder et al., 1993; Cosentino et al., 2008). Importantly, however, homozygous *APOEε3* AD patients still account for the majority of LOAD cases, suggesting that additional genetic or environmental

factors are relevant to disease progression. The question, however, if APOE4 isoform is deleterious or less protective, remains unanswered, with evidence supporting both claims (Kanekiyo et al., 2014). While the global deletion of APOE is associated with a drastic reduction of compact amyloid plaques in brain of APP expressing mice (Bales et al., 1997; Fitz et al., 2015; Holtzman et al., 2000; Holtzman et al., 1999) the phenotypes of those mice have not been extensively examined to improve our understanding of the role of APOE in the development of AD. Recent studies provided new insight on the role of microglia in the phenotype of APP expressing mice with global deletion of mouse *Apoe* – their reduced microglia recruitment and altered plaque morphology indicated a role beyond APP processing and deposition (Ulrich et al., 2018).

Using mouse models for AD, it has been established that human APOE differentially impacts Aβ deposition in a dose-dependent, as well as isoform-specific manner with APOE4 > APOE3 > APOE2 (Bales et al., 2009; Castellano et al., 2011; Fitz et al., 2012; Kim et al., 2011). Interestingly, recent publications implicated APOE as essential for plaque formation during early seeding stages of Aβ deposition (Huynh et al., 2017; Liu et al., 2017). Utilizing APOE3 or APOE4 inducible mice Liu et al. have shown that APOE4 but not APOE3 increases amyloid pathology when expressed during the early seeding stages of amyloid deposition (Liu et al., 2017). This impact was not seen in APOE3 mice and was lost when APOE4 was expressed only in later stages of plaque development, indicating APOE4 has the greatest impact on amyloid deposition during the initial seeding stages (Liu et al., 2017). By dosing with anti-sense oligonucleotides from birth, Huynh et al. showed a reduction in Aβ deposition in APOE4 mice, whereas there was no effect when the treatment began after the onset of Aβ plaque formation (Huynh et al., 2017).

Data from animal models suggest that APOE affects also Aβ clearance in an isoform-dependent manner (Castellano et al., 2011; Fitz et al., 2012), and the lipidation of the protein seems

to be of importance (Liao et al., 2018). There are two major Aβ clearance pathways in the brain: receptor-mediated clearance via microglia (Clayton et al., 2017), and astrocytes (Acosta et al., 2017), BBB (Chakraborty et al., 2016) or through interstitial fluid drainage pathways (Bakker et al., 2016). Cell facilitated clearance mechanisms are likely to be, in part, mediated by APOE and APOE receptors. APOE receptor-mediated internalization of Aβ seems to be most functional in microglia (El Khoury and Luster, 2008) and astrocytes (Koistinaho et al., 2004). ABCA1 functions to alter the lipidation state of APOE in the brain which consequently impacts Aβ fibrillization (reviewed in (Koldamova et al., 2010, 2014)). In APP transgenic mice, targeted disruption of Abca1 decreases APOE lipidation and increases amyloid deposition (Hirsch-Reinshagen et al., 2005; Koldamova et al., 2005a; Wahrle et al., 2005). Conversely, overexpression of Abca1 increases APOE lipidation and decreases amyloid deposition (Wahrle et al., 2008).

A second hallmark of AD, aside from Aβ deposition, is the formation of tau tangles. Early studies demonstrated isoform-specific binding of APOE to human tau *in vitro*, suggesting an isoform-specific impact on tau pathology (Fleming et al., 1996; Strittmatter et al., 1994). Recently, APOE4 has been shown to exacerbate tau-mediated neurodegeneration, while the absence of APOE altogether is protective (Shi et al., 2017). Using a P301S tauopathy mouse model on human APOE KI or APOE KO background Shi et al. found no changes at 3 months, but by 9 months the P301S/E4 mice had significantly more brain atrophy than P301S/E2, or P301S/E3, and that APOE KO mice were largely protected from this effect (Shi et al., 2017).

As a result of the relationship between APOE and AD, it has been suggested that targeting APOE may have a therapeutic potential for AD (reviewed in (Yamazaki et al., 2016)). There are two potential therapeutic interventions: regulation of APOE quantity and modification of APOE properties. The former entails the upregulation of APOE levels via LXR and PPARγ agonists

(Jiang et al., 2008b; Koldamova et al., 2005b; Mandrekar-Colucci et al., 2012; Skerrett et al., 2014; Vanmierlo et al., 2011). The administrations of RXR agonist, bexarotene, was shown to increase APOE level and its lipidation resulting in a reversal of cognitive deficits observed in APP mouse models (Boehm-Cagan and Michaelson, 2014; Cramer et al., 2012; Fitz et al., 2013; Mounier et al., 2015). However, bexarotene effect on Aβ deposition in AD mouse models is controversial (Price et al., 2013; Tesseur et al., 2013; Veeraraghavalu et al., 2013). Another therapeutic approach is the use of specific antibodies to alter the protein levels of APOE (Kim et al., 2012). A recent study demonstrated that using an anti-APOE antibody that recognizes human APOE isoforms, targets and specifically binds to non-lipidated forms making it effective in reducing amyloid burden in APP transgenic mice (Liao et al., 2018). The modulation of APOE properties by structural modification through small molecule correctors (Brodbeck et al., 2011; Chen et al., 2011), or by inhibiting APOE-Aβ interactions with small molecule inhibitors (Kuszczyk et al., 2013; Pankiewicz et al., 2014) have also been proposed for therapeutic interventions in AD.

## 3.5.2 TREM2 and Alzheimer's Disease

As the resident immune cells of the brain, microglia continuously monitor the brain and respond to damage-related signals that perturb the environment, (reviewed in (Butovsky and Weiner, 2018)). The proposed function of microglial recruitment is to form a physical barrier that encapsulates neurotoxic Aβ, thereby restricting plaque growth and containing any neurotoxic effects (Wang et al., 2016; Yuan et al., 2016). Deficiency in TREM2 or its adaptor protein TYROBP prevents myeloid cell accumulation around Aβ plaques in a dose-dependent manner (Jay et al., 2015; Ulrich et al., 2017; Wang et al., 2015; Wang et al., 2016; Yuan et al., 2016). In AD patients, heterozygous for the R47H or R62H variants, there are fewer plaque-associated microglia

than in those with nonmutant TREM2 (Krasemann et al., 2017). This lack of microglial response in R47H carrying patients has also been shown to increase plaque-associated neuronal dystrophy and reduced microglial coverage (Yuan et al., 2016).

Multiple groups have examined the effects of *Trem2* deficiency on amyloid pathology with different results based on the mouse model used, as well as the stage of amyloid pathology. Wang et al. examined the effect of *TREM2* deficiency in 5XFAD and found that at 8.5 months there is a significant increase of amyloid load in the hippocampus but not in the cortex (Wang et al., 2015). Using 5xFAD mice at an earlier age (4 months) the same group found that Aβ accumulation was similar in TREM2 deficient and TREM2-WT 5XFAD mice (Wang et al., 2016). Likewise, Jay et al. utilizing APPPS1-21 mice found no change in the amyloid pathology in the cortex and a significant decrease in the hippocampus in Trem2-/- mice at 4 months (Jay et al., 2015). Interestingly, the same AD mouse model, when examined at 8 months, showed an increased Aβ staining in the cortex and no changes in the hippocampus of Trem2-/- mice (Jay et al., 2017). Jay et al. concluded that in the early stages of amyloid deposition (2-month cortex, 4-month hippocampus) *Trem2* deficiency reduces both plaque number and size and at later stages (8-month cortex) it increases plaque size and area. Yuan et al. showed that *Trem2* deficiency resulted in an increase of diffuse amyloid plaques with longer and more branched amyloid fibrils thus, covering a larger surface area (Yuan et al., 2016). They conclude that lack of TREM2 may disrupt the microglia barrier around the plaques that regulates amyloid compaction and has a protective role (Fig. 4).

Recently transgenic mouse models expressing TREM2 R47H variant have been generated that demonstrate a diminished response to amyloid deposition exemplified by the reduced cell

number and activation of microglia surrounding the plaques (Cheng-Hathaway et al., 2018; Song et al., 2018). These data suggest that TREM2 R47H is loss a of function variant.

In regard to sTREM2, an early study demonstrated that sTREM2 levels were reduced in the CSF of AD patients (Kleinberger et al., 2014). However, emerging evidence suggests the opposite: sTREM2 is increased in AD and is positively correlated with tau but not Aβ42 levels (Heslegrave et al., 2016; Piccio et al., 2016; Rauchmann et al., 2018; Suarez-Calvet et al., 2016). sTREM2 has also been shown to be impacted by TREM2 variants, in which R47H carriers had significantly higher, and T96K, L211P, as well as W199X had significantly lower sTREM2 levels than TREM2 WT controls (Piccio et al., 2016). A recent meta-analysis study comprising of 17 reports and 1,593 patients found sTREM2 levels increased in the early course of AD progression, indicating its potential use as a biomarker for AD progression (Liu et al., 2018).
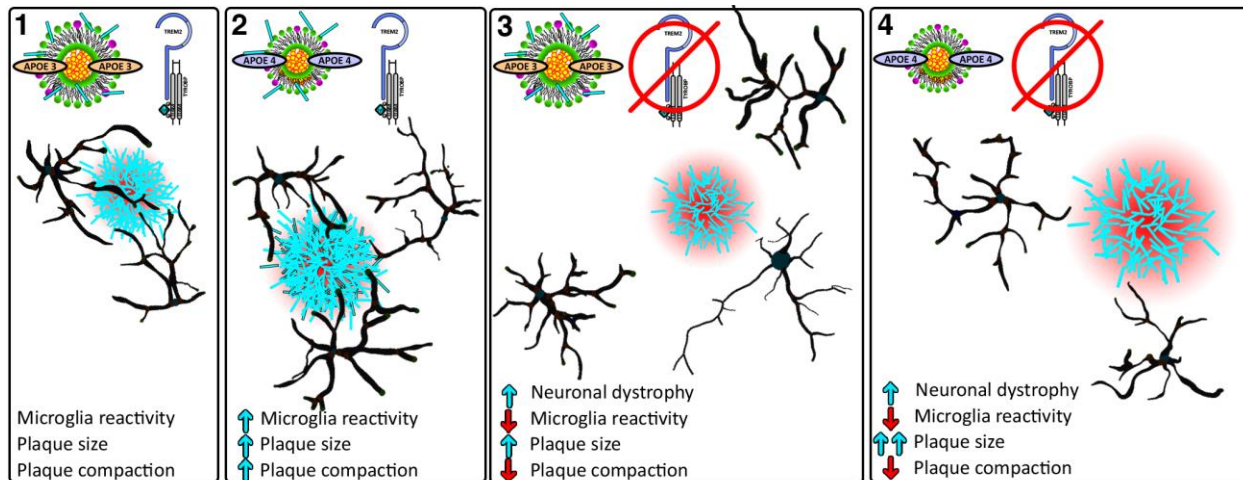


**Figure 4. Schematic illustration of the relationship between APOE and TREM2.**
Microglia in black cluster around amyloid deposits which impacts plaque morphology and the microenvironment surrounding the plaques. Boxes 1 and 2 illustrate TREM2 in an active state and shown an increase in plaque size, compaction, and microglia reactivity in APOE4 compared to APOE3. Microglia which are TREM2 deficient (boxes 3 and 4) fail to contain the plaques allowing them to become more diffuse and increase the surrounding dystrophic area. Arrows are relative to APOE3, TREM2 active (box 1).

### 3.5.3 APOE, TREM2, and AD

APOE$\varepsilon$4 and TREM2-R47H variant were identified as independent risk factors for LOAD (Corder et al., 1993; Guerreiro et al., 2018; Jonsson et al., 2013; Schmechel et al., 1993). Interestingly both APOE and TREM2 are part of a large group of genes associated with LOAD risk that are expressed in glia cells and related immune response (Villegas-Llerena et al., 2016). Several groups have shown that TREM2 binds to APOE using TREM2-Fc fusion pulldown (Bailey et al., 2015), dot blot assays (Atagi et al., 2015), and high throughput protein microarrays (Yeh et al., 2016) (Fig. 4). Atagi et al. showed that APOE increases the phagocytosis of apoptotic neurons via TREM2 pathway and that TREM2 R47H variant was shown to reduces TREM2 affinity to bind APOE (Atagi et al., 2015). Interestingly APOE lipidation appears to enhance its binding to TREM2 and microglia are more efficient at A$\beta$ uptake when A$\beta$ forms a complex with LDL, APOE, or CLU (Yeh et al., 2016). In contrast, the same study showed that TREM2-deficient microglia have a reduced uptake of A$\beta$-APOE or A$\beta$-LDL complexes (Yeh et al., 2016). A recent study by Jendresen et al. suggests that amino acids 130-149 of human APOE contain the binding site for TREM2, and that there is an APOE-isoform-dependent binding to TREM2 (Jendresen et al., 2017). Although other groups have shown no APOE isoform differences in binding (Atagi et al., 2015; Bailey et al., 2015), possibly due to the sensitivity of binding assays and the lipidation state of APOE.

Microglia as resident macrophages in CNS account for the immune response in the brain, therefore impaired microglia function through either *TREM2* deficiency or APOE isoform-specific differences have significant implications. Consistently TREM2 haplodeficient, knockout, or the TREM2 R47H variant, have shown a dose-dependent reduction in microglial activation surrounding amyloid plaques resulting in more diffuse and less compact amyloid plaques. In

agreement with these results, overexpression of TREM2 and increasing TREM2 protein level cause a significant reduction in plaque area, plaque-associated neuronal dystrophy, and amelioration of cognitive deficit in 5xFAD mice (Lee et al., 2018). Recent reports identified novel microglia type associated with neurodegenerative diseases (also called disease associated microglia or DAM) characterized by a specific transcriptional profile with both Apoe and Trem2 part of this program (Keren-Shaul et al., 2017; Krasemann et al., 2017). Accordingly, during the progression of neurodegeneration in APP transgenic mice and possible AD brain microglia transcriptome convert from homeostatic to disease associated profile. Interestingly, in APP mice that are either TREM2 or APOE deficient microglia fail to convert from a homeostatic into a fully activated state (Keren-Shaul et al., 2017; Krasemann et al., 2017). One explanation for these findings may be the significantly decreased plaque load observed in APP transgenic and APOE or TREM2 knockout mice reported by Krasemann et al. (Krasemann et al., 2017). Another explanation is that TREM2 and possibly APOE deficiency prevent microglia conversion from homeostatic to disease oriented state thus impairing essential defense functions such as chemotaxis, proliferation, phagocytosis, and survival (Keren-Shaul et al., 2017; Krasemann et al., 2017; Mazaheri et al., 2017; Ulrich et al., 2018; Wang et al., 2015).

In the end, we can conclude that during the last decade significant progress has been made towards understanding the biology of APOE and TREM2, as well as the biochemical aspects of their interactions and their impact on AD pathogenesis. And although there are still many unanswered questions our knowledge of the most significant risk factors of AD will be soon implemented in successful diagnostic and therapeutic strategies against a devastating disease.

# 4.0 Trem2 Deficiency Differentially Affects Phenotype and Transcriptome of Human APOE3 and APOE4 Mice

Nicholas F Fitz[1†], Cody M Wolfe[1†], Brittany E Playso[1], Richard J Biedrzycki[1], Yi Lu[1], Kyong Nyon Nam[1], Iliya Lefterov[1]*, Radosveta Koldamova[1]*

[1] Department of Environmental & Occupational Health, University of Pittsburgh, Pittsburgh, PA, USA 15261

[†] These authors contributed equally

## 4.1 Abstract

**Background**: Alzheimer's Disease (AD) is a neurodegenerative disorder influenced by aging and genetic risk factors. The inheritance of *APOEε*4 and variants of Triggering Receptor Expressed on Myeloid cells 2 (*TREM2*) are major genetic risk factors for AD. Recent studies showed that APOE binds to TREM2, thus raising the possibility of an APOE-TREM2 interaction that can modulate AD pathology.

**Methods:** The aim of this study was to investigate this interaction using complex AD model mice - a crossbreed of Trem2[ko] and APP/PSEN1dE9 mice expressing human APOE3 or APOE4 isoforms (APP/E3 and APP/E4 respectively), and their WT littermates (E3 and E4), and

evaluate cognition, steady-state amyloid load, plaque compaction, plaque growth rate, glial response, and brain transcriptome.

**Results:** In both, APP/E3 and APP/E4 mice, *Trem2* deletion reduced plaque compaction but did not significantly affect steady-state plaque load. Importantly, the lack of TREM2 increased plaque growth that negatively correlated to the diminished microglia barrier, an effect most pronounced at earlier stages of amyloid deposition. We also found that *Trem2* deficiency significantly decreased plaque-associated APOE protein in APP/E4 but not in APP/E3 mice in agreement with RNA-seq data. Interestingly, we observed a significant decrease of *Apoe* mRNA expression in plaque-associated microglia of APP/E4/Trem2$^{ko}$ vs APP/E4 mice. The absence of TREM2, worsened cognitive performance in APP transgenic mice but not their WT littermates.

Gene expression analysis identified *Trem2* signature - a cluster of highly connected immune response genes, commonly downregulated as a result of *Trem2* deletion in all genotypes including APP and WT littermates. Furthermore, we identified sets of genes that were affected in TREM2- and APOE isoform-dependent manner. Among them were *Clec7* and *Csf1r* upregulated in APP/E4 vs APP/E3 mice, a result further validated by *in situ* hybridization analysis. In contrast, *Tyrobp* and several genes involved in the C1Q complement cascade had a higher expression level in APP/E3 versus their APP/E4 counterparts.

**Conclusions:** Our data demonstrate that lack of *Trem2* differentially impacts the phenotype and brain transcriptome of APP mice expressing human APOE isoforms. The changes probably reflect the different effect of APOE isoforms on amyloid deposition.

## 4.2 Keywords

*Trem2*, APOE, Transcriptomics, Microglia, Neuroinflammation, Alzheimer's disease, Amyloid plaques, Neurodegeneration, APP transgenic mice, RNA-sequencing

## 4.3 Background

The inheritance of ε4 allele of apolipoprotein E (APOE) is the major genetic risk factor for late-onset Alzheimer's disease (AD) (Corder et al., 1993; Saunders et al., 1993). APOE is an apolipoprotein which, in the central nervous system, is secreted by glia; it facilitates the transport of cholesterol and phospholipids between cells (Kanekiyo et al., 2014; Wolfe et al., 2018). GWAS have identified TREM2 missense variants that are related to AD risk, with the largest risk conferred by the loss of function R47H variant (Cruchaga et al., 2013; Guerreiro et al., 2013a; Jansen et al., 2019; Jonsson et al., 2013). TREM2 is a receptor of the innate immune system, expressed in mononuclear phagocytes, including microglia in brain (Colonna and Wang, 2016). The proteolytic cleavage of TREM2 generates soluble TREM2, which can be detected in CSF and has been proposed as a biomarker and shown to be increased in AD (Piccio et al., 2016; Suarez-Calvet et al., 2016). Recent data showed that APOE can bind to TREM2, thus raising the possibility of an APOE-TREM2 interaction affecting TREM2 signaling (Atagi et al., 2015; Bailey et al., 2015; Yeh et al., 2016). Interestingly, Jendersen et al. showed that while all three human isoforms of APOE bind TREM2, APOE4 exhibits diminished interaction when compared to APOE2 and APOE3 (Jendresen et al., 2017).

In AD, microglia are important for the phagocytosis of debris, clearance of Aβ, release of pro-inflammatory cytokines, and development of a plaque-associated barrier (Hansen et al., 2018). Recently, Keren-Shaul et al. identified a subset of microglia named "disease-associated microglia" (DAM) that accumulate in AD and other neurodegenerative diseases (Keren-Shaul et al., 2017). DAM are characterized by the upregulation of genes involved in lysosomal, phagocytic, and lipid metabolism pathways, including genes known as AD risk factors, such as *APOE* and *TREM2* (Deczkowska et al., 2018). Simultaneously with the upregulation of DAM, Keren-Shaul et al. detected a significant downregulation of the so-called "homeostatic microglial" genes (Keren-Shaul et al., 2017). Furthermore, genetic ablation of *Trem2* suppressed mouse *Apoe* expression and restored homeostatic microglial function in AD-model mice (Krasemann et al., 2017). This implicates TREM2 in the maintenance of the microglial response to amyloid pathology, further connecting APOE, TREM2, microglia function, and amyloid pathology. Loss of functional TREM2 in mice has been shown to increase plaque seeding, reduce plaque-associated microglia barrier, reduced plaque compaction, reduce the level of APOE in APP mice, and increased dystrophic neurites surrounding plaques (Jay et al., 2017; Jay et al., 2015; Parhizkar et al., 2019; Ulrich et al., 2014; Wang et al., 2016). The effect of TREM2 on amyloid deposition in AD mice is controversial, however, with some studies showing the lack of TREM2 increasing (Griciuc et al., 2019; Wang et al., 2015) and others decreasing the amyloid load (Jay et al., 2015; Krasemann et al., 2017). Interestingly though, increased soluble TREM2 has been shown to increase microglia survival, reduce amyloid plaque load, increase microglia clustering and phagocytic activity in AD model mice (Zhong et al., 2017).

While APOE and TREM2 are two major genetic risk factors for LOAD, surprisingly little is known about the interplay between these two, regarding amyloid deposition, microglial

phenotype or transcriptomic profile. In this study, we hypothesized that *Trem2* deletion would have a differential effect on the phenotype and transcriptome of APP and WT mice expressing human APOE3 or APOE4.

## 4.4 Results

### 4.4.1 *Trem2* Deficiency Worsens Cognitive Performance, Affects Plaque Compaction, and Impacts Microglia Recruitment in APP/E3 and APP/E4 Mice

To determine the impact of *Trem2* deficiency on AD-like phenotype we used APP/PSEN1dE9 mice expressing human *APOE3* or *APOE4* genes (referred to as APP/E3, APP/E3/Trem2$^{ko}$, APP/E4, and APP/E4/Trem2$^{ko}$). For all behavioral and histological analysis we tested the mice at an average age of 6.5 months when amyloid pathology is readily detectable in mice expressing either APOE isoform and we previously have shown significant cognitive differences between APP/E3 and APP/E4 mice (Fitz et al., 2013; Fitz et al., 2012). The controls were age and gender-matched non-APP transgenic littermates expressing human *APOE3* or *APOE4* (referred to as E3, E3/Trem2$^{ko}$, E4, and E4/Trem2$^{ko}$) (Fig. 5A). To reveal differences in cognitive behavior, we used novel object recognition and contextual fear conditioning paradigms that demonstrated both factors - *Trem2* deficiency and APOE isoform, significantly affected cognition in APP mice, but not in their non-APP transgenic littermates (Fig. 5B). While *Trem2* deficiency was a significant factor in the behavioral performance, APP/E4 mice performed at the lower limits of both tasks and thus we were unable to observe a significant reduction in their Trem2$^{ko}$ counterparts. The deterioration of memory was hippocampal-based as there was no

significant difference during the amygdala-dependent cued phase (Fig. 6A-B). There were no

changes during the learning phase or novel phase of fear conditioning as well as no significant

change in locomotor activity between genotypes (Fig. 6C-H).
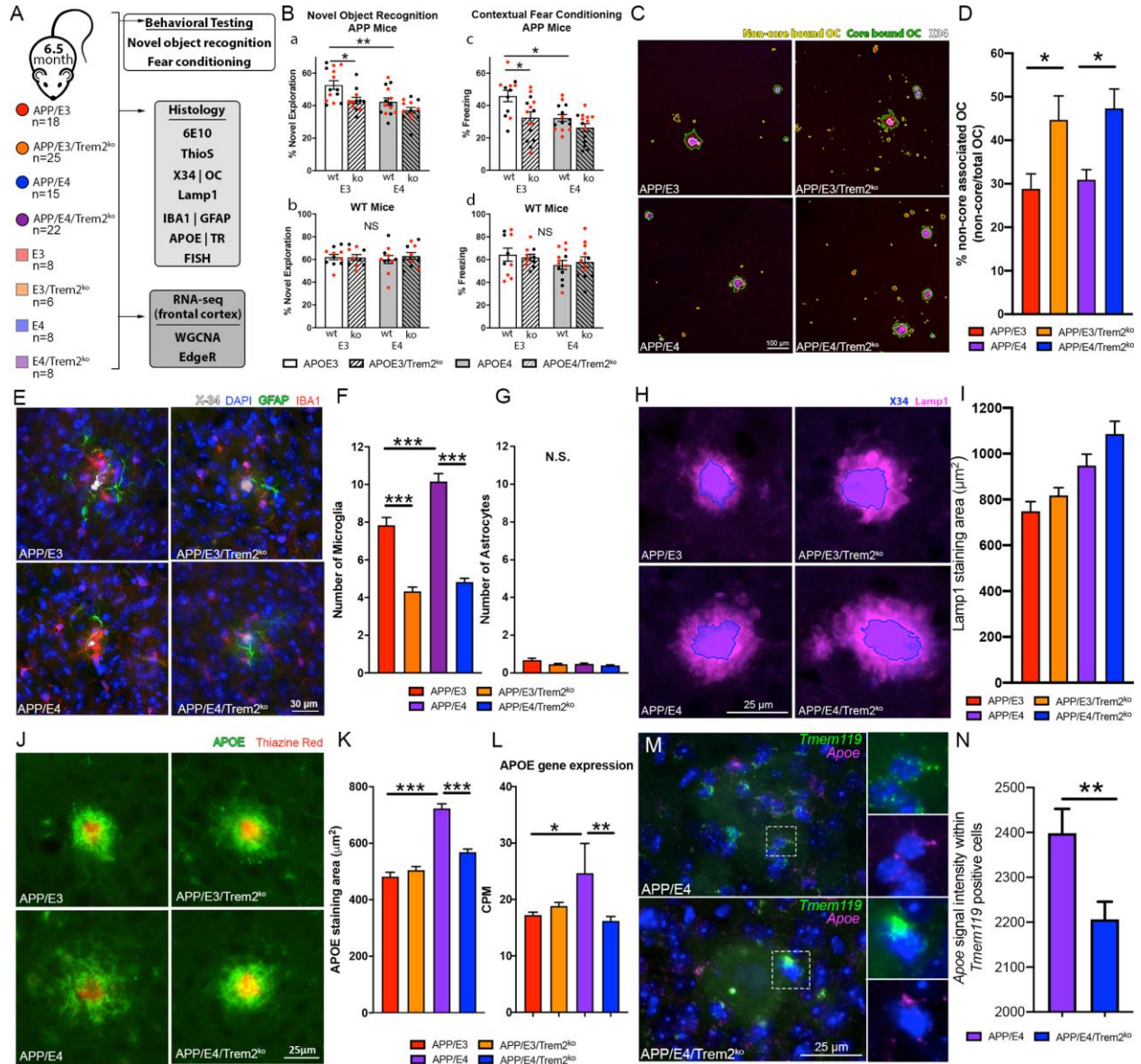


**Figure 5. *Trem2* deficiency impacts cognition, plaque compaction, and microglia recruitment in APP/E3 and APP/E4 mice.**
(A) Schematic timeline showing groups and experimental procedures of 6.5-month-old mice used for behavioral, histological, and transcriptional analysis. (B) Novel object recognition (NOR), and Contextual fear conditioning. Analysis by two-way ANOVA showed no interaction between APOE isoform and Trem2 status and a significant main effect of APOE isoform ($F_{(1, 49)} = 13.28$, $p<0.01$) and Trem2 status ($F_{(1, 49)} = 11.06$, $p<0.01$) for NOR (a, b), and Contextual fear conditioning (c, d) APOE isoform effect ($F_{(1, 50)} = 11.39$, $p <0.01$) and Trem2 status ($F_{(1,50)} = 10.86$, $p<0.01$). ** $p<0.01$; * $p<0.05$, Sidak multiple comparisons test. n = 6 -14 mice per group. For APP mice n = 6-7 mice/genotype/sex (12-14 mice/genotype). For non-APP mice, n = 4-7 mice/genotype/sex (8-14 mice/genotype).

54

On the graphs, red symbols indicate female and black symbols indicate male mice. (C) Representative images of X34 and OC labeled amyloid deposits showing core-bound and non-core bound OC. (D) Bar plot depicting the ratio of non-core bound OC to total OC. n = 15-26 mice per group. (E) Representative images of glial cells (Iba1+ microglia and GFAP+ astrocytes) recruited to amyloid plaques. (F) Bar plots depicting the number of microglia nuclei within 60 µm of plaque border. (G) Bar plots depicting the number of astrocyte nuclei within 60 µm of plaque border. n = 80-120 plaques from 6 mice per group. (H) Representative images of X34 and LAMP1 label showing neuronal dystrophy surrounding amyloid deposits. X34 is shown as a blue region of interest defined by NIS elements thresholding. (I) Bar plot depicting the area of plaque-associated LAMP1 staining. Analysis by two-way ANOVA showed no interaction between APOE isoform and Trem2 status and a significant main effect of APOE isoform ($F_{(1, 476)} = 25.41$, p<0.0001) and Trem2 status ($F_{(1, 476)} = 4.99$, p<0.05) for LAMP1 area. Sidak multiple comparison test found no difference in plaque-associated LAMP1 staining area between APP/E3 vs APP/E3/Trem2$^{ko}$ or APP/E4 vs APP/E4/Trem2$^{ko}$. n = 120 plaques from 4 mice per group. (J) Representative images of plaque-associated APOE (green) and TR (red) staining to visualize compact amyloid plaques. (K) Bar plots showing the area of APOE staining that surrounds TR positive amyloid plaques. n = 874-2719 plaques from 4-6 mice per group. (L) Bar plots depicting *Apoe* gene expression as identified by RNA-seq, which closely follows the genotypic pattern of plaque-associated APOE protein levels. For histological analyses, one-way ANOVA was used followed by Tukey's multiple comparison test. (M) Representative images of FISHanalyses of gene expression near amyloid plaques (*Tmem119* – green, *Apoe* – Pink, Nuclei – Blue). (N) Bar plot depicting the *Apoe* gene expression within *Tmem119*-positive microglia cells. The intensity of *Apoe* FISH signal was normalized to the number of *Tmem119*-positive microglial cells. n = 279-313 microglia per group. Bars represent mean ± SEM, with all red bars = APP/E3, orange = APP/E3/Trem2$^{ko}$, purple = APP/E4, and blue = APP/E4/Trem2$^{ko}$. *** p<0.001; ** p<0.01; * p<0.05.

The examination of total amyloid (6E10, ThioS, X34, and OC staining) in cortex and hippocampus of the same 6.5 month mice assessed for cognitive changes revealed an effect of APOE isoform but no TREM2 effect (Fig. 7A-G) - a result that was confirmed by ELISA (Fig. 6I-J). To assess the proportion of compact to diffuse plaques we used X34 staining for compact amyloid and OC antibody that binds protofibrilar deposits (Kayed et al., 2007). As visible from Fig. 7I-J, OC/X34 ratio was increased in Trem2$^{ko}$ mice indicating reduced plaque compaction in both APOE isoforms caused by *Trem2* deletion. The assessment OC outside dense amyloid core (X34), determined that *Trem2* deletion significantly increased the percent of non-core bound OC (Fig. 5C-D, Fig. 7H). Therefore, lack of *Trem2* did not affect total amyloid coverage but reduced plaque compaction and increased the presence of diffuse deposits which have not been sequestered into a dense core amyloid plaque.
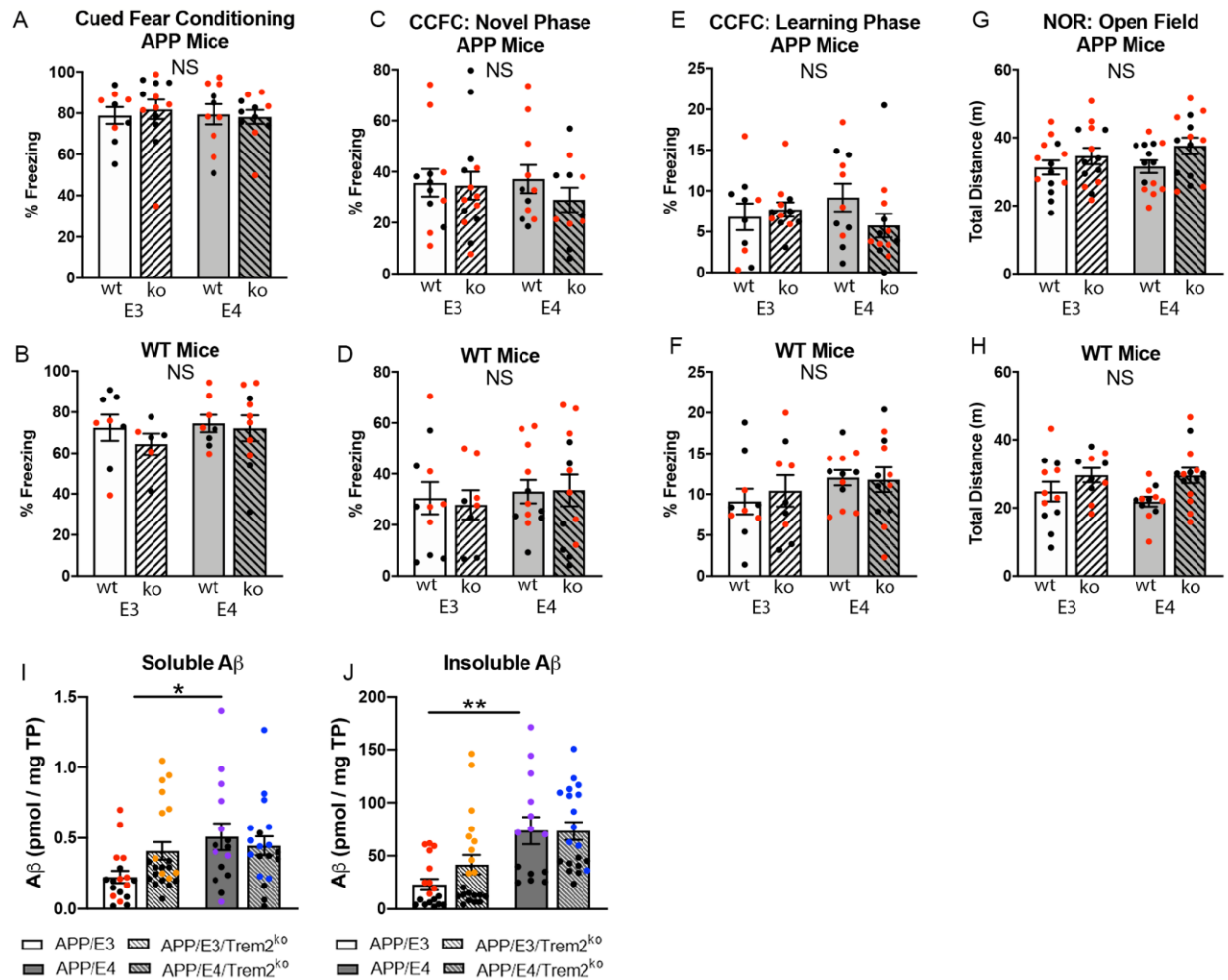
**Figure 6. No significant differences in locomotor activity, learning during novel object recognition and fear conditioning, and Aβ ELISA, as a result of *Trem2* deletion.**
Cued fear conditioning in APP mice (A & B) and all behavioral analysis for wild-type controls showed no significant effect of APOE or Trem2. There was no significant difference in percent freezing during the novel phase (C & D) or learning phase (E & F) of the contextual-cued fear conditioning (CCFC) for all experimental groups assessed. There was also no significant difference in total distance (m) traveled during the Open Field phase of NOR in APP/E3, APP/E4, APP/E3/Trem2[ko], and APP/E4/Trem2[ko] mice (G) or wild-type controls (H). n = 6-14 mice per group. For APP mice n = 6-7 mice/genotype/sex (12-14 mice/genotype). For non-APP mice, n = 4-7 mice/genotype/sex (8-14 mice/genotype). Analysis of cortical soluble Aβ (I) and cortical insoluble Aβ (J) ELISA levels by two-way ANOVA did not show an interaction between main factors: APOE and Trem2. There was a main effect of APOE isoform but not Trem2 status. Sidak multiple comparisons test showed statistical significance between APP/E3 and APP/E4 mice. n = 4-22 mice per group (equal males and females). On the graphs, colored symbols indicate female and black symbols male mice.

To investigate if *Trem2* deficiency affects the number of glial cells recruited to amyloid plaques, brain sections were stained with IBA1 to label activated microglia and GFAP to label astrocytes (Fig. 5E-G). The lack of *Trem2* significantly reduced the number of microglia around

the plaques in both APP/E3 and APP/E4 mice (Fig. 5F). Importantly, there was significantly more activated microglia in APP/E4 mice when compared to APP/E3, possibly reflecting the more advanced brain pathology of those mice. However, we did not find any difference between microglia numbers of APP/E3/Trem2[ko] vs APP/E4/Trem2[ko] mice suggesting that *Trem2* deletion blocks the conventional microglia response. Interestingly, there were very few astrocytes when compared to the number of microglia and their quantity was not significantly affected by *Trem2* deficiency (Fig. 5G). To investigate if *Trem2* deficiency affects plaque-associated neuronal dystrophy we used immunostaining for LAMP1, a lysosomal protein enriched in dystrophic neurites (Condello et al., 2011b; Condello et al., 2015). Analysis by two-way ANOVA demonstrated main effects of APOE and *Trem2* deficiency but no significant post hoc effect between Trem2[ko] mice and their WT counterparts (Fig. 5H-I).

Next, we determined the impact of *Trem2* deficiency on the level of APOE protein within the vicinity of amyloid plaques. We found that there was significantly more plaque-associated APOE in APP/E4 vs APP/E4/Trem2[ko] mice, but *Trem2* deficiency did not impact APOE level in APP/E3 mice (Fig. 5J-K). This result correlated to the *Apoe* mRNA expression, as identified by RNA-seq. As shown on Fig. 5L, the lack of *Trem2* significantly affected *Apoe* expression level only in APP/E4 and not in APP/E3 mice or in their WT littermates (Fig. 14B).

To determine the effect of *Trem2* deletion on *Apoe* expression in microglia, we used in situ hybridization (FISH) to compare APP/E4 and APP/E4/Trem2[ko] mice. Microglia were identified using the microglia-specific marker *Tmem119*. Our data demonstrated that *Apoe* mRNA expression is significantly higher in microglia surrounding amyloid plaques in APP/E4 compared to APP/E4/Trem2[ko] thus, validating the RNA-seq data (Fig. 5M-N). We conclude that the absence of *Trem2* similarly impairs microglia recruitment to plaques
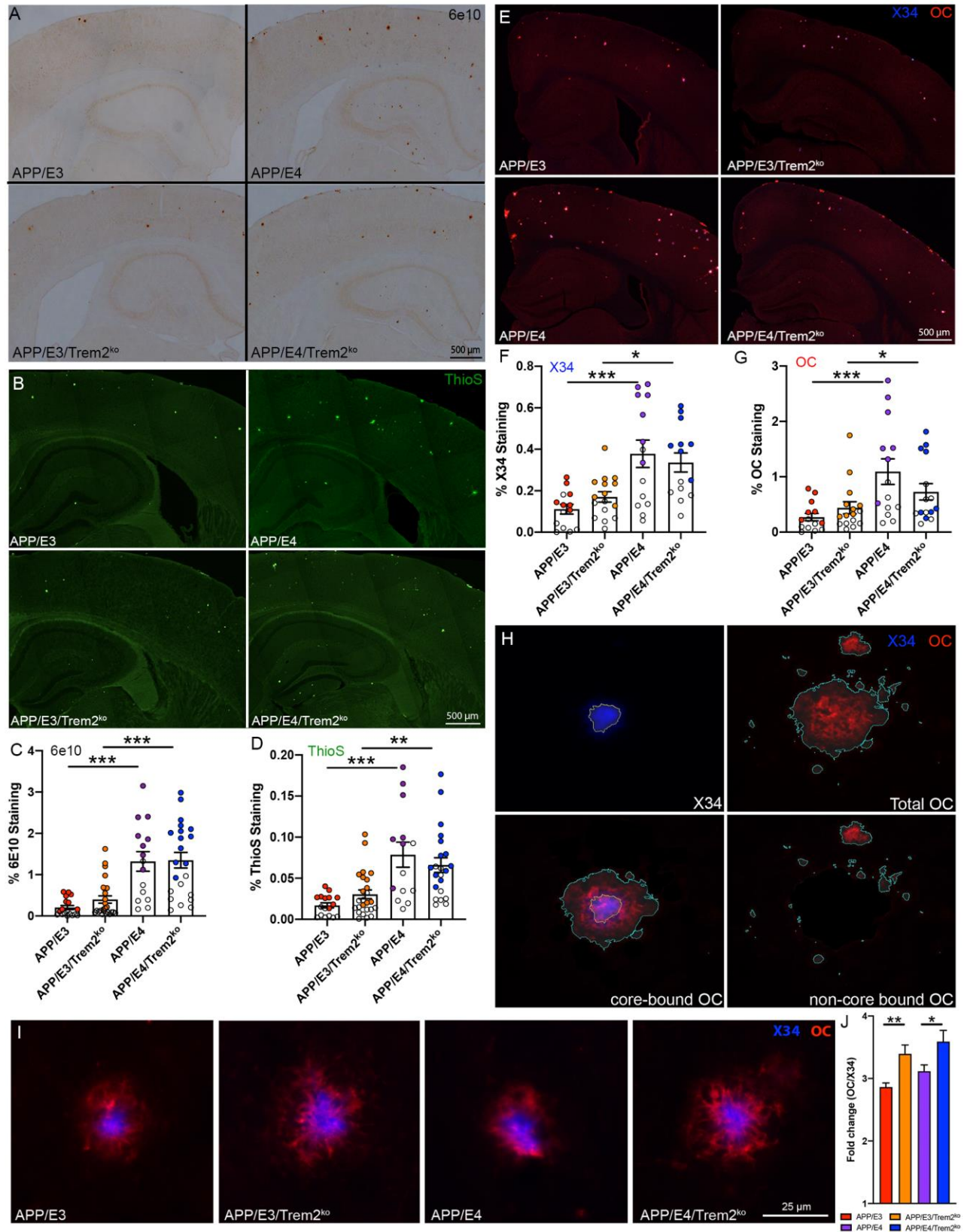
**Figure 7. The absence of Trem2 similarly impacts plaque diffusivity but has no effect on steady-state amyloid load.**
(A) Representative images of 6E10 anti-Aβ immunostaining showing both diffuse and compact plaques (4X magnification). (B) Representative images of ThioS staining showing compact plaques (4X magnification). (C) 6E10-positive plaques were analyzed by two-way ANOVA showing no interaction between Trem2 and APOE as factors. There was a significant main effect of APOE isoform (p<0.0001), but no effect of *Trem2* deficiency. Sidak multiple comparisons test shows no significant differences between APP/E3 and APP/E3/Trem2$^{ko}$ or between APP/E4 and APP/E4/Trem2$^{ko}$ mice. n = 22–30 mice per group (equal males and females). (D) ThioS staining confirmed 6E10 staining results with no significant main effect of Trem2 status or interaction. (E) Representative images of X34 and OC staining showing both diffuse and compact plaques (4X magnification). (F-G) X34 and OC staining confirmed 6E10 and ThioS staining results with no significant main effect of Trem2 status or interaction for either X34 or OC. Sidak multiple comparisons test showed a statistical significance between APP/E3 and APP/E4 mice (p<0.05). n = 14-16 mice per group (equal males and females). Colored dots represent female mice. (H) A visual depiction of what is counted as core-bound OC, total OC, and non-core bound OC used to generate data in Fig. 5D. (I) Representative images of individual X34 and OC labeled amyloid deposits. (J) Analysis of the OC/X34 ratio. n = 896-1569 plaques from 8 mice per group (equal male and female). For all histological analyses, one-way ANOVA was used followed by Tukey's multiple comparison test. Bars represent mean ± SEM. *** p<0.001; ** p<0.01; * p<0.05; NS, not significant*Trem2* deletion affects plaque growth depending on the stage of amyloid deposition

and increases neuronal dystrophy but has a differential effect on plaque-associated APOE protein

and mRNA levels in APP/E3 and APP/E4 mice.

## 4.4.2 *Trem2* Deletion Affects Plaque Growth Depending on the Stage of Amyloid Deposition

We showed that *Trem2* deficiency did not affect steady-state amyloid load (Fig. 7). Here

we evaluated whether the lack of *Trem2* affects the growth rate of individual amyloid plaques and

if this correlates to the surrounding microglia barrier. To reveal this, we employed an *in vivo*

labeling technique using the amyloid binding dye X04 followed by postmortem staining with TR

(Condello et al., 2011b). Intraperitoneally injected X04 readily crosses the blood-brain barrier

(Klunk et al., 2002) and remains bound to plaques for at least 90 days post injection (Condello et

al., 2011b). We injected the mice with X04 at 5.5 months of age and they were sacrificed 30 days

later, followed by TR staining of sectioned tissues (Fig. 8). Plaque growth was assessed using

high-resolution confocal images in Imaris to generate 3D volumetric renderings of amyloid

plaques by subtracting the volume of the plaque at the time of injection (X04 staining) from the

volume of the plaque at the time of sacrifice (TR staining). For each individual plaque, IBA1

staining for activated microglia was used to determine the plaque surface area that is not covered by microglia i.e. "exposed" (see Fig. 8H for details). As shown on Fig. 9A-B, *Trem2* deficiency significantly increased the growth of amyloid plaques in APP/E3 but not in APP/E4 mice. The examination of exposed plaque surface area follows the same pattern as plaque growth rate and is significantly affected only in APP/E3 mice (Fig. 9C&E). Subsequently, in all genotypes, we identified a very strong correlation between plaque growth rate and the exposed surface area suggesting that with the decrease of microglia barrier plaques grow faster (Fig. 9D). Our data also imply that *Trem2* deficiency may have a higher impact on plaque growth rate at earlier stages of amyloid deposition. Considering that amyloid deposition advances faster in APP/E4 mice and that there is a significant difference between the steady-state load of APP/E4 vs APP/E3 mice (Fig. 7), it is possible that TREM2 affects APP/E4 plaque growth rate at an earlier age. To test this, we performed the same experiment in younger mice injected with X04 at 3.5 and sacrificed at 4.5 months (Fig. 10). Interestingly, we found that in the younger group, *Trem2* deficiency significantly increased amyloid plaque growth only in APP/E4 mice in agreement with significantly reduced microglia barrier around the plaques (Fig. 10). At this age, we observed that in contrast to APP/E4, age-matched APP/E3 had very little compact amyloid with almost no detectable X04 deposits in APP/E3/Trem2$^{ko}$ mice that complicated the assessment of amyloid plaque growth in this genotype. Our data indicate that the absence of *Trem2* affects plaque growth depending on the stage of amyloid deposition and at different ages for APP/E3 and APP/E4 mice.
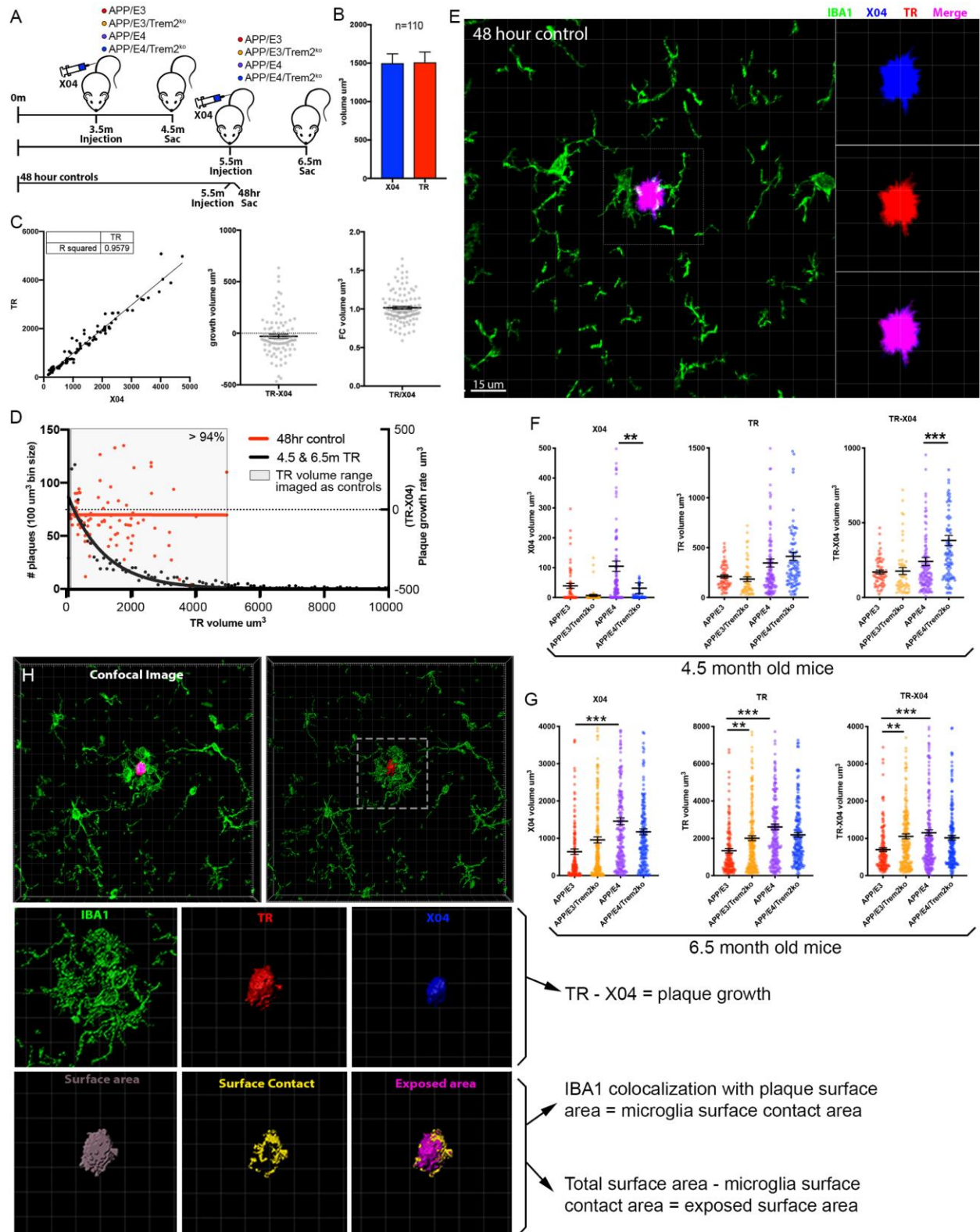
**Figure 8.** *In vivo* **plaque labeling using X04.**

(A) Schematic timeline of *in vivo* plaque labeling using an injection of X04 30 days prior to tissue harvesting. (B) Analysis of the plaques imaged from mice injected at 5.5 months and sacrificed 48 hours later shows no difference in

the volume of X04 and TR (n =110 plaques). (C) Plotting TR against X04 shows minimal deviation from the expected 1:1 ratio (R2 = 0.9579), a growth volume near 0, and FC near 1. (D) Scatterplot wherein red dots denote the plaque growth rate in the 48-hour control plaques (right axis), and the TR volume on the X axis. Black dots represent the entire experimental dataset binned by plaque size, with 94% of the plaques falling within the grey shaded box of the min and max values analyzed in the 48-hour control plaques. (E) Representative confocal imaging of an amyloid plaque 48 hours following X04 injection with IBA1 in green, X04 in blue, TR in red and the X04-TR merge in pink. Quantification of the volume of X04, TR and growth rate (TR-X04) in 4.5-month-old mice (F) and 6.5-month-old mice (G). (H) Representative images depicting how analysis metrics were derived. Confocal images were loaded into Imaris and 3D renderings generated for X04 and TR to calculate the volume. Plaque growth rate was calculated by subtracting the volume of the plaque at the time of *in vivo* labeling (X04, blue) from the volume of the plaque at the time of sacrifice (TR, red). 3D renderings were created to assess IBA1 (green) colocalization with the surface of the TR plaque. The plaque surface area contacted by microglia (yellow) is subtracted from the total surface area (grey) to quantify the exposed surface area of each plaque (purple, the surface area not covered by microglia). Analysis by one-way ANOVA followed by Tukey's multiple comparison test. Bars represent mean ± SEM. * $p<0.05$; ** $p<0.01$; *** $p<0.001$.
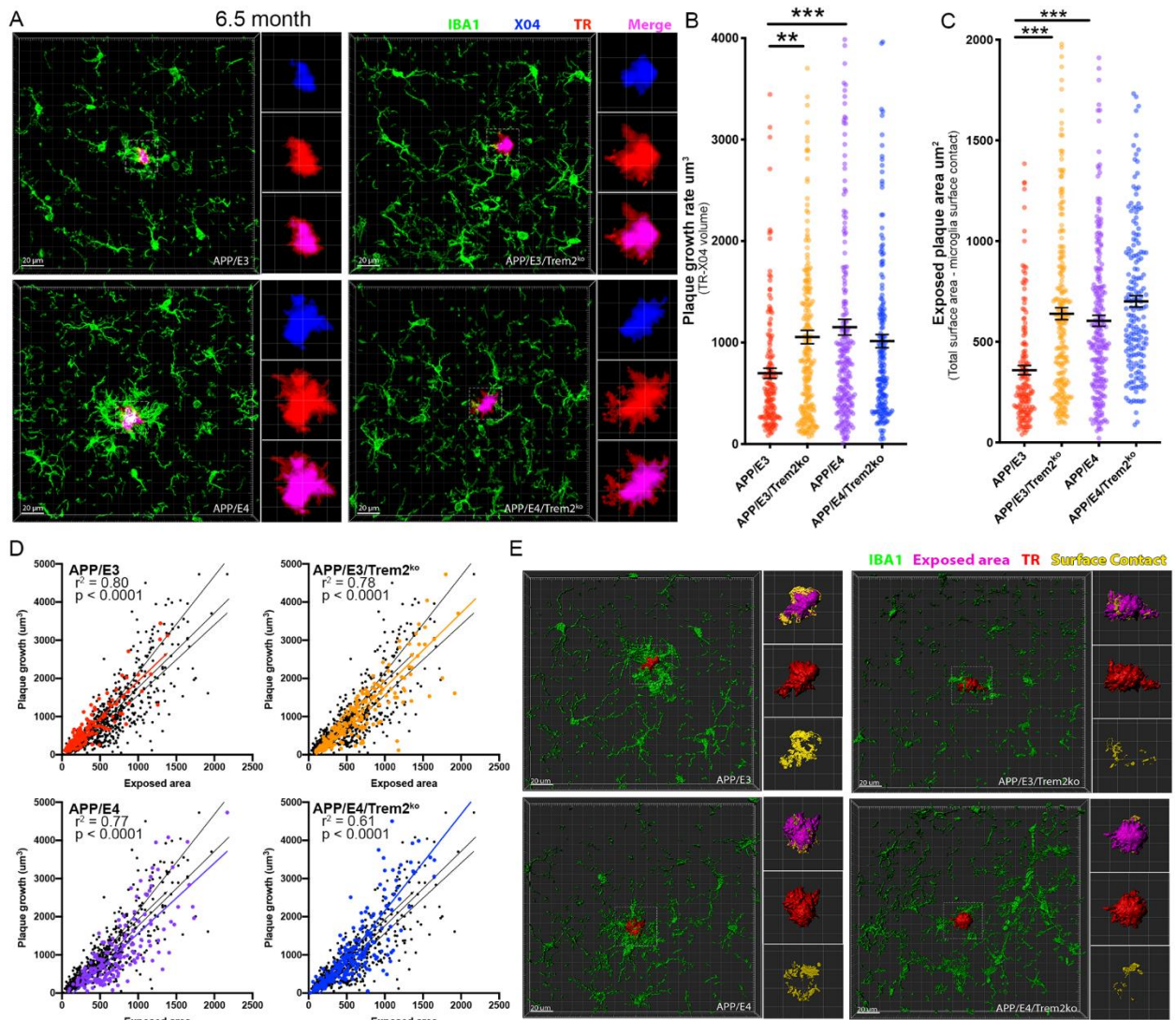


**Figure 9.** *Trem2* **deletion affects plaque growth in correlation with microglia barrier at 6.5 months of age.**

(A) Representative confocal imaging of an amyloid plaque from the 6.5-month-old groups with IBA1 in green, X04 in blue, TR in red and the merge of X04-TR in pink. n = 6 mice/group (3 male and 3 female). APP/E3 n = 148, APP/E3/Trem2$^{ko}$ n = 219, APP/E4 n = 219, APP/E4/Trem2$^{ko}$ n = 180 individual plaques. (B) Quantification of the growth volume in 30 days for individual plaques. (C) The exposed area for each plaque is determined by the area in which microglia processes are not contacting the surface of TR (purple color in panel E). (D) Correlation between plaque growth and exposed surface area for each plaque and genotype. (E) Imaris generated 3D volumetric representations of an amyloid plaque from the 6.5-month-old group with IBA1 in green, exposed area in purple, TR in red, and surface contact in yellow. Analysis by one-way ANOVA followed by Tukey's multiple comparison test. Bars represent mean ± SEM. *** p<0.001; ** p<0.01; * p<0.05.



**Figure 10. *Trem2* deletion affects microglia barrier and plaque growth at 4.5 months of age.**
(A) Representative confocal imaging of an amyloid plaque from the 4.5-month-old groups with IBA1 in green, X04 in blue, TR in red and the merge of X04/TR in pink. n = 6 mice per group (3 male and 3 female). APP/E3 n = 57, APP/E3/Trem2$^{ko}$ n = 54, APP/E4 n = 130, APP/E4/Trem2$^{ko}$ n = 94 individual plaques. (B) Quantification of the growth volume in 30 days for individual plaques. (C) The exposed area for each plaque is determined by the area in which microglia processes are not contacting the surface of TR (purple color in panel E). (D) Correlation between plaque growth and exposed surface area for each plaque and genotype. (E) Imaris generated 3D volumetric

representations of an amyloid plaque from the 4.5-month-old group with IBA1 in green, exposed area in purple, TR in red, and surface contact in yellow. Analysis by one-way ANOVA followed by Tukey's multiple comparison test. Bars represent mean ± SEM. * $p<0.05$; ** $p<0.01$; *** $p<0.001$.

### 4.4.3 Lack of *Trem2* Significantly Affects Brain Transcriptome in APOE3 or APOE4 Mice

The effect of *Trem2* deficiency on brain transcriptome was examined by mRNA-seq on cortical tissue from all 8 genotypes shown on Fig.5A. First, we used weighted gene co-expression network analysis (WGCNA) to correlate gene expression to four traits - *Trem2* deficiency, APOE isoform, APP transgene/amyloid deposition and sex (Fig. 11A). The top three most significant modules correlated either to *Trem2* deficiency (lightcyan) or APOE isoform (turquoise and lightyellow). The turquoise module negatively correlates with APOE4 isoform and is associated with biological processes such as transport, translation, and mRNA processing and oxidation-reduction (Fig. 12). The lightyellow module positively correlates with APOE4 isoform and biological processes associated with it are related to intermediate filament organization, immune system process, and innate immune response (Fig. 12). In addition to lightyellow, another APOE isoform-specific module (darkturquoise) was positively associated with APOE4 isoform and represented GO terms such as acute-phase response, cholesterol efflux, and response to cytokines. Interestingly, this module contained *Apoe* and several members of *Serpina* family that were previously reported by us (Castranio et al., 2017) and others (Zhao et al., 2020) to be increased in an APOE4 dependent manner.
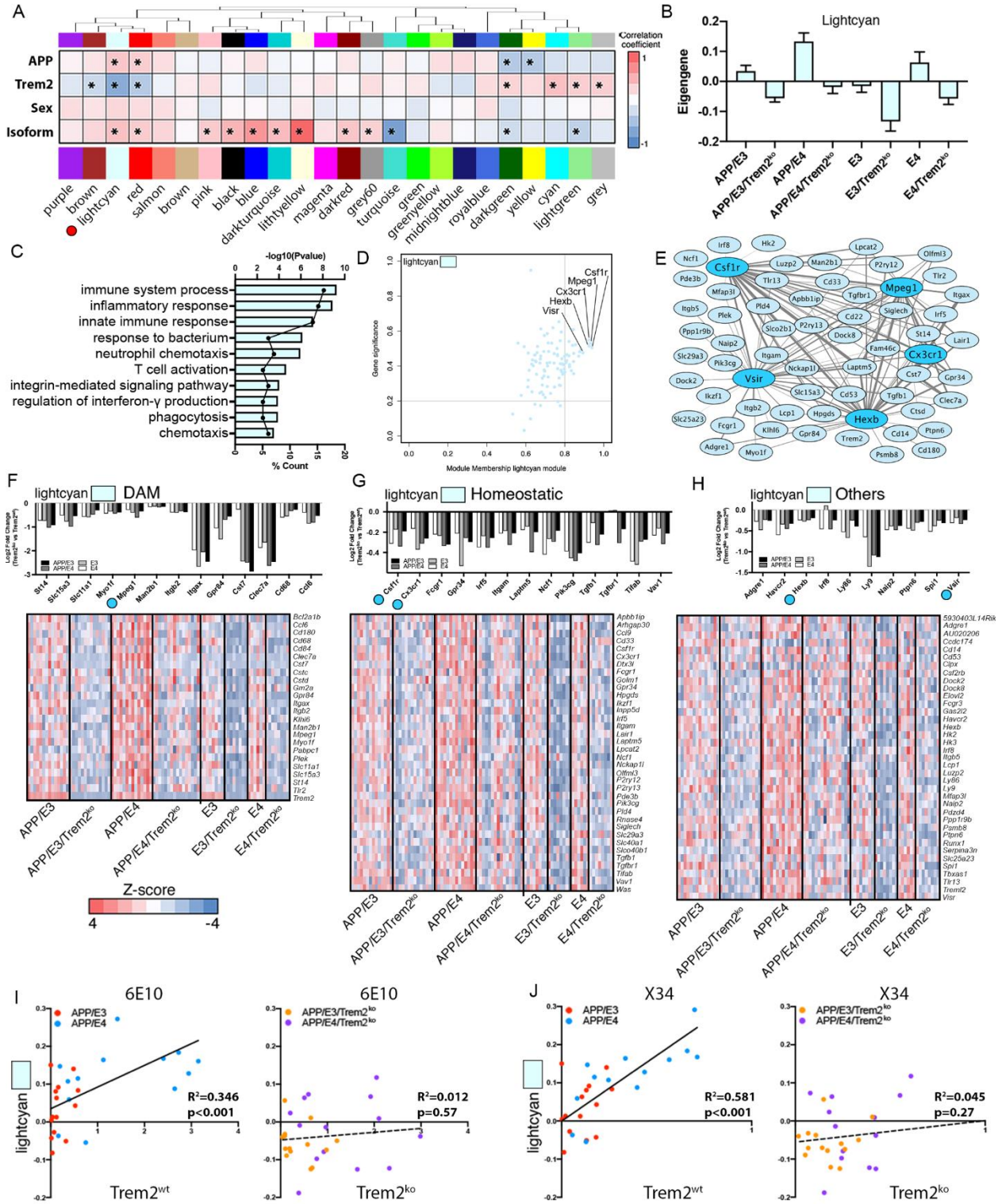
**Figure 11. Lack of Trem2 significantly affects brain transcriptome of mice expressing human APOE3 or APOE4.**

Gene expression profiling was performed by RNA-seq on cortical tissue from the same 6-7 months old mice shown on Fig. 5A. (A) WGCNA was used to identify correlations between gene expression and four traits: APOE isoform,

sex, *Trem2* genotype, and human APP transgene. The relationship table shows the correlation between the module eigengene (row) traits (column). Red denotes a positive correlation and blue a negative correlation, with * denoting a significant correlation (* p<0.05). Trem2 signature module is marked with a red circle. (B) Bar plots show the aggregated module eigengene for each genotype in the modules of interest. (C) GO term bar plots indicate the -log10P value for each term. The associated point in the center of each bar represents the percent of submitted genes found in each GO term. (D) Scatterplot depicts the MM vs GS plot for genes in the lightcyan module relating to the *Trem2* genotype, with hub genes defined as MM>0.8 and GS>0.2. (E) The network generated from all connections within the module from the top 5 hub genes (indicated by darker blue color). Characterization of the lightcyan module with fold change bar plots and heatmaps for disease associated microglial genes (DAM) (F), homeostatic (G) microglia genes and genes outside these two categories (others) (H). Heatmaps depict the Z-score for genes downregulated in Trem2$^{ko}$ mice from the lightcyan module. N: E3/Trem2$^{ko}$ = 8; E4/Trem2$^{ko}$ = 8; E3 = 8; E4 = 6; APP/E3/Trem2$^{ko}$ = 14; APP/E4/Trem2$^{ko}$ = 16; APP/E3 = 14; APP/E4 = 14; (equal number males and females). (I-J) Integration of co-expressed gene network of interest to amyloid deposition. The expression profile of lightcyan was used to identify correlations between gene expression patterns in each of the four APP groups to the percent coverage of 6E10 (I), and percent coverage of X34 (J). Correlation between histological data and RNA-seq data is done with Pearson r correlation.

The lightcyan module was highly and negatively correlated to *Trem2* status in all genotypes regardless of amyloid deposition or APOE isoform, indicating a decreased expression of these genes in all Trem2$^{ko}$ mice (Fig. 11B). This module represented processes such as immune response, innate immune response, inflammatory response, integrin-mediated signaling pathway, phagocytosis, and chemotaxis (Fig. 11C). The top hub genes (i.e. the most interconnected genes) in lightcyan module were *Csf1r*, *Mpeg1*, *Cx3cr1*, *Hexb,* and *Vsir* and were used to generate a representative network (Fig. 11D-E). This module is highly enriched in microglial-specific genes (48 out of 99 genes are microglia specific genes), indicating a strong impact of *Trem2* deficiency on microglial gene expression. As shown on the heat maps in Fig. 11F-H, the gene list of the lightcyan module is comprised of 26 DAM genes (such as *Clec7a*, *Cst7*, *Cd68*, *Itgax*/CD11c, *Mpeg1*), 36 homeostatic genes (*P2ry12*, *P2ry13*, *Cx3cr1*, *Itgam*/CD11b, *Tgfb1*), and a group of 37 genes (*Spi1*/PU.1, *Runx1*, *Treml2*, *Vsir*) not associated with DAM or homeostatic microglia. These genes are downregulated in Trem2$^{ko}$ mice in all of the four respective genotypes and represent the common signature of *Trem2* deficiency. Interestingly, two important DAM genes, *Apoe* (Keren-Shaul et al., 2017; Krasemann et al., 2017) and *Tyrobp* (Keren-Shaul et al., 2017), were not present in this module. The reason *Apoe* was missing from the Trem2 signature list of genes is that as
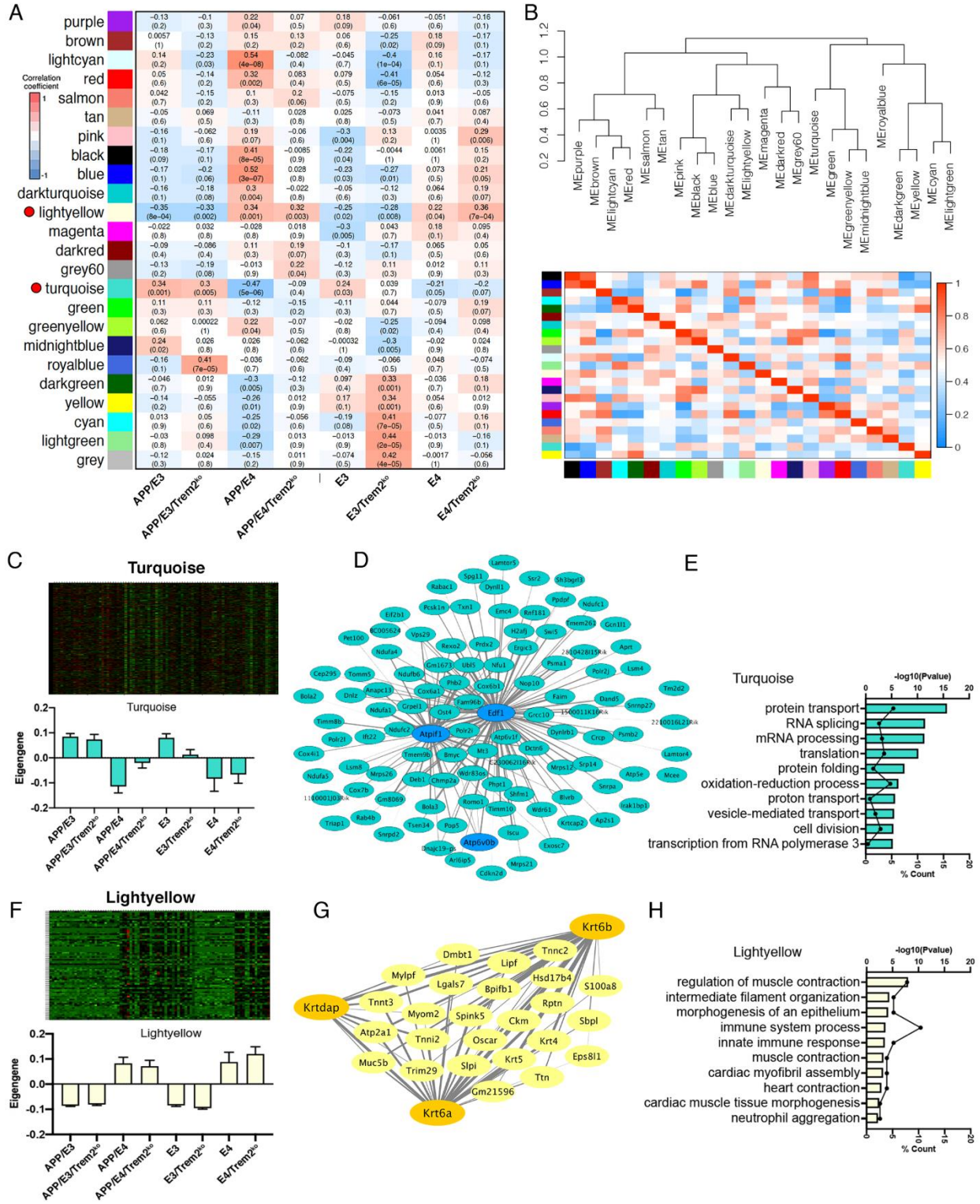
**Figure 12. WGCNA identifies patterns of gene expression characteristic to each of the eight experimental groups.**

(A) WGCNA was used to identify correlations between gene expression and each of the 8 genotypes: APP/E3, APP/E3/Trem2[ko], APP/E4, APP/E4/Trem2[ko] and their corresponding non-APP counterparts (E3, E3/Trem2[ko], E4, E4/Trem2[ko]). Numbers on the heatmap represent Pearson correlation and p-value in parenthesis. Modules of interest

67

are marked with red circles. (B) The dendrogram visualizes the relative similarity between identified modules, with modules that appear close to each other having a more similar expression profile. Heatmap of the Pearson correlation coefficient between each module. (C) Gene expression heatmap and bar plots for each animal from turquoise – correlates positively to all APOE3 mice, as well as a network generated from top 3 hub genes (D) and GO term bar plots indicate the -log10P value for each term. The associated point in the center of each bar represents the percent of submitted genes found in each GO term (E). (F-H) Heatmap, bar plots, network, and GO terms for the lightyellow module – correlates positively to all APOE4 mice.

shown on Fig. 5L, it was upregulated only in APP/E4 mice vs APP/E3 in response to the higher

level of amyloid pathology in these mice (also see Fig. 14B). *Tyrobp* was uniquely downregulated

only in APP/E3/Trem2$^{ko}$ vs APPE3 mice as well as in E3/Trem2$^{ko}$ vs E3 mice. Furthermore,

*Tyrobp* (a member of turquoise module) had a higher expression level in APP/E3 and E3 mice vs

their APOE4 counterparts (see Fig. 13G).

To associate the Trem2 signature to the phenotype of the APP mice, we correlated the gene

expression levels of the lightcyan module to amyloid deposition. As shown in Fig. 11I-J, percent

coverage of 6E10 and X34 in the mice expressing wild-type *Trem2* correlated significantly and

positively to the lightcyan module indicating that this module, enriched in microglial-specific

genes, represents the transcriptional response of microglia to increasing amyloid deposition. In

contrast, there was no significant correlation in APP/E3/Trem2$^{ko}$ or APP/E4/Trem2$^{ko}$ mice

between amyloid deposition and lightcyan module eigengene expression, demonstrating that as

deposition increases in Trem2 deficient APP mice, there is no corresponding increase of microglial

gene expression suggesting that *Trem2* deletion blocks the normal response of microglia to the

increased pathology.

**4.4.4 APOE Isoform-specific Effect on Gene Expression**

Since we found a significant APOE isoform-specific effect (Fig. 11A, Fig.12), we

determined differentially expressed genes that are characteristic for each genotype by comparing

brain transcriptome of APP/E4 vs APP/E3 mice, E4 vs E3 mice as well as their respective Trem2$^{ko}$ counterparts (Fig. 13A-D). We observed more than twice as many differentially expressed genes when comparing APP/E4 vs APP/E3 mice (Fig. 13A) than in APP/E4/Trem2$^{ko}$ vs APP/E3/Trem2$^{ko}$ mice (Fig. 13B). Finding a high number of differentially expressed genes in brain transcriptomes of APP/E4 vs APP/E3 mice is expected because it reflects the difference in amyloid pathology that elicits a stronger response in APP/E4 than in APP/E3 mice. However, a reduced number of differentially expressed genes in APP/E4/Trem2$^{ko}$ vs APP/E3/Trem2$^{ko}$ mice, at approximately the same level of neurodegeneration as in the wild-type *Trem2* mice, suggests that *Trem2* deficiency impairs the normal response to the disease progression and "blunts" the differences between the transcriptomes.

We next searched for DAM and homeostatic genes that are significantly affected in Trem2 and APOE isoform-dependent manner in APP mice. Fig. 13E-F shows heatmaps of DAM and homeostatic genes that have a higher expression level in APP/E4 vs APP/E3 mice and are affected by *Trem2* deficiency. As shown on the line patterning graphs (Fig. 13E-F) some of these, such as DAM genes *Clec7a*, *Itgax,* and *Mpeg1* or homeostatic *Pik3cg* gene, are part of the Trem2 signature and are downregulated in all Trem2$^{ko}$ mice. However, they still retain a higher level of expression in APP/E4/Trem2$^{ko}$ vs APP/E3/Trem2$^{ko}$ as in APP/E4 vs APP/E3 mice, suggesting that these genes respond, at least to a degree, to the more advanced level of neurodegeneration in APP/E4 mice even as *Trem2* is absent. Another group of DAM genes (*Slc15a3*) and homeostatic genes (*Csf1r, Itgam/*Cd11b*, Laptm5,* and *Nckap1l*) had a significantly higher expression in APP/E4 vs APP/E3 mice but this difference disappeared between their Trem2$^{ko}$ counterparts, suggesting an increased dependence on the presence of *Trem2*. Similarly, we identified *Trem2*-dependent genes with significantly higher expression in APP/E3 vs APP/E4 mice that failed to elicit the same
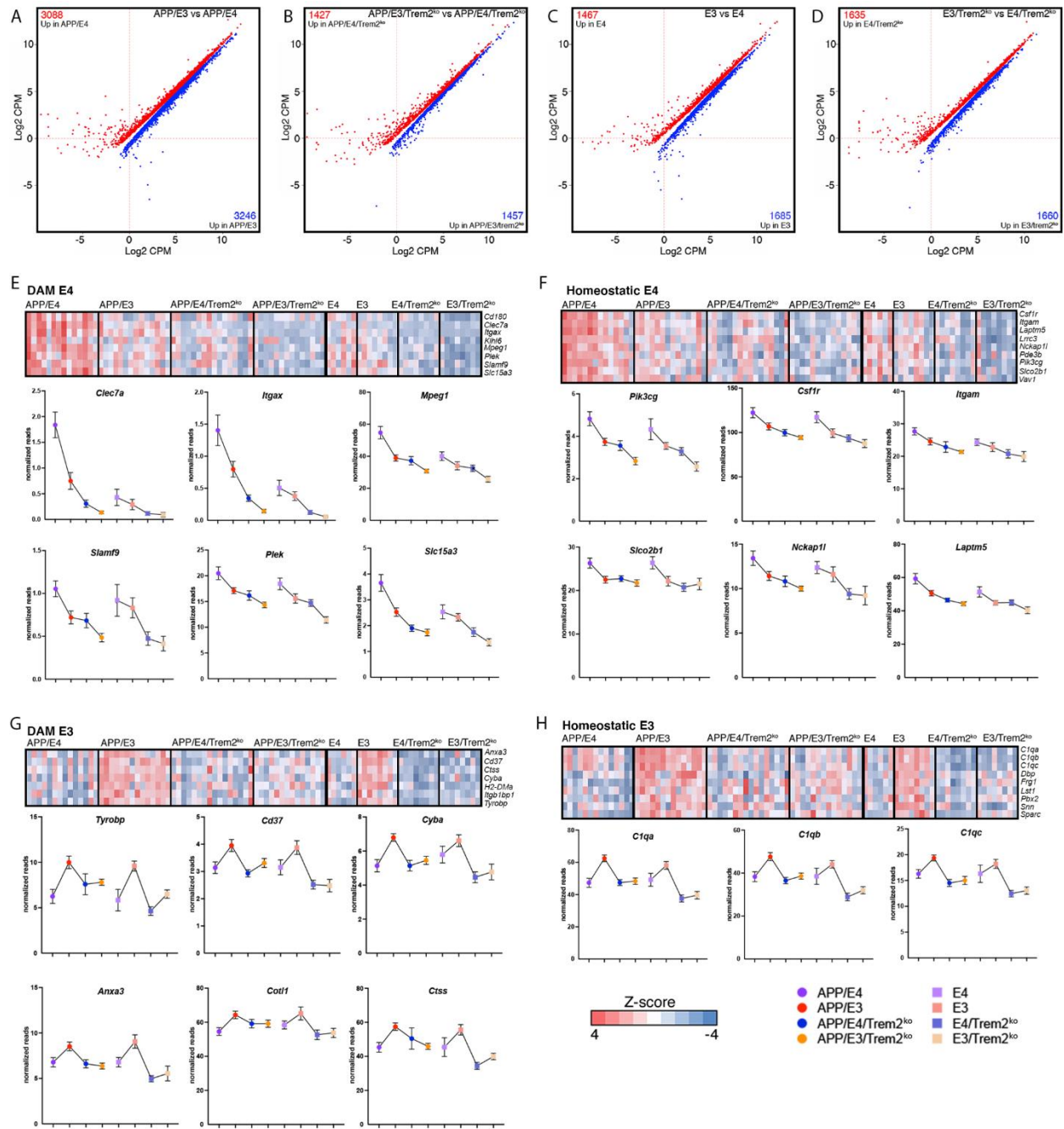
**Figure 13. APOE isoform-specific effect on gene expression.**
RNA-seq data shown in Fig. 11 were analyzed using edgeR to identify differentially expressed genes between APOE isoforms. Scatterplots depict differentially expressed genes between APP/E3 vs APP/E4 (A), APP/E3/Trem2[ko] vs APP/E4/Trem2[ko] (B) E3 vs E4 (C), and E3/Trem2[ko] vs E4/Trem2[ko] mice (D). Shown are genes at p<0.05 cutoff. Heatmaps and line patterning graphs of DAM and homeostatic microglia genes that are upregulated in either APOE4 (E-F) or in APOE3 mice (G-H) mice in a *Trem2* and APOE-isoform dependent manner. Genes of interest are marked with colored circles and shown as line patterning.

response when *Trem2* was deleted. A few examples are shown on Fig. 13G-H: DAM associated (*Tyrobp, Cd37, Cyba,* and *Ctss*) and homeostatic genes (*C1qa, C1qb,* and *C1qc*).

In addition, we also identified APOE isoform-specific genes that were not associated with *Trem2* deficiency or amyloid pathology (Fig. 14A). Among the genes upregulated in APOE4 mice were several members of *Serpina3* family (*Serpina3h*, *Serpina3k*, *Serpina3m*, *Serpina3n*), as well as *Ptprh*, *Abcg1*, and *Picalm* which have all previously been reported by us (Castranio et al., 2017) and others (Zhao et al., 2020). All of *Serpina3* genes and *Ptprh* were upregulated and statistically significant in every E4 vs E3 comparison (APP/E3 vs APP/E4, APP/E3/Trem2[ko] vs APP/E4/Trem2[ko], E3 vs E4, and E3/Trem2[ko] vs E4/Trem2[ko]) confirming that they were neither TREM2 nor amyloid dependent but strictly APOE isoform dependent.
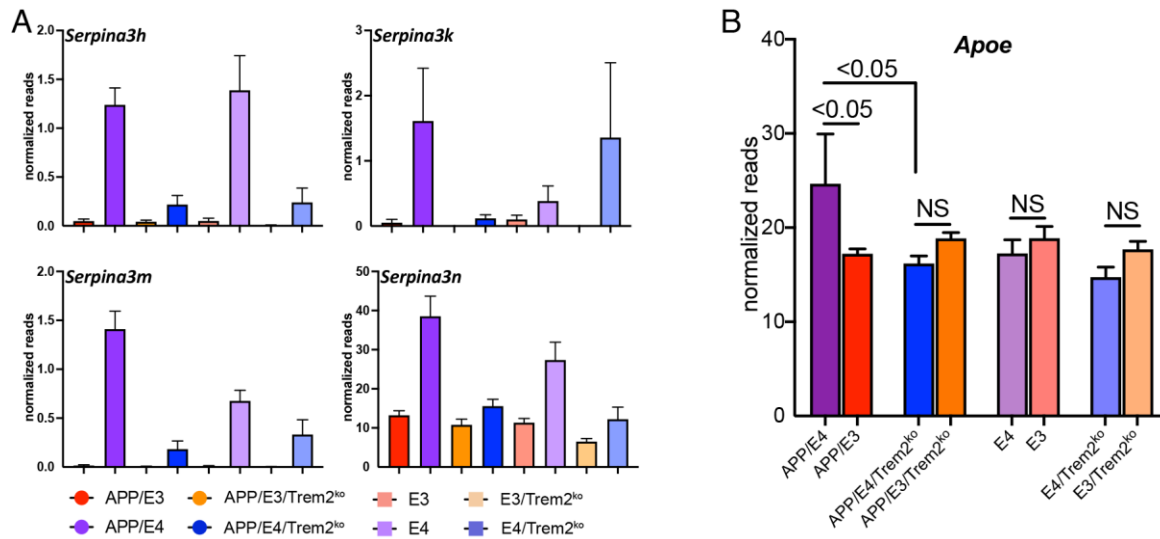


**Figure 14. The expression of Serpina3 family is higher in APOE4 than in APOE3 mice and cell type specific differentially expressed genes.**
(A) Bar plots of *Serpina3h*, *Serpina3k*, *Serpina3m*, and *Serpina3n* from the same 6.5-month-old WT and APP mice as shown on Fig.11 and 13. (B) Bar plots depicting the average *Apoe* gene expression in APOE3 and APOE4 mice as identified by RNA-seq and statistics generated using edgeR.

**4.4.5 FISH Identifies Alterations in Microglial Gene Expression Within the Plaque**

**Microenvironment as a Result of *Trem2* Deficiency and APOE Isoform**

Our next goal was to validate RNA-seq data and characterized the spatial distribution of expressed mRNAs of three genes in relation to compact amyloid plaques at 6.5 months of age. We chose three genes that are part of Trem2 signature– two significantly affected homeostatic genes (*Tmem119* and *Csf1r*), and one significantly affected DAM gene (*Clec7a*) (Fig. 15). We selected these genes because *Tmem119* is a microglia-specific gene and *Csf1r* was the most connected hub gene in the network (Fig. 11E) and *Clec7a* was the top down-regulated gene in all Trem2 deficient mice. We performed FISH using RNAscope probes, coupled with histological detection of X34 positive Aβ plaques. We found that in the microenvironment surrounding plaques (<50 μm), mRNA expression of all three genes was significantly decreased in both APP/E3/Trem2$^{ko}$ and APP/E4/Trem2$^{ko}$ mice when compared to their wild-type *Trem2* counterparts (Fig. 15B-D). In confirmation to RNA-seq results, *Csf1r* and *Clec7a* expression was also significantly higher in APP/E4 vs APP/E3 mice and the expression of *Tmem119* was not affected in APOE isoform-specific manner. This suggests that in addition to being *Trem2* dependent, *Csf1r* and *Clec7a* are also affected by APOE isoform as shown above on Fig. 13E-F. In contrast, there was no difference in gene expression of any of the analyzed genes away from the plaques (> than 50 μm away). The most probable explanation for the spatial difference in gene expression between Trem2$^{ko}$ and Trem2 wild-type mice is the significant reduction in microglia recruitment around plaques in Trem2 deficient mice (Fig. 5F). We then compared the magnitude of the effect seen in the RNA-seq and FISH data using Z-scores to normalize each dataset to comparable levels. The FISH data collected within 50 μm of plaque center parallels the expression profile seen by RNA-seq (Fig.

15E-G). Thus, this experiment validated RNA-seq result confirming TREM2 and APOE isoform-specific effects on gene expression.
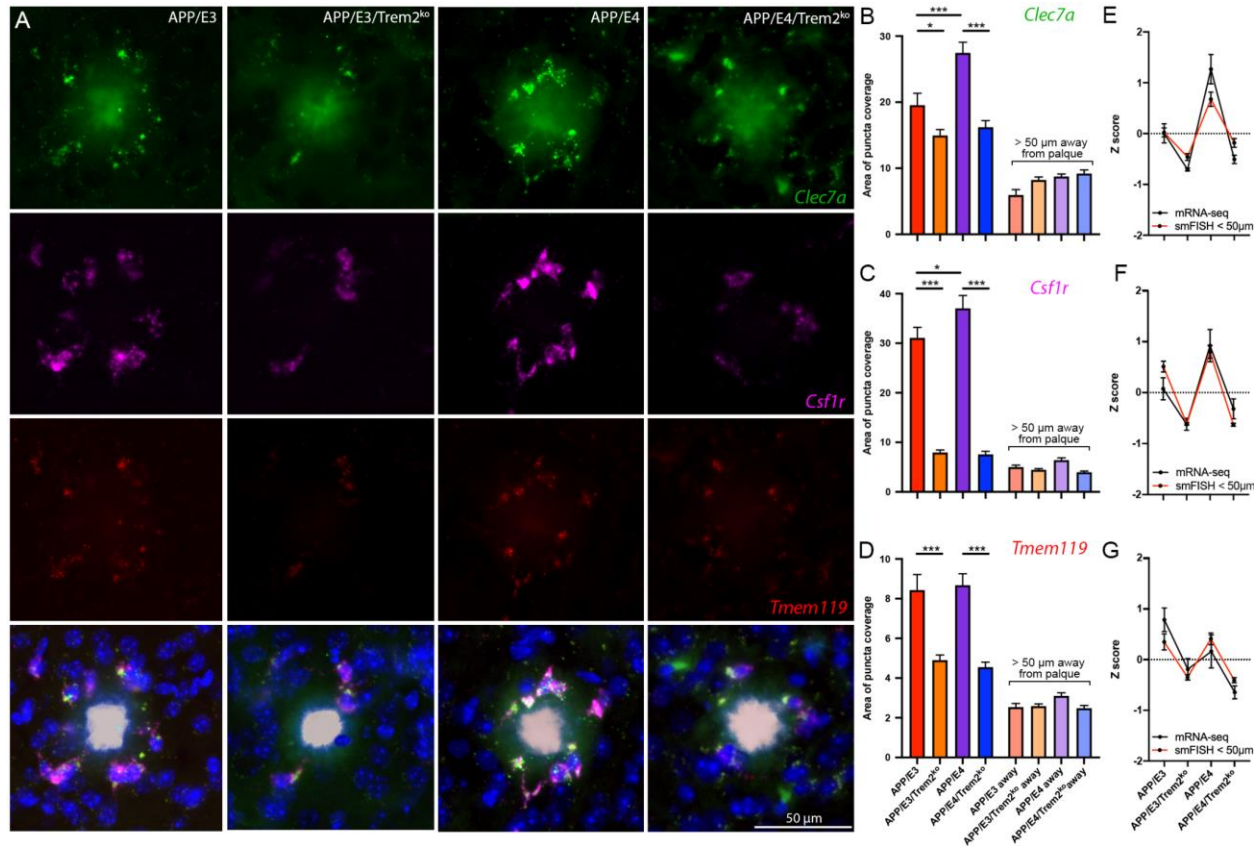


**Figure 15. FISH identifies alterations in gene expression within plaque microenvironment as a result of *Trem2* deficiency.**

(A) Representative images of FISH analyses of microglia gene expression near amyloid plaques at 6.5 months of age (*Tmem119* – red, *Csf1r* – Pink, *Clec7a* – Green, Nuclei – Blue, Amyloid plaque - White). The area occupied by the puncta was quantified adjacent to plaques (<50 μm) as well as away from plaques (>50 μm) for APP/E3, APP/E3/Trem2$^{ko}$, APP/E4, and APP/E4/Trem2$^{ko}$ mice. Bar plots showing the area of puncta coverage adjacent to and away from plaques, and line patterning depicting the Z-score of RNA-seq data and FISHdata together for *Clec7a* DAM marker (B & E), *Csf1r* homeostatic microglia marker (C & F), and *Tmem119* homeostatic microglia marker (D & G). FISHanalysis by one-way ANOVA followed by Tukey's multiple comparison test. n = 4 mice per group (equal males and females), an average of 86 plaques analyzed per genotype, bars represent mean ± SEM, and *** p<0.001; * p<0.05 using Tukey's multiple comparison testing.

## 4.5 Discussion

In the present study, we investigated the effect of *Trem2* deletion on the phenotype of APP transgenic mice expressing human APOE3 or APOE4 isoforms. We show that the absence of *Trem2* exacerbated cognitive impairments in APP transgenic mice but not in their non-APP littermates. Examination of the behavioral data showed that APP/E4 mice performed at the lower limit in these tasks and we were unable to observe a significant reduction in their Trem2$^{ko}$ counterparts. The behavioral data demonstrate that APOE isoform impacts memory significantly more than Trem2 status, which is not surprising considering the higher impact of APOE isoform compared to TREM2 variants on the risk of late-onset AD (Corder et al., 1993; Cruchaga et al., 2013; Guerreiro et al., 2013a; Jansen et al., 2019; Jonsson et al., 2013; Saunders et al., 1993). These data are consistent with previous studies showing that increased human *TREM2* gene dosage in 5XFAD mice improved contextual fear conditioning memory (Friedman et al., 2018). In contrast, another study using the same AD model (5XFAD mice) has shown no impact of *Trem2* deficiency on spatial learning (Griciuc et al., 2019). The observed diminished cognitive performance could be associated with the lack of microglial barrier around plaques and increased neuronal dystrophy observed in the TREM2 deficient mice. This is in agreement with previous data that showed *Trem2* haplodeficiency diminished the plaque-associated microglial barrier resulting in severe neuronal dystrophy (Yuan et al., 2016).

The examination of amyloid plaque load revealed that while APOE isoform was a significant factor, *Trem2* deletion resulted in no change in steady-state plaque level in either APOE genotype at 6.5 months of age. This is an age where APP/E3 mice are characteristic of early Aβ pathology and APP/E4 mice exhibit a more advanced stage. Many of the studies aimed at better understanding the link between TREM2 function and AD have focused on amyloid plaque

pathology however, with conflicting results. Using different AD models (5xFAD), *Trem2* deletion was shown to increase Aβ pathology during the very advanced stages of plaque pathology in a region-specific manner (Colonna and Wang, 2016; Griciuc et al., 2019). Other studies demonstrated that *Trem2* deletion reduced plaque load early but increased it later with the disease progression (Friedman et al., 2018; Jay et al., 2015). Conversely, amyloid PET imaging of the same AD model (APPPS-21) revealed that *Trem2* knockout resulted in accelerated fibrillar amyloid early, which equalized during the later stages of pathogenesis (Parhizkar et al., 2019). Our study is unique in that we utilized AD model mice expressing human APOE isoforms. We identified significant differences in the ratio of compact plaques to the protofibular halo amyloid staining, indicating a *Trem2* mediated effect on plaque compaction in agreement with previous reports (Colonna and Wang, 2016; Wang et al., 2016).

There are several aspects of TREM2 function that could explain a decreased ability of Trem2[ko] to perform their function. The loss of TREM2 cell-surface signaling may lead to a diminished capacity of microglia to recognize Aβ followed by a decreased uptake. Furthermore, the reduced numbers of microglia around amyloid plaques suggest that microglial chemotaxis was inhibited in APP expressing / Trem2[ko] mice, thus restricting microglia movement towards Aβ, or any other damage in surrounding areas. As a consequence, the rate of plaque growth strongly correlated to the significant reduction of microglia barrier around the plaques (Fig. 9-10). Our transcriptomic data support this hypothesis, demonstrating a downregulation of genes associated with both phagocytosis and chemotaxis in Trem2[ko] versus wild-type Trem2 mice (Fig. 11).

The novelty of our study is that we tested the effect of APOE isoform as an additional factor that could interact with TREM2 to contribute to neurodegeneration. Previously, it was shown that, following microglial depletion, microglia derived APOE protein is reduced in Trem2[ko]

mice (Parhizkar et al., 2019). Here we have examined *Trem2* effect in an APOE isoform-dependent and amyloid-dependent manner by directly comparing age-matched APP/E3 and APP/E4 mice that are at different stages of amyloid pathology. We observed a difference in the number of microglia but not astrocytes (Fig. 5E-G), as well as APOE protein surrounding plaques between APP/E3 and APP/E4 mice that was not recapitulated in their Trem2$^{ko}$ counterparts (Fig. 5J-K). Similar pattern of *Apoe* mRNA expression was detected by RNA-seq in APP and their WT littermates, confirming that *Apoe,* as a DAM gene (Keren-Shaul et al., 2017), responds to the differences in the amyloid pathology in APP/E4 vs APP/E3 mice (Fig. 5L and Fig. 14B). Furthermore, our results suggest the effect of *Trem2* deletion on *Apoe* expression is apparent only in APP mice and depends on the amyloid deposition. APOE is secreted mainly by astrocytes and less by microglia, but since *Trem2* is microglia-specific gene, it is reasonable to expect that *Trem2* deletion will directly affect *Apoe* expression in microglia. In order to identify microglia, we used the microglia-specific gene *Tmem119* (Bonham et al., 2019; Unger et al., 2018). It should be noted that *Tmem119* is a homeostatic gene and in our study its expression was decreased by *Trem2* deficiency. However, as in previous studies (Bonham et al., 2019; Unger et al., 2018) we used it only as a marker to label microglia without assessing its expression. Our results using in situ hybridization confirmed that microglial *Apoe* depends on *Trem2* presence and is decreased in APP/E4/Trem2$^{ko}$ microglia vs APP/E4 counterparts (Fig. 5M-N).

Our data also indicate that the effect of *Trem2* deficiency on plaque growth is stronger at earlier stages of amyloid deposition when plaques are smaller. Considering that APP/E4 mice show earlier onset of amyloid pathology, the TREM2 effect on plaque growth in mice expressing this isoform is observed in mice younger than their APOE3 counterparts. A possible explanation for the observed APOE isoform effects is the difference in their abilities to transport lipids and

cholesterol (Mahley, 2016) that can impact APOE receptor-binding properties. Recently, we reported a significant difference in brain phospholipid content of APOE2, E3, and E4 in AD patients (Lefterov et al., 2019) and APOE4-containing lipoproteins were shown to be less lipidated than APOE3 (DeMattos et al., 2001). Thus, APOE4 may impede Aβ phagocytosis via reduced affinity for receptor binding (including TREM2 receptor), or changes in proteolytic degradation of Aβ (reviewed in (Wolfe et al., 2018; Zhao et al., 2018a)).

There is an apparent inconsistency between the role of TREM2 in plaque growth, albeit at different ages for APP/E3 and APP/E4, and its lack of effect on steady-state amyloid load in APP/Trem2$^{ko}$ mice. This could be explained by the balance between Aβ clearance mechanisms at different phases of amyloid pathology, i.e. microglia phagocytosis vs efflux via the BBB. At the earlier stages of amyloid deposition, the prevailing Aβ species in brain interstitial fluid are monomers and low molecular weight oligomers that are easily cleared out of the brain by efflux via BBB with half-life 1.5 hours (Cirrito et al., 2003; Fitz et al., 2012). In contrast, with the progression of the pathology, there is an increase of high molecular weight Aβ oligomers (Takeda et al., 2013) leading to the increase of Aβ half-life in interstitial fluid (Cirrito et al., 2003; Fitz et al., 2015). Thus, in mice with significant amyloid pathology, the faster BBB clearance mechanism is impeded and defects in microglia-mediated clearance mechanisms result in an increase of its deposition into plaques (Fig. 16).
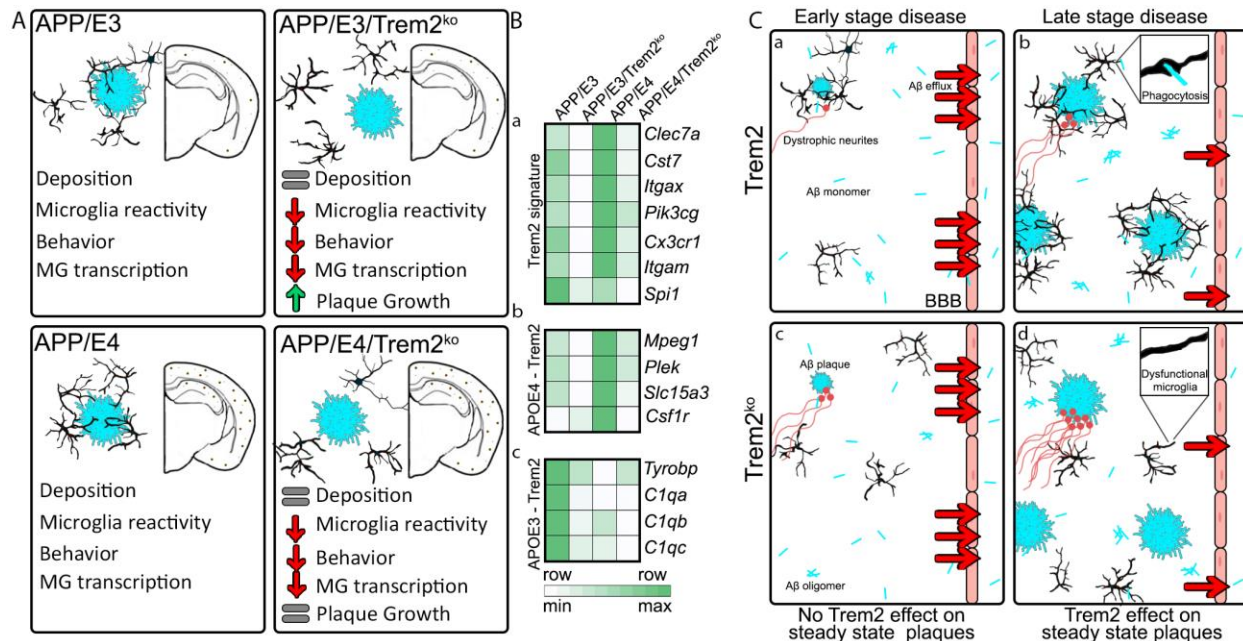
**Figure 16. Suggested model, illustrating the impact of *Trem2* deletion on the phenotype and transcriptome in APP/E3 and APP/E4 mice.**
(A) Lack of *Trem2* does not impact steady state amyloid deposition, impacts plaque growth, reduces microglia reactivity and worsens behavior in APP/E3/Trem2ko and APP/E4/Trem2ko mice as compared to their *Trem2*-expressing counterparts. Arrows are relative to their Trem2-expressing counterparts. (B) Differential effects of *Trem2* deficiency on microglia transcriptome in the same mice. a) Topmost affected Trem2 signature genes; b-c) Examples of Trem2-APOE dependent genes with expression higher in APP/E4 mice (b) or APP/E3 mice (c). (C) A graphical hypothesis regarding the importance of microglia barrier on the accumulation of Aβ and plaque dynamics. (a) and (c), In the early stage of amyloid deposition low molecular weight Aβ species are prevailing in interstitial fluid and are cleared mainly via efflux through the blood-brain barrier. (b) and (d), In the later stages of amyloid deposition, high molecular weight Aβ oligomers accumulate in interstitial fluid that impedes Aβ efflux via blood-brain barrier and microglia phagocytosis becomes a major component of Aβ removal. We hypothesize that there is increased reliance on functional *Trem2* on Aβ clearance in the late stages of amyloid pathology.

The lightcyan module represents the Trem2 signature which is enriched for microglial-specific genes indicating that *Trem2* deficiency has a robust effect on microglial gene expression. Because of the limitations of bulk RNA-seq data, this conclusion needs to be confirmed by single cell RNA-seq data. The main hubs of lightcyan module network are *Csf1r*, *Mpeg1*, *Cx3cr1*, *Hexb* and *Visr*. Previously, few of these genes such as *Cx3cr1*, *Hexb*, *P2ry12*, *P2ry13*, and *Siglech* were classified as *Trem2* dependent (Keren-Shaul et al., 2017). However, as part of the Trem2 signature, we also identified a group of genes which had never before been linked to *Trem2* deficiency, including *Spi1*/PU.1 (Gosselin et al., 2014), *Adgre1* (Gordon et al., 2011), *Ctsc* (Zhang et al.,

2013), *Fcgr1* (Minett et al., 2016), *Cd68* (Hopperton et al., 2018), and the hub gene *Visr* (Li et al., 2017). These genes are enriched in immune cells (Lein et al., 2007) and follow similar expression patterns in microglia expressing either APOE isoform. Our topmost downregulated genes in Trem2$^{ko}$ mice in all four sets of comparisons were *Clec7a* and *Itgax*. Both, *Clec7a* and *Itgax* have been previously identified as drivers of a "primed" microglia phenotype associated with neurodegeneration and aging (Holtman et al., 2015). We found no change in a few genes, previously found downregulated in Trem2$^{ko}$ mice, namely *Axl, Csf1,* and *Spp1* (Friedman et al., 2018; Griciuc et al., 2019; Krasemann et al., 2017; Mazaheri et al., 2017). It should be noted that the Trem2 signature as identified in this study, incorporates only the genes that are commonly affected by *Trem2* deficiency in APP as well in their WT littermates. DAM genes that respond mainly to the increased neurodegeneration such as *Apoe* and *Lpl* were not identified as part of the common Trem2 signature. Both *Apoe* and *Lpl* were upregulated only in APP/E4 mice vs APP/E3 in response to the higher level of amyloid pathology seen in these mice.

Interestingly, *Tyrobp* implicated in the TREM2 checkpoint (Keren-Shaul et al., 2017) was downregulated in Trem2$^{ko}$ mice in an APOE isoform-specific manner in both APP/E3 mice and in their WT non-APP littermates (see Fig. 5G). The most probable reason is that we are exploring an effect of *Trem2* deletion in mice expressing human *APOE* instead of mouse *Apoe* and as mentioned above the differences in APOE3 and APOE4 lipidation could affect receptor binding and signal transduction pathways reflecting on brain transcriptome. In addition to *Tyrobp*, we identified as uniquely upregulated in APP/E3 vs APP/E3/Trem2$^{ko}$ mice, i.e. in an APOE3-*Trem2* dependent manner, several genes involved in the C1q complement cascade. *Tyrobp* has been previously regarded as a regulator of genes involved in the complement pathway (Haure-Mirande et al., 2017;

Haure-Mirande et al., 2019), and is part of a predicted protein-protein interaction network along with *C1qa*, *C1qb*, *C1qc,* and *Ctss* (Szklarczyk et al., 2019).

We have previously shown an APOE4 isoform-specific increase of several *Serpina3* genes and *Ptprh* in human APOE targeted replacement mice (Castranio et al., 2017). In the current study, we confirmed that four members of *Serpina3* family (*Serpina3h*, *Serpina3k*, *Serpina3m*, *Serpina3n*), as well as *Ptprh,* are increased in both APP/E4 vs APP/E3 mice and their non-transgenic littermates (E4 vs E3) suggesting that their expression was not affected by amyloid deposition. We also established that the expression of the *Serpina3* genes was not affected by *Trem2* deficiency. Recently, Zhao et al. (Zhao et al., 2020) demonstrated a transcriptional upregulation of several genes from *Serpina3* family in the same APOE4 vs APOE3 mice. They also reported that the expression level of *SERPINA3* (human ortholog of *Serpina3n*) is higher in APOE4 carriers vs non-carriers, but is not significantly different when adjusted by AD status (Zhao et al., 2020). Interestingly, in a recent study examining the effect of APOE isoform on the transcriptome in human AD cortex (right inferior parietal lobule), we found that the expression of *SERPINA3*, as well as *PTPRH,* was significantly higher in APOE2 carriers vs APOE4 carriers (Lefterov et al., 2019). The APOE isoform-dependent effect on the expression of members of this gene family in human and mouse data warrants further research.


### 4.6 Conclusion


In conclusion, the results of this study provide insight into the complex effect of TREM2 on phenotype, and brain transcriptomes in mice expressing human APOE isoforms. We show that the absence of *Trem2* exacerbated cognitive impairments in APP transgenic mice but not in their

WT littermates. *Trem2* deletion significantly reduced microglia barrier around the plaques in correlation with the increased plaque growth rate. The differences in expression levels identified a Trem2 signature - a cluster of highly connected immune response genes, commonly downregulated as a result of *Trem2* deletion and regardless of the APOE isoform. Surprisingly, the lack of TREM2 significantly decreased *Apoe* mRNA expression in APP/E4 but not in APP/E3 mice a result that was confirmed by APOE protein analysis. Future studies are needed to better understand the role of TREM2 through the normal aging and in microglial response to neuronal injury and amyloid deposition.

## 5.0 Final Conclusions

AD is the most common form of dementia worldwide and is characterized by extracellular β-amyloid plaques and intracellular neurofibrillary tau tangles. *APOEε4* and *TREM2* deficiency caused by the R47H mutation are two major genetic risk factors for LOAD. However, surprisingly little is known about the interplay between these two genes regarding amyloid deposition, microglial phenotype, or transcriptomic profile. We hypothesized that APOE isoform would differentially impact transcriptional gene expression and aspects of amyloid pathology, potentially in a *Trem2*-dependent manner, with APOE4 exhibiting worse outcomes than APOE3. We addressed this hypothesis through three aims: First, we undertook a comprehensive literature review encompassing all published data about the proposed hypothesis (Chapter 3). Second, an analysis of the phenotypic changes observed in WT and APP-expressing APOE3, APOE4, APOE3/Trem2$^{ko}$, and APOE4/Trem2$^{ko}$ mice (Chapter 4) was completed. Third, transcriptional profiling of both WT and APP mice expressing human APOE3, APOE4, APOE3/Trem2$^{ko}$, or APOE4/Trem2$^{ko}$ was accomplished (Chapter 4). Logistically, Chapter 3 established the conceptual bases for investigating the impact of APOE isoform and *Trem2* deficiency and pointed to gaps in the knowledge base revolving around these two eminent AD risk factors that Chapter 4 set about addressing.

Our second aim was to elucidate the phenotypic characteristics of APOE3, APOE4, APOE3/Trem2$^{ko}$, and APOE4/Trem2$^{ko}$ AD-like mice at a time in which we have previously established a noticeable difference in amyloid pathology between APOE isoforms. This aim provided evidence that *Trem2* deletion worsened cognitive performance, restricted microglia recruitment to amyloid plaques, increased neuronal dystrophy, and impacted growth kinetics of

plaques, but showed no impact on steady-state amyloid load in either APOE genotype. Additionally, *Trem2* deletion resulted in reduced microglia surface contact and a subsequent increase in the plaque growth rate, exhibiting the strongest effects on smaller plaques. This ultimately leads to the conclusion that early plaque development is a critical window for modulating aspects of the microglia – amyloid relationship, which has lasting impacts as deposition progresses.

Recently, Parhizkar et al. used *in vivo* μPET imaging at multiple ages in APPPS1/Trem2[ko] mice to detect an increase in cortical amyloid load early that diminishes in later stages of amyloid deposition of *Trem2* deletion mice. We found no change in overall amyloid load as a result of *Trem2* deletion at 6.5 months but did elucidate alterations in plaque compaction. Hence, we addressed the changes in the growth rate of individual plaques. Our data showed that Trem2[ko] increased the growth rate of plaques at the earlier, but not later stages of plaque development. Reduced microglial recruitment to amyloid deposits has been consistently observed in the Trem2[ko] genotype (Jay et al., 2017; Jay et al., 2015; Parhizkar et al., 2019; Wang et al., 2015; Wang et al., 2016; Yuan et al., 2016). The data presented here confirm this observation by examining reduced microglia – plaque surface contact in Trem2[ko] established plaques (APP/E4: 4.5-month; both 6.5-month groups), although no change in surface contact from the early plaque growth group (APP/E3 4.5 month) was detected. The microglial barrier provides a physical reduction in the surface area exposed to the microenvironment surrounding the plaque, while at the same time providing more surface area for microglia phagocytosis to occur. This is noteworthy because TREM2-dependent Aβ phagocytosis is more efficient when the Aβ forms complexes with APOE (Yeh et al., 2016).

Previously, it has been shown that newly formed, and specifically fast-growing plaques are surrounded by a disproportionately large area of neuronal dystrophy (Condello et al., 2011a).

Interestingly, *Trem2* haploinsufficiency and full deletion have both been shown to increase dystrophic neurites surrounding filamentous and small compact plaques (Yuan et al., 2016). The increase in plaque growth seen early in Trem2$^{ko}$ mice may not be enough to influence overall amyloid deposition, as we observed at 6.5 months, but the early, rapid expansion of amyloid plaques can have lasting effects on the tissue surrounding the plaques. To this end, elevated *Trem2* gene dosage in microglia has been shown to significantly reduce plaque-associated neuronal dystrophy and rescue cognitive deficits in AD mice (Lee et al., 2018). However, the protective effect of a well-established microglia barrier does seem to have limitations. Our data show that in the 6.5-month APP/E4 group, the plaques have significantly increased surface coverage compared to either of the Trem2$^{ko}$ groups, although they still retain a similar growth volume. This emphasizes the importance of surface contact in very small plaques and how a better microglial acquisition and coverage of small plaques can delay the exponential growth phase.

In the third aim, we assessed transcriptional changes in each group and identified a common Trem2 signature in all groups analyzed. The APP/E4 genotype is associated with an increased number of differentially expressed genes, specifically DAM and homeostatic genes, compared to E4. This is presumably influenced by the presence of amyloid pathology and is a driving force behind the genetic response in these mice. Within that context, *Trem2* deletion leads to a down-regulation of immune response genes (*Csf1r*, *Mpeg1*, *Cx3cr1*, *Hexb,* and *Vsir*), and drives APP/E3 and APP/E4 mice to have a more similar gene expression profile than expected based on differences in amyloid pathology. The reduction of gene expression for both DAM and homeostatic genes implies that *Trem2* deficiency not only impedes the adoption of an increased activation state by microglia but also constrains the maintenance of proper homeostasis. In some

instances, APP/E4 mice still demonstrate elevated expression of DAM and homeostatic markers in APP/E4 compared to APP/E3 mice, likely driven by baseline differences in the amyloid load.

Without access to transcriptional data from mice with relatively similar levels of amyloid deposition but different APOE genotypes, it is hard to disentangle the transcriptional effects seen as a result of APOE4 isoform from that of increased pathology. That being said, two of the strongest drivers of the APOE4-Trem2 dependent expression pattern are *Clec7a* and *Itgax*. Both have been previously identified as part of the DAM signature (Keren-Shaul et al., 2017) and even implicated in the APOE-TREM2 pathway (Krasemann et al., 2017), but never in an APOE isoform-specific manner. Furthermore, both of these genes have been identified as characteristic drivers of a "primed" microglia phenotype derived from neurodegeneration and aging (Holtman et al., 2015). This indicates that these genes are involved in the natural aging process, but their upregulation can result in the adoption of an accelerated, more aggravated phenotype. These genes along with *Mpeg1* are severely reduced in the absence of functional *Trem2*, but they still remain elevated in the APP/E4/Trem2$^{ko}$ compared to the APP/E3/Trem2$^{ko}$, indicating that they are still being at least partially activated by a pathway other than *Trem2*, specifically in response to the presence of APOE4.

We noted that several genes involved in the C1q complement cascade (*C1qa*, *C1qb*, and *C1qc)* within the group of *Trem2* dependent genes were increased in APOE3 compared to APOE4 mice. The activation of the complement system has been previously identified in human AD brain tissue, specifically in the microenvironment of amyloid deposits (Hong et al., 2016; Zanjani et al., 2005). C1q protein accumulates in the brain with aging, especially in the hippocampus, in an APOE isoform-specific manner; the APOE4 genotype shows the most accumulation, whereas APOE2 displays the least (Chung et al., 2016). Given the higher binding affinity of APOE3 to

C1q, the uniquely elevated expression of these genes in APOE3 mice may indicate that they have a more heavily relied upon and robust C1q complement system than the APOE4 genotype. It should be noted that a similar expression pattern is seen in the WT mice, indicating that APOE3 mice are activating and utilizing the *Trem2* dependent C1q complement system as a defense response to normal aging, whereas APOE4 mice are not. Thus, at a baseline level as well as in the early stages of amyloid deposition, C1q activation could play a protective role in neurodegeneration by restricting the adoption of an inflammatory phenotype in APOE3 mice in a Trem2 dependent manner.

The activation of TREM2 leads to intracellular signal transduction through the adaptor protein TYROBP, making its function intimately connected to TREM2. In AD, *Tyrobp* has been previously identified as a potential driver for microglial activation and the immune response through the regulation of genes involved in the complement pathway (Zhang et al., 2013). Our data delineated that *Tyrobp* expression displays an isoform-specific response to *Trem2* deletion and is downregulated only in APOE3 comparisons. This is driven by the fact that *Tyrobp*, along with the complement cascade genes, have a higher expression in APP/E3 and E3 mice compared to their APOE4 counterparts, and the deletion of *Trem2* drives expression down to the levels seen in APOE4-expressing mice. *Tyrobp* deficiency has been shown to modulate plaque morphology and alter gene expression of many AD-related genes including *C1qa*, *C1qbp*, and *C1qc* (Haure-Mirande et al., 2017; Haure-Mirande et al., 2019). We also found that *Cd37*, a downstream component of the *Tyrobp* causal network (Zhang et al., 2013), expressed the same signature as *Tyrobp*. All of this points to the conclusion that APOE3 mice rely more heavily on the use of the C1q complement system to regulate microglia activation and regulate inflammation. Thus, when

*Trem2* is knocked out, a larger transcriptional response is observed in these genes in APOE3 than APOE4 mice.

When examining the totality of the evidence presented here, the decreased cognitive performance in Trem2$^{ko}$ mice at 6.5 months of age combined with the lack of difference in overall amyloid load between the WT Trem2 and Trem2$^{ko}$ mice is interesting, given the fact that we also established that plaques from Trem2$^{ko}$ mice have an increased growth rate early in amyloid deposition. It has been established that faster-growing plaques are more damaging to the surrounding microenvironment (Condello et al., 2011b). The plaque growth rate, aside from overall amyloid deposition, may be a factor that contributes to reduced cognitive performance even if the steady-state amyloid load is not significantly different. It also should be noted that increased activation of APOE4 microglia could ultimately cause long term problems for the surrounding cells. In this instance, the homeostatic lock imposed as a result of *Trem2* deletion may reduce some of the negative effects caused by chronic activation, since microglia can never reach full activation. This brings into question the dual role of *TREM2* and provides insight into why the phenotypic characteristics derived as a result of deficiencies in this gene have been hard to define.

The use of transgenic mouse models constitutes an inherent limitation of these studies. The addition of the human APOE3 or APOE4 transgene into the mouse genome may influence aspects of the model outside of what was intended. Additionally, interactions between human APOE and murine TREM2 are known to be biologically possible (Jendresen et al., 2017) but clearly do not function as the systems were intended. Furthermore, the distinction between Trem2$^{ko}$ and *TREM2* deficiency must be made clear: the rare biallelic mutations in *TREM2* that result in a true loss of function in humans manifests as Nasu–Hakola disease, which is clinically different than the AD risk modifying aspects of *TREM2* deficiency via the R47H mutation (Paloneva et al., 2002). There

are known differences in the transcriptomic regulation between human and mouse microglia which invariably play a part in the interpretation of mouse derived data (Zhou et al., 2020). Microglia in particular have been shown to have divergent activation profiles between human and mouse, although in both species, the deletion or mutation of TREM2 similarly blunted the response to amyloid accumulation (Zhou et al., 2020).

Accepting the necessity of the use of transgenic models to further our understanding of a complex disease such as AD is requisite, as they provide the means to examine systems that replicate the human disease in a time and cost-efficient manner. It would be very interesting to examine the transcriptomic profile of mice at a younger (3.5 months) as well as an older age (13.5 months) using this model. The younger age would provide a glimpse into the early transcriptional changes behind the onset of amyloid deposition as well as uncover potential first responders that work in a *Trem2* dependent manner. It would also be interesting to investigate the transcriptomic profiles of these groups at a later time point as the deposition differences between APOE isoforms become more similar. This would allow for the determination of whether or not the more chronic nature of the APOE4 deposition has exhibited a lasting impact on the gene expression, or if the transcriptional profiles between APOE isoforms will become more similar once the deposition levels begin to converge.

One practical application of the data presented here would be the use of TREM2 as a therapeutic in AD. There are some inherent challenges in this with the first being the relative infrequency in TREM2 mutations in humans with risk variants occurring in less than one percent of the population. This contrasts with the other gene investigated here APOE, which has the risk variant of APOE4 occurring in around 20% of the global population. Secondarily, there is the potential that targeting of TREM2 in non-risk carrying individuals (which represent the vast majority of all people) would have consequences outside the intended therapy. The most

commonly reported effect of TREM2 deficiency is the loss of ability to acquire an activated microglia signature state. The stimulation of TREM2 signaling before, or at the onset of amyloid accumulation could boost the microglia reactivity to the amyloid thereby slowing the initial onset of accumulation and delaying symptoms. It remains to be solved as to is the adoption of an activated microglia state is detrimental long-term thought as chronic microglial activation is potentially detrimental as well.

Collectively, this dissertation has elucidated unique phenotypic and transcriptional differences in the response to Aβ deposition when in the presence of either human APOE3 or APOE4 in conjunction with *Trem2* deficiency. We have identified a unique transcriptomic signature which mostly impacts microglia gene expression, behavioral deficits, increases in plaque growth at early stages of amyloid deposition, and no impact on steady state amyloid deposition in both APOE genotypes following *Trem2* deletion. Additionally, we found and a reduction of APOE protein and gene expression surrounding amyloid plaques which was unique to APOE4 expressing mice following *Trem2* deletion. The assessment and characterization of these two genetic risk factors and how they impact Alzheimer's disease progression provides a critical knowledge base that can be implemented in the creation of successful early diagnostic and therapeutic strategies against such a devastating disease.

# Bibliography

Acosta, C., Anderson, H.D., and Anderson, C.M. (2017). Astrocyte dysfunction in Alzheimer disease. J Neurosci Res *95*, 2430-2447.

Agosta, F., Vossel, K.A., Miller, B.L., Migliaccio, R., Bonasera, S.J., Filippi, M., Boxer, A.L., Karydas, A., Possin, K.L., and Gorno-Tempini, M.L. (2009). Apolipoprotein E epsilon4 is associated with disease-specific effects on brain atrophy in Alzheimer's disease and frontotemporal dementia. Proceedings of the National Academy of Sciences of the United States of America *106*, 2018-2022.

Alzheimer's, W.R. (2018). World Alzheimer Report 2018. The state of the art of dementia research: New frontiers.

Association, A. (2019). 2019 Alzheimer's disease facts and figures.

Atagi, Y., Liu, C.C., Painter, M.M., Chen, X.F., Verbeeck, C., Zheng, H., Li, X., Rademakers, R., Kang, S.S., Xu, H.*, et al.* (2015). Apolipoprotein E Is a Ligand for Triggering Receptor Expressed on Myeloid Cells 2 (TREM2). J Biol Chem *290*, 26043-26050.

Azarnia Tehran, D., Kuijpers, M., and Haucke, V. (2018). Presynaptic endocytic factors in autophagy and neurodegeneration. Curr Opin Neurobiol *48*, 153-159.

Bailey, C.C., DeVaux, L.B., and Farzan, M. (2015). The Triggering Receptor Expressed on Myeloid Cells 2 Binds Apolipoprotein E. J Biol Chem *290*, 26033-26042.

Bakker, E.N., Bacskai, B.J., Arbel-Ornath, M., Aldea, R., Bedussi, B., Morris, A.W., Weller, R.O., and Carare, R.O. (2016). Lymphatic Clearance of the Brain: Perivascular, Paravascular and Significance for Neurodegenerative Diseases. Cell Mol Neurobiol *36*, 181-194.

Bales, K.R., Liu, F., Wu, S., Lin, S., Koger, D., DeLong, C., Hansen, J.C., Sullivan, P.M., and Paul, S.M. (2009). Human APOE isoform-dependent effects on brain beta-amyloid levels in PDAPP transgenic mice. The Journal of neuroscience : the official journal of the Society for Neuroscience *29*, 6771-6779.

Bales, K.R., Verina, T., Dodel, R.C., Du, Y., Altstiel, L., Bender, M., Hyslop, P., Johnstone, E.M., Little, S.P., Cummins, D.J.*, et al.* (1997). Lack of apolipoprotein E dramatically reduces amyloid beta-peptide deposition. NatGenet *17*, 263-264.

Benitez, B.A., Jin, S.C., Guerreiro, R., Graham, R., Lord, J., Harold, D., Sims, R., Lambert, J.C., Gibbs, J.R., Bras, J.*, et al.* (2014). Missense variant in TREML2 protects against Alzheimer's disease. Neurobiol Aging *35*, 1510 e1519-1526.

Bjorkhem, I., and Meaney, S. (2004). Brain cholesterol: long secret life behind a barrier. Arteriosclerosis, thrombosis, and vascular biology *24*, 806-815.

Boche, D., Perry, V.H., and Nicoll, J.A. (2013). Review: activation patterns of microglia and their identification in the human brain. Neuropathology and applied neurobiology *39*, 3-18.

Boehm-Cagan, A., and Michaelson, D.M. (2014). Reversal of apoE4-driven brain pathology and behavioral deficits by bexarotene. The Journal of neuroscience : the official journal of the Society for Neuroscience *34*, 7293-7301.

Bonham, L.W., Sirkis, D.W., and Yokoyama, J.S. (2019). The Transcriptional Landscape of Microglial Genes in Aging and Neurodegenerative Disease. Front Immunol *10*, 1170-1170.

Borchelt, D.R., Thinakaran, G., Eckman, C.B., Lee, M.K., Davenport, F., Ratovitsky, T., Prada, C.M., Kim, G., Seekins, S., Yager, D.*, et al.* (1996). Familial Alzheimer's disease-linked

presenilin 1 variants elevate Abeta1-42/1-40 ratio in vitro and in vivo. Neuron *17*, 1005-1013.

Brier, M.R., Gordon, B., Friedrichsen, K., McCarthy, J., Stern, A., Christensen, J., Owen, C., Aldea, P., Su, Y., Hassenstab, J.*, et al.* (2016). Tau and Aβ imaging, CSF measures, and cognition in Alzheimer's disease. Sci Transl Med *8*, 338ra366-338ra366.

Brodbeck, J., McGuire, J., Liu, Z., Meyer-Franke, A., Balestra, M.E., Jeong, D.E., Pleiss, M., McComas, C., Hess, F., Witter, D.*, et al.* (2011). Structure-dependent impairment of intracellular apolipoprotein E4 trafficking and its detrimental effects are rescued by small-molecule structure correctors. J Biol Chem *286*, 17217-17226.

Bu, G. (2009). Apolipoprotein E and its receptors in Alzheimer's disease: pathways, pathogenesis and therapy. Nat Rev Neurosci *10*, 333-344.

Butovsky, O., and Weiner, H.L. (2018). Microglial signatures and their role in health and disease. Nat Rev Neurosci.

Cady, J., Koval, E.D., Benitez, B.A., Zaidman, C., Jockel-Balsarotti, J., Allred, P., Baloh, R.H., Ravits, J., Simpson, E., Appel, S.H.*, et al.* (2014). TREM2 variant p.R47H as a risk factor for sporadic amyotrophic lateral sclerosis. JAMA neurology *71*, 449-453.

Campion, D., Dumanchin, C., Hannequin, D., Dubois, B., Belliard, S., Puel, M., Thomas-Anterion, C., Michon, A., Martin, C., Charbonnier, F.*, et al.* (1999). Early-onset autosomal dominant Alzheimer disease: prevalence, genetic heterogeneity, and mutation spectrum. American journal of human genetics *65*, 664-670.

Carbajosa, G., Malki, K., Lawless, N., Wang, H., Ryder, J.W., Wozniak, E., Wood, K., Mein, C.A., Dobson, R.J.B., Collier, D.A.*, et al.* (2018). Loss of Trem2 in microglia leads to widespread disruption of cell coexpression networks in mouse brain. Neurobiol Aging *69*, 151-166.

Carrasquillo, M.M., Barber, I., Lincoln, S.J., Murray, M.E., Camsari, G.B., Khan, Q., Nguyen, T., Ma, L., Bisceglio, G.D., Crook, J.E.*, et al.* (2016). Evaluating pathogenic dementia variants in posterior cortical atrophy. Neurobiol Aging *37*, 38-44.

Carter, A.Y., Letronne, F., Fitz, N.F., Mounier, A., Wolfe, C.M., Nam, K.N., Reeves, V.L., Kamboh, H., Lefterov, I., and Koldamova, R. (2017). Liver X receptor agonist treatment significantly affects phenotype and transcriptome of APOE3 and APOE4 Abca1 haplo-deficient mice. PloS one *12*, e0172161.

Castellano, J.M., Kim, J., Stewart, F.R., Jiang, H., DeMattos, R.B., Patterson, B.W., Fagan, A.M., Morris, J.C., Mawuenyega, K.G., Cruchaga, C.*, et al.* (2011). Human apoE isoforms differentially regulate brain amyloid-beta peptide clearance. Sci Transl Med *3*, 89ra57.

Castranio, E.L., Mounier, A., Wolfe, C.M., Nam, K.N., Fitz, N.F., Letronne, F., Schug, J., Koldamova, R., and Lefterov, I. (2017). Gene co-expression networks identify Trem2 and Tyrobp as major hubs in human APOE expressing mice following traumatic brain injury. Neurobiology of disease *105*, 1-14.

Caughey, B., and Lansbury, P.T. (2003). Protofibrils, pores, fibrils, and neurodegeneration: separating the responsible protein aggregates from the innocent bystanders. Annu Rev Neurosci *26*, 267-298.

Chakraborty, A., de Wit, N.M., van der Flier, W.M., and de Vries, H.E. (2016). The blood brain barrier in Alzheimer's disease. Vascular pharmacology.

Chen, H.K., Ji, Z.S., Dodson, S.E., Miranda, R.D., Rosenblum, C.I., Reynolds, I.J., Freedman, S.B., Weisgraber, K.H., Huang, Y., and Mahley, R.W. (2011). Apolipoprotein E4 domain

interaction mediates detrimental effects on mitochondria and is a potential therapeutic target for Alzheimer disease. J Biol Chem *286*, 5215-5221.

Chen, X., Chen, Y., Wei, Q., Guo, X., Cao, B., Ou, R., Zhao, B., and Shang, H.F. (2015a). Assessment of TREM2 rs75932628 association with amyotrophic lateral sclerosis in a Chinese population. Journal of the neurological sciences *355*, 193-195.

Chen, Y., Chen, X., Guo, X., Song, W., Cao, B., Wei, Q., Ou, R., Zhao, B., and Shang, H.F. (2015b). Assessment of TREM2 rs75932628 association with Parkinson's disease and multiple system atrophy in a Chinese population. Neurological sciences : official journal of the Italian Neurological Society and of the Italian Society of Clinical Neurophysiology *36*, 1903-1906.

Chen, Y., Durakoglugil, M.S., Xian, X., and Herz, J. (2010). ApoE4 reduces glutamate receptor function and synaptic plasticity by selectively impairing ApoE receptor recycling. Proceedings of the National Academy of Sciences of the United States of America *107*, 12011-12016.

Cheng-Hathaway, P.J., Reed-Geaghan, E.G., Jay, T.R., Casali, B.T., Bemiller, S.M., Puntambekar, S.S., von Saucken, V.E., Williams, R.Y., Karlo, J.C., Moutinho, M.*, et al.* (2018). The Trem2 R47H variant confers loss-of-function-like phenotypes in Alzheimer's disease. Molecular neurodegeneration *13*, 29.

Chitu, V., and Stanley, E.R. (2006). Colony-stimulating factor-1 in immunity and inflammation. Current opinion in immunology *18*, 39-48.

Chouery, E., Delague, V., Bergougnoux, A., Koussa, S., Serre, J.L., and Megarbane, A. (2008). Mutations in TREM2 lead to pure early-onset dementia without bone cysts. Human mutation *29*, E194-204.

Chung, W.-S., Verghese, P.B., Chakraborty, C., Joung, J., Hyman, B.T., Ulrich, J.D., Holtzman, D.M., and Barres, B.A. (2016). Novel allele-dependent role for APOE in controlling the rate of synapse pruning by astrocytes. Proceedings of the National Academy of Sciences of the United States of America *113*, 10186-10191.

Cirrito, J.R., May, P.C., O'Dell, M.A., Taylor, J.W., Parsadanian, M., Cramer, J.W., Audia, J.E., Nissen, J.S., Bales, K.R., Paul, S.M.*, et al.* (2003). In vivo assessment of brain interstitial fluid with microdialysis reveals plaque-associated changes in amyloid-beta metabolism and half-life. The Journal of neuroscience : the official journal of the Society for Neuroscience *23*, 8844-8853.

Clayton, K.A., Van Enoo, A.A., and Ikezu, T. (2017). Alzheimer's Disease: The Role of Microglia in Brain Homeostasis and Proteopathy. Front Neurosci *11*, 680.

Colonna, M., and Butovsky, O. (2017). Microglia Function in the Central Nervous System During Health and Neurodegeneration. Annual review of immunology *35*, 441-468.

Colonna, M., and Wang, Y. (2016). TREM2 variants: new keys to decipher Alzheimer disease pathogenesis. Nat Rev Neurosci *17*, 201-207.

Condello, C., Schain, A., and Grutzendler, J. (2011a). Multicolor time-stamp reveals the dynamics and toxicity of amyloid deposition. Scientific reports *1*, 19.

Condello, C., Schain, A., and Grutzendler, J. (2011b). Multicolor time-stamp reveals the dynamics and toxicity of amyloid deposition. Sci Rep *1*, 19-19.

Condello, C., Yuan, P., Schain, A., and Grutzendler, J. (2015). Microglia constitute a barrier that prevents neurotoxic protofibrillar Aβ42 hotspots around plaques. Nat Commun *6*, 6176-6176.

Corder, E.H., Saunders, A.M., Strittmatter, W.J., Schmechel, D.E., Gaskell, P.C., Small, G.W., Roses, A.D., Haines, J.L., and Pericak-Vance, M.A. (1993). Gene dose of apolipoprotein E type 4 allele and the risk of Alzheimer's disease in late onset families. Science (New York, NY) *261*, 921-923.

Cosentino, S., Scarmeas, N., Helzner, E., Glymour, M.M., Brandt, J., Albert, M., Blacker, D., and Stern, Y. (2008). APOE epsilon 4 allele predicts faster cognitive decline in mild Alzheimer disease. Neurology *70*, 1842-1849.

Cramer, P.E., Cirrito, J.R., Wesson, D.W., Lee, C.Y., Karlo, J.C., Zinn, A.E., Casali, B.T., Restivo, J.L., Goebel, W.D., James, M.J.*, et al.* (2012). ApoE-directed therapeutics rapidly clear beta-amyloid and reverse deficits in AD mouse models. Science (New York, NY) *335*, 1503-1506.

Crous-Bou, M., Minguillon, C., Gramunt, N., and Molinuevo, J.L. (2017). Alzheimer's disease prevention: from risk factors to early intervention. Alzheimer's research & therapy *9*, 71.

Cruchaga, C., Kauwe, J.S., Harari, O., Jin, S.C., Cai, Y., Karch, C.M., Benitez, B.A., Jeng, A.T., Skorupa, T., Carrell, D.*, et al.* (2013). GWAS of cerebrospinal fluid tau levels identifies risk variants for Alzheimer's disease. Neuron *78*, 256-268.

Cuyvers, E., Bettens, K., Philtjens, S., Van Langenhove, T., Gijselinck, I., van der Zee, J., Engelborghs, S., Vandenbulcke, M., Van Dongen, J., Geerts, N.*, et al.* (2014). Investigating the role of rare heterozygous TREM2 variants in Alzheimer's disease and frontotemporal dementia. Neurobiol Aging *35*, 726 e711-729.

Daws, M.R., Sullam, P.M., Niemi, E.C., Chen, T.T., Tchao, N.K., and Seaman, W.E. (2003). Pattern recognition by TREM-2: binding of anionic ligands. Journal of immunology (Baltimore, Md : 1950) *171*, 594-599.

Deczkowska, A., Keren-Shaul, H., Weiner, A., Colonna, M., Schwartz, M., and Amit, I. (2018). Disease-Associated Microglia: A Universal Immune Sensor of Neurodegeneration. Cell *173*, 1073-1081.

DeMattos, R.B., Brendza, R.P., Heuser, J.E., Kierson, M., Cirrito, J.R., Fryer, J., Sullivan, P.M., Fagan, A.M., Han, X., and Holtzman, D.M. (2001). Purification and characterization of astrocyte-secreted apolipoprotein E and J-containing lipoproteins from wild-type and human apoE transgenic mice. Neurochem Int *39*, 415-425.

Dong, L.M., and Weisgraber, K.H. (1996). Human apolipoprotein E4 domain interaction. Arginine 61 and glutamic acid 255 interact to direct the preference for very low density lipoproteins. J Biol Chem *271*, 19053-19057.

Dubois, B., Feldman, H.H., Jacova, C., Hampel, H., Molinuevo, J.L., Blennow, K., DeKosky, S.T., Gauthier, S., Selkoe, D., Bateman, R.*, et al.* (2014). Advancing research diagnostic criteria for Alzheimer's disease: the IWG-2 criteria. Lancet Neurol *13*, 614-629.

Dubois, B., Hampel, H., Feldman, H.H., Scheltens, P., Aisen, P., Andrieu, S., Bakardjian, H., Benali, H., Bertram, L., Blennow, K.*, et al.* (2016). Preclinical Alzheimer's disease: Definition, natural history, and diagnostic criteria. Alzheimer's & dementia : the journal of the Alzheimer's Association *12*, 292-323.

Dumanis, S.B., Tesoriero, J.A., Babus, L.W., Nguyen, M.T., Trotter, J.H., Ladu, M.J., Weeber, E.J., Turner, R.S., Xu, B., Rebeck, G.W.*, et al.* (2009). ApoE4 decreases spine density and dendritic complexity in cortical neurons in vivo. The Journal of neuroscience : the official journal of the Society for Neuroscience *29*, 15317-15322.

El Khoury, J., and Luster, A.D. (2008). Mechanisms of microglia accumulation in Alzheimer's disease: therapeutic implications. Trends in pharmacological sciences *29*, 626-632.

Fitz, N.F., Castranio, E.L., Carter, A.Y., Kodali, R., Lefterov, I., and Koldamova, R. (2014). Improvement of memory deficits and amyloid-beta clearance in aged APP23 mice treated with a combination of anti-amyloid-beta antibody and LXR agonist. Journal of Alzheimer's disease : JAD *41*, 535-549.

Fitz, N.F., Cronican, A., Pham, T., Fogg, A., Fauq, A.H., Chapman, R., Lefterov, I., and Koldamova, R. (2010). Liver X receptor agonist treatment ameliorates amyloid pathology and memory deficits caused by high-fat diet in APP23 mice. The Journal of neuroscience : the official journal of the Society for Neuroscience *30*, 6862-6872.

Fitz, N.F., Cronican, A.A., Lefterov, I., and Koldamova, R. (2013). Comment on "ApoE-directed therapeutics rapidly clear β-amyloid and reverse deficits in AD mouse models". Science (New York, NY) *340*, 924-992c.

Fitz, N.F., Cronican, A.A., Saleem, M., Fauq, A.H., Chapman, R., Lefterov, I., and Koldamova, R. (2012). Abca1 deficiency affects Alzheimer's disease-like phenotype in human ApoE4 but not in ApoE3-targeted replacement mice. The Journal of neuroscience : the official journal of the Society for Neuroscience *32*, 13125-13136.

Fitz, N.F., Tapias, V., Cronican, A.A., Castranio, E.L., Saleem, M., Carter, A.Y., Lefterova, M., Lefterov, I., and Koldamova, R. (2015). Opposing effects of Apoe/Apoa1 double deletion on amyloid-beta pathology and cognitive performance in APP mice. Brain *138*, 3699-3715.

Fleming, L.M., Weisgraber, K.H., Strittmatter, W.J., Troncoso, J.C., and Johnson, G.V. (1996). Differential binding of apolipoprotein E isoforms to tau and other cytoskeletal proteins. Experimental neurology *138*, 252-260.

Friedman, B.A., Srinivasan, K., Ayalon, G., Meilandt, W.J., Lin, H., Huntley, M.A., Cao, Y., Lee, S.-H., Haddick, P.C.G., Ngu, H.*, et al.* (2018). Diverse Brain Myeloid Expression Profiles Reveal Distinct Microglial Activation States and Aspects of Alzheimer's Disease Not Evident in Mouse Models. Cell Rep *22*, 832-847.

Fryer, J.D., Demattos, R.B., McCormick, L.M., O'Dell, M.A., Spinner, M.L., Bales, K.R., Paul, S.M., Sullivan, P.M., Parsadanian, M., Bu, G.*, et al.* (2005). The low density lipoprotein receptor regulates the level of central nervous system human and murine apolipoprotein E but does not modify amyloid plaque pathology in PDAPP mice. J Biol Chem *280*, 25754-25759.

Gatz, M., Reynolds, C.A., Fratiglioni, L., Johansson, B., Mortimer, J.A., Berg, S., Fiske, A., and Pedersen, N.L. (2006). Role of genes and environments for explaining Alzheimer disease. Archives of general psychiatry *63*, 168-174.

Ghiso, J., Matsubara, E., Koudinov, A., Choi-Miura, N.H., Tomita, M., Wisniewski, T., and Frangione, B. (1993). The cerebrospinal-fluid soluble form of Alzheimer's amyloid beta is complexed to SP-40,40 (apolipoprotein J), an inhibitor of the complement membrane-attack complex. Biochem J *293 ( Pt 1)*, 27-30.

Giraldo, M., Lopera, F., Siniard, A.L., Corneveaux, J.J., Schrauwen, I., Carvajal, J., Munoz, C., Ramirez-Restrepo, M., Gaiteri, C., Myers, A.J.*, et al.* (2013). Variants in triggering receptor expressed on myeloid cells 2 are associated with both behavioral variant frontotemporal lobar degeneration and Alzheimer's disease. Neurobiol Aging *34*, 2077 e2011-2078.

Gordon, S., Hamann, J., Lin, H.-H., and Stacey, M. (2011). F4/80 and the related adhesion-GPCRs. Eur J Immunol *41*, 2472-2476.

Gosselin, D., Link, V.M., Romanoski, C.E., Fonseca, G.J., Eichenfield, D.Z., Spann, N.J., Stender, J.D., Chun, H.B., Garner, H., Geissmann, F.*, et al.* (2014). Environment drives selection

and function of enhancers controlling tissue-specific macrophage identities. Cell *159*, 1327-1340.

Griciuc, A., Patel, S., Federico, A.N., Choi, S.H., Innes, B.J., Oram, M.K., Cereghetti, G., McGinty, D., Anselmo, A., Sadreyev, R.I.*, et al.* (2019). TREM2 Acts Downstream of CD33 in Modulating Microglial Pathology in Alzheimer's Disease. Neuron *103*, 820-835.e827.

Guerreiro, R., Orme, T., Naj, A.C., Kuzma, A.B., Schellenberg, G.D., and Bras, J. (2018). Is APOE epsilon4 required for Alzheimer's disease to develop in TREM2 p.R47H variant carriers? Neuropathology and applied neurobiology.

Guerreiro, R., Wojtas, A., Bras, J., Carrasquillo, M., Rogaeva, E., Majounie, E., Cruchaga, C., Sassi, C., Kauwe, J.S., Younkin, S.*, et al.* (2013a). TREM2 variants in Alzheimer's disease. The New England journal of medicine *368*, 117-127.

Guerreiro, R.J., Gustafson, D.R., and Hardy, J. (2012). The genetic architecture of Alzheimer's disease: beyond APP, PSENs and APOE. Neurobiol Aging *33*, 437-456.

Guerreiro, R.J., Lohmann, E., Bras, J.M., Gibbs, J.R., Rohrer, J.D., Gurunlian, N., Dursun, B., Bilgic, B., Hanagasi, H., Gurvit, H.*, et al.* (2013b). Using exome sequencing to reveal mutations in TREM2 presenting as a frontotemporal dementia-like syndrome without bone involvement. JAMA neurology *70*, 78-84.

Gyoneva, S., and Ransohoff, R.M. (2015). Inflammatory reaction after traumatic brain injury: therapeutic potential of targeting cell-cell communication by chemokines. Trends in pharmacological sciences *36*, 471-480.

Hansen, D.V., Hanson, J.E., and Sheng, M. (2018). Microglia in Alzheimer's disease. The Journal of cell biology *217*, 459-472.

Hansson, O., Lehmann, S., Otto, M., Zetterberg, H., and Lewczuk, P. (2019). Advantages and disadvantages of the use of the CSF Amyloid β (Aβ) 42/40 ratio in the diagnosis of Alzheimer's Disease. Alzheimer's research & therapy *11*, 34.

Harold, D., Abraham, R., Hollingworth, P., Sims, R., Gerrish, A., Hamshere, M.L., Pahwa, J.S., Moskvina, V., Dowzell, K., Williams, A.*, et al.* (2009). Genome-wide association study identifies variants at CLU and PICALM associated with Alzheimer's disease. Nature genetics *41*, 1088-1093.

Haure-Mirande, J.-V., Audrain, M., Fanutza, T., Kim, S.H., Klein, W.L., Glabe, C., Readhead, B., Dudley, J.T., Blitzer, R.D., Wang, M.*, et al.* (2017). Deficiency of TYROBP, an adapter protein for TREM2 and CR3 receptors, is neuroprotective in a mouse model of early Alzheimer's pathology. Acta neuropathologica *134*, 769-788.

Haure-Mirande, J.-V., Wang, M., Audrain, M., Fanutza, T., Kim, S.H., Heja, S., Readhead, B., Dudley, J.T., Blitzer, R.D., Schadt, E.E.*, et al.* (2019). Integrative approach to sporadic Alzheimer's disease: deficiency of TYROBP in cerebral Aβ amyloidosis mouse normalizes clinical phenotype and complement subnetwork molecular pathology without reducing Aβ burden. Molecular psychiatry *24*, 431-446.

Herz, J., Clouthier, D.E., and Hammer, R.E. (1992). LDL receptor-related protein internalizes and degrades uPA-PAI-1 complexes and is essential for embryo implantation. Cell *71*, 411-421.

Heslegrave, A., Heywood, W., Paterson, R., Magdalinou, N., Svensson, J., Johansson, P., Ohrfelt, A., Blennow, K., Hardy, J., Schott, J.*, et al.* (2016). Increased cerebrospinal fluid soluble TREM2 concentration in Alzheimer's disease. Molecular neurodegeneration *11*, 3.

Hiesberger, T., Trommsdorff, M., Howell, B.W., Goffinet, A., Mumby, M.C., Cooper, J.A., and Herz, J. (1999). Direct binding of Reelin to VLDL receptor and ApoE receptor 2 induces tyrosine phosphorylation of disabled-1 and modulates tau phosphorylation. Neuron *24*, 481-489.

Hirsch-Reinshagen, V., Maia, L.F., Burgess, B.L., Blain, J.F., Naus, K.E., McIsaac, S.A., Parkinson, P.F., Chan, J.Y., Tansley, G.H., Hayden, M.R.*, et al.* (2005). The Absence of ABCA1 Decreases Soluble ApoE Levels but Does Not Diminish Amyloid Deposition in Two Murine Models of Alzheimer Disease. Journal of Biological Chemistry *280*, 43243-43256.

Holtman, I.R., Raj, D.D., Miller, J.A., Schaafsma, W., Yin, Z., Brouwer, N., Wes, P.D., Möller, T., Orre, M., Kamphuis, W.*, et al.* (2015). Induction of a common microglia gene expression signature by aging and neurodegenerative conditions: a co-expression meta-analysis. Acta neuropathologica communications *3*, 31-31.

Holtzman, D.M., Bales, K.R., Tenkova, T., Fagan, A.M., Parsadanian, M., Sartorius, L.J., Mackey, B., Olney, J., McKeel, D., Wozniak, D.*, et al.* (2000). Apolipoprotein E isoform-dependent amyloid deposition and neuritic degeneration in a mouse model of Alzheimer's disease. Proceedings of the National Academy of Sciences of the United States of America *97*, 2892-2897.

Holtzman, D.M., Bales, K.R., Wu, S., Bhat, P., Parsadanian, M., Fagan, A.M., Chang, L.K., Sun, Y., and Paul, S.M. (1999). Expression of human apolipoprotein E reduces amyloid-beta deposition in a mouse model of Alzheimer's disease. J Clin Invest *103*, R15-R21.

Holtzman, D.M., Morris, J.C., and Goate, A.M. (2011). Alzheimer's disease: the challenge of the second century. Sci Transl Med *3*, 77sr71.

Hong, S., Beja-Glasser, V.F., Nfonoyim, B.M., Frouin, A., Li, S., Ramakrishnan, S., Merry, K.M., Shi, Q., Rosenthal, A., Barres, B.A.*, et al.* (2016). Complement and microglia mediate early synapse loss in Alzheimer mouse models. Science (New York, NY) *352*, 712-716.

Hooli, B.V., Lill, C.M., Mullin, K., Qiao, D., Lange, C., Bertram, L., and Tanzi, R.E. (2015). PLD3 gene variants and Alzheimer's disease. Nature *520*, E7-8.

Hopperton, K.E., Mohammad, D., Trépanier, M.O., Giuliano, V., and Bazinet, R.P. (2018). Markers of microglia in post-mortem brain samples from patients with Alzheimer's disease: a systematic review. Molecular Psychiatry *23*, 177-198.

Hsia, A.Y., Masliah, E., McConlogue, L., Yu, G.Q., Tatsuno, G., Hu, K., Kholodenko, D., Malenka, R.C., Nicoll, R.A., and Mucke, L. (1999). Plaque-independent disruption of neural circuits in Alzheimer's disease mouse models. Proceedings of the National Academy of Sciences of the United States of America *96*, 3228-3233.

Hsieh, C.L., Koike, M., Spusta, S.C., Niemi, E.C., Yenari, M., Nakamura, M.C., and Seaman, W.E. (2009). A role for TREM2 ligands in the phagocytosis of apoptotic neuronal cells by microglia. J Neurochem *109*, 1144-1156.

Hu, X., Leak, R.K., Shi, Y., Suenaga, J., Gao, Y., Zheng, P., and Chen, J. (2015). Microglial and macrophage polarization-new prospects for brain repair. Nature reviews Neurology *11*, 56-64.

Huang, D.W., Sherman, B.T., and Lempicki, R.A. (2009). Systematic and integrative analysis of large gene lists using DAVID bioinformatics resources. Nat Protoc *4*, 44-57.

Huynh, T.V., Liao, F., Francis, C.M., Robinson, G.O., Serrano, J.R., Jiang, H., Roh, J., Finn, M.B., Sullivan, P.M., Esparza, T.J.*, et al.* (2017). Age-Dependent Effects of apoE Reduction

Using Antisense Oligonucleotides in a Model of beta-amyloidosis. Neuron *96*, 1013-1023.e1014.

Jansen, I.E., Savage, J.E., Watanabe, K., Bryois, J., Williams, D.M., Steinberg, S., Sealock, J., Karlsson, I.K., Hagg, S., Athanasiu, L.*, et al.* (2019). Genome-wide meta-analysis identifies new loci and functional pathways influencing Alzheimer's disease risk. Nature genetics *51*, 404-413.

Jay, T.R., Hirsch, A.M., Broihier, M.L., Miller, C.M., Neilson, L.E., Ransohoff, R.M., Lamb, B.T., and Landreth, G.E. (2017). Disease Progression-Dependent Effects of TREM2 Deficiency in a Mouse Model of Alzheimer's Disease. The Journal of neuroscience : the official journal of the Society for Neuroscience *37*, 637-647.

Jay, T.R., Miller, C.M., Cheng, P.J., Graham, L.C., Bemiller, S., Broihier, M.L., Xu, G., Margevicius, D., Karlo, J.C., Sousa, G.L.*, et al.* (2015). TREM2 deficiency eliminates TREM2+ inflammatory macrophages and ameliorates pathology in Alzheimer's disease mouse models. J Exp Med *212*, 287-295.

Jellinger, K.A. (2020). Neuropathological assessment of the Alzheimer spectrum. J Neural Transm (Vienna) *127*, 1229-1256.

Jendresen, C., Arskog, V., Daws, M.R., and Nilsson, L.N. (2017). The Alzheimer's disease risk factors apolipoprotein E and TREM2 are linked in a receptor signaling pathway. Journal of neuroinflammation *14*, 59.

Jeon, H., and Blacklow, S.C. (2005). Structure and physiologic function of the low-density lipoprotein receptor. Annual review of biochemistry *74*, 535-562.

Ji, Y., Gong, Y., Gan, W., Beach, T., Holtzman, D.M., and Wisniewski, T. (2003). Apolipoprotein E isoform-specific regulation of dendritic spine morphology in apolipoprotein E transgenic mice and Alzheimer's disease patients. Neuroscience *122*, 305-315.

Jiang, Q., Lee, C.Y., Mandrekar, S., Wilkinson, B., Cramer, P., Zelcer, N., Mann, K., Lamb, B., Willson, T.M., Collins, J.L.*, et al.* (2008a). ApoE promotes the proteolytic degradation of Abeta. Neuron *58*, 681-693.

Jiang, Q., Lee, C.Y., Mandrekar, S., Wilkinson, B., Cramer, P., Zelcer, N., Mann, K., Lamb, B., Willson, T.M., Collins, J.L.*, et al.* (2008b). ApoE promotes the proteolytic degradation of Abeta. Neuron *58*, 681-693.

Jin, S.C., Carrasquillo, M.M., Benitez, B.A., Skorupa, T., Carrell, D., Patel, D., Lincoln, S., Krishnan, S., Kachadoorian, M., Reitz, C.*, et al.* (2015). TREM2 is associated with increased risk for Alzheimer's disease in African Americans. Molecular neurodegeneration *10*, 19.

Jonsson, T., Stefansson, H., Steinberg, S., Jonsdottir, I., Jonsson, P.V., Snaedal, J., Bjornsson, S., Huttenlocher, J., Levey, A.I., Lah, J.J.*, et al.* (2013). Variant of TREM2 associated with the risk of Alzheimer's disease. The New England journal of medicine *368*, 107-116.

Jun, G., Naj, A.C., Beecham, G.W., Wang, L.S., Buros, J., Gallins, P.J., Buxbaum, J.D., Ertekin-Taner, N., Fallin, M.D., Friedland, R.*, et al.* (2010). Meta-analysis confirms CR1, CLU, and PICALM as alzheimer disease risk loci and reveals interactions with APOE genotypes. Archives of neurology *67*, 1473-1484.

Kanekiyo, T., and Bu, G. (2014). The low-density lipoprotein receptor-related protein 1 and amyloid-beta clearance in Alzheimer's disease. Frontiers in aging neuroscience *6*, 93.

Kanekiyo, T., Xu, H., and Bu, G. (2014). ApoE and Abeta in Alzheimer's disease: accidental encounters or partners? Neuron *81*, 740-754.

Karch, C.M., Cruchaga, C., and Goate, A.M. (2014). Alzheimer's disease genetics: from the bench to the clinic. Neuron *83*, 11-26.

Kayed, R., Head, E., Sarsoza, F., Saing, T., Cotman, C.W., Necula, M., Margol, L., Wu, J., Breydo, L., Thompson, J.L.*, et al.* (2007). Fibril specific, conformation dependent antibodies recognize a generic epitope common to amyloid fibrils and fibrillar oligomers that is absent in prefibrillar oligomers. Molecular neurodegeneration *2*, 18-18.

Kelker, M.S., Foss, T.R., Peti, W., Teyton, L., Kelly, J.W., Wuthrich, K., and Wilson, I.A. (2004). Crystal structure of human triggering receptor expressed on myeloid cells 1 (TREM-1) at 1.47 A. Journal of molecular biology *342*, 1237-1248.

Keren-Shaul, H., Spinrad, A., Weiner, A., Matcovitch-Natan, O., Dvir-Szternfeld, R., Ulland, T.K., David, E., Baruch, K., Lara-Astaiso, D., Toth, B.*, et al.* (2017). A Unique Microglia Type Associated with Restricting Development of Alzheimer's Disease. Cell *169*, 1276-1290.e1217.

Kim, J., Eltorai, A.E., Jiang, H., Liao, F., Verghese, P.B., Kim, J., Stewart, F.R., Basak, J.M., and Holtzman, D.M. (2012). Anti-apoE immunotherapy inhibits amyloid accumulation in a transgenic mouse model of Abeta amyloidosis. J Exp Med *209*, 2149-2156.

Kim, J., Jiang, H., Park, S., Eltorai, A.E., Stewart, F.R., Yoon, H., Basak, J.M., Finn, M.B., and Holtzman, D.M. (2011). Haploinsufficiency of human APOE reduces amyloid deposition in a mouse model of amyloid-beta amyloidosis. The Journal of neuroscience : the official journal of the Society for Neuroscience *31*, 18007-18012.

Kleinberger, G., Yamanishi, Y., Suarez-Calvet, M., Czirr, E., Lohmann, E., Cuyvers, E., Struyfs, H., Pettkus, N., Wenninger-Weinzierl, A., Mazaheri, F.*, et al.* (2014). TREM2 mutations implicated in neurodegeneration impair cell surface transport and phagocytosis. Sci Transl Med *6*, 243ra286.

Klesney-Tait, J., Turnbull, I.R., and Colonna, M. (2006). The TREM receptor family and signal integration. Nat Immunol *7*, 1266-1273.

Klunemann, H.H., Ridha, B.H., Magy, L., Wherrett, J.R., Hemelsoet, D.M., Keen, R.W., De Bleecker, J.L., Rossor, M.N., Marienhagen, J., Klein, H.E.*, et al.* (2005). The genetic causes of basal ganglia calcification, dementia, and bone cysts: DAP12 and TREM2. Neurology *64*, 1502-1507.

Klunk, W.E., Bacskai, B.J., Mathis, C.A., Kajdasz, S.T., McLellan, M.E., Frosch, M.P., Debnath, M.L., Holt, D.P., Wang, Y., and Hyman, B.T. (2002). Imaging Abeta plaques in living transgenic mice with multiphoton microscopy and methoxy-X04, a systemically administered Congo red derivative. J Neuropathol Exp Neurol *61*, 797-805.

Knopman, D.S., Petersen, R.C., and Jack, C.R., Jr. (2019). A brief history of "Alzheimer disease": Multiple meanings separated by a common name. Neurology *92*, 1053-1059.

Kober, D.L., Alexander-Brett, J.M., Karch, C.M., Cruchaga, C., Colonna, M., Holtzman, M.J., and Brett, T.J. (2016). Neurodegenerative disease mutations in TREM2 reveal a functional surface and distinct loss-of-function mechanisms. eLife *5*.

Koffie, R.M., Hyman, B.T., and Spires-Jones, T.L. (2011). Alzheimer's disease: synapses gone cold. Molecular neurodegeneration *6*, 63.

Koistinaho, M., Lin, S., Wu, X., Esterman, M., Koger, D., Hanson, J., Higgs, R., Liu, F., Malkani, S., Bales, K.R.*, et al.* (2004). Apolipoprotein E promotes astrocyte colocalization and degradation of deposited amyloid-beta peptides. Nature medicine *10*, 719-726.

Koldamova, R., Fitz, N.F., and Lefterov, I. (2010). The role of ATP-binding cassette transporter A1 in Alzheimer's disease and neurodegeneration. Biochim Biophys Acta *1801*, 824-830.

Koldamova, R., Fitz, N.F., and Lefterov, I. (2014). ATP-binding cassette transporter A1: from metabolism to neurodegeneration. Neurobiology of disease *72 Pt A*, 13-21.

Koldamova, R., Staufenbiel, M., and Lefterov, I. (2005a). Lack of ABCA1 considerably decreases brain ApoE level and increases amyloid deposition in APP23 mice. J Biol Chem *280*, 43224-43235.

Koldamova, R.P., Lefterov, I.M., Lefterova, M.I., and Lazo, J.S. (2001). Apolipoprotein A-I directly interacts with amyloid precursor protein and inhibits A beta aggregation and toxicity. Biochemistry *40*, 3553-3560.

Koldamova, R.P., Lefterov, I.M., Staufenbiel, M., Wolfe, D., Huang, S., Glorioso, J.C., Walter, M., Roth, M.G., and Lazo, J.S. (2005b). The Liver X Receptor Ligand T0901317 Decreases Amyloid {beta} Production in Vitro and in a Mouse Model of Alzheimer's Disease. Journal of Biological Chemistry *280*, 4079-4088.

Kowal, R.C., Herz, J., Weisgraber, K.H., Mahley, R.W., Brown, M.S., and Goldstein, J.L. (1990). Opposing effects of apolipoproteins E and C on lipoprotein binding to low density lipoprotein receptor-related protein. J Biol Chem *265*, 10771-10779.

Krasemann, S., Madore, C., Cialic, R., Baufeld, C., Calcagno, N., El Fatimy, R., Beckers, L., O'Loughlin, E., Xu, Y., Fanek, Z*., et al.* (2017). The TREM2-APOE Pathway Drives the Transcriptional Phenotype of Dysfunctional Microglia in Neurodegenerative Diseases. Immunity *47*, 566-581.e569.

Kuszczyk, M.A., Sanchez, S., Pankiewicz, J., Kim, J., Duszczyk, M., Guridi, M., Asuni, A.A., Sullivan, P.M., Holtzman, D.M., and Sadowski, M.J. (2013). Blocking the interaction between apolipoprotein E and Abeta reduces intraneuronal accumulation of Abeta and inhibits synaptic degeneration. Am J Pathol *182*, 1750-1768.

LaDu, M.J., Falduto, M.T., Manelli, A.M., Reardon, C.A., Getz, G.S., and Frail, D.E. (1994). Isoform-specific binding of apolipoprotein E to beta-amyloid. J Biol Chem *269*, 23403-23406.

Lambert, J.C., Ibrahim-Verbaas, C.A., Harold, D., Naj, A.C., Sims, R., Bellenguez, C., DeStafano, A.L., Bis, J.C., Beecham, G.W., Grenier-Boley, B*., et al.* (2013). Meta-analysis of 74,046 individuals identifies 11 new susceptibility loci for Alzheimer's disease. Nature genetics *45*, 1452-1458.

Lane-Donovan, C., Philips, G.T., and Herz, J. (2014). More than cholesterol transporters: lipoprotein receptors in CNS function and neurodegeneration. Neuron *83*, 771-787.

Lane-Donovan, C., Wong, W.M., Durakoglugil, M.S., Wasser, C.R., Jiang, S., Xian, X., and Herz, J. (2016). Genetic Restoration of Plasma ApoE Improves Cognition and Partially Restores Synaptic Defects in ApoE-Deficient Mice. The Journal of neuroscience : the official journal of the Society for Neuroscience *36*, 10141-10150.

Langfelder, P., and Horvath, S. (2008). WGCNA: an R package for weighted correlation network analysis. BMC Bioinformatics *9*, 559.

Larson, E.B., Yaffe, K., and Langa, K.M. (2013). New insights into the dementia epidemic. The New England journal of medicine *369*, 2275-2277.

Le Ber, I., De Septenville, A., Guerreiro, R., Bras, J., Camuzat, A., Caroppo, P., Lattante, S., Couarch, P., Kabashi, E., Bouya-Ahmed, K*., et al.* (2014). Homozygous TREM2 mutation in a family with atypical frontotemporal dementia. Neurobiol Aging *35*, 2419.e2423-2419.e2425.

Lee, C.Y., Tse, W., Smith, J.D., and Landreth, G.E. (2012). Apolipoprotein E promotes beta-amyloid trafficking and degradation by modulating microglial cholesterol levels. J Biol Chem *287*, 2032-2044.

Lee, C.Y.D., Daggett, A., Gu, X., Jiang, L.L., Langfelder, P., Li, X., Wang, N., Zhao, Y., Park, C.S., Cooper, Y.*, et al.* (2018). Elevated TREM2 Gene Dosage Reprograms Microglia Responsivity and Ameliorates Pathological Phenotypes in Alzheimer's Disease Models. Neuron *97*, 1032-1048.e1035.

Lefterov, I., Wolfe, C.M., Fitz, N.F., Nam, K.N., Letronne, F., Biedrzycki, R.J., Kofler, J., Han, X., Wang, J., Schug, J.*, et al.* (2019). APOE2 orchestrated differences in transcriptomic and lipidomic profiles of postmortem AD brain. Alzheimer's research & therapy *11*, 113-113.

Lein, E.S., Hawrylycz, M.J., Ao, N., Ayres, M., Bensinger, A., Bernard, A., Boe, A.F., Boguski, M.S., Brockway, K.S., Byrnes, E.J.*, et al.* (2007). Genome-wide atlas of gene expression in the adult mouse brain. Nature *445*, 168-176.

Lessard, C.B., Malnik, S.L., Zhou, Y., Ladd, T.B., Cruz, P.E., Ran, Y., Mahan, T.E., Chakrabaty, P., Holtzman, D.M., Ulrich, J.D.*, et al.* (2018). High-affinity interactions and signal transduction between Abeta oligomers and TREM2. EMBO Mol Med *10*.

Li, N., Xu, W., Yuan, Y., Ayithan, N., Imai, Y., Wu, X., Miller, H., Olson, M., Feng, Y., Huang, Y.H.*, et al.* (2017). Immune-checkpoint protein VISTA critically regulates the IL-23/IL-17 inflammatory axis. Sci Rep *7*, 1485.

Li, Y., Du, X.F., and Du, J.L. (2013). Resting microglia respond to and regulate neuronal activity in vivo. Communicative & integrative biology *6*, e24493.

Liao, F., Li, A., Xiong, M., Bien-Ly, N., Jiang, H., Zhang, Y., Finn, M.B., Hoyle, R., Keyser, J., Lefton, K.B.*, et al.* (2018). Targeting of nonlipidated, aggregated apoE with antibodies inhibits amyloid accumulation. J Clin Invest *128*, 2144-2155.

Liao, Y., Smyth, G.K., and Shi, W. (2013). The Subread aligner: fast, accurate and scalable read mapping by seed-and-vote. Nucleic Acids Res *41*, e108-e108.

Liao, Y., Smyth, G.K., and Shi, W. (2019). The R package Rsubread is easier, faster, cheaper and better for alignment and quantification of RNA sequencing reads. Nucleic Acids Res *47*, e47-e47.

Lill, C.M., Rengmark, A., Pihlstrom, L., Fogh, I., Shatunov, A., Sleiman, P.M., Wang, L.S., Liu, T., Lassen, C.F., Meissner, E.*, et al.* (2015). The role of TREM2 R47H as a risk factor for Alzheimer's disease, frontotemporal lobar degeneration, amyotrophic lateral sclerosis, and Parkinson's disease. Alzheimer's & dementia : the journal of the Alzheimer's Association *11*, 1407-1416.

Liu, C.C., Kanekiyo, T., Xu, H., and Bu, G. (2013). Apolipoprotein E and Alzheimer disease: risk, mechanisms and therapy. Nature reviews Neurology *9*, 106-118.

Liu, C.C., Zhao, N., Fu, Y., Wang, N., Linares, C., Tsai, C.W., and Bu, G. (2017). ApoE4 Accelerates Early Seeding of Amyloid Pathology. Neuron *96*, 1024-1032.e1023.

Liu, D., Cao, B., Zhao, Y., Huang, H., McIntyre, R.S., Rosenblat, J.D., and Zhou, H. (2018). Soluble TREM2 changes during the clinical course of Alzheimer's disease: A meta-analysis. Neuroscience letters.

Liu, Q., Zerbinatti, C.V., Zhang, J., Hoe, H.S., Wang, B., Cole, S.L., Herz, J., Muglia, L., and Bu, G. (2007). Amyloid precursor protein regulates brain apolipoprotein E and cholesterol metabolism through lipoprotein receptor LRP1. Neuron *56*, 66-78.

Love, M.I., Huber, W., and Anders, S. (2014). Moderated estimation of fold change and dispersion for RNA-seq data with DESeq2. Genome Biology *15*, 550.

Love, S., Siew, L.K., Dawbarn, D., Wilcock, G.K., Ben-Shlomo, Y., and Allen, S.J. (2006). Premorbid effects of APOE on synaptic proteins in human temporal neocortex. Neurobiol Aging *27*, 797-803.

Mahley, R.W. (2016). Central Nervous System Lipoproteins: ApoE and Regulation of Cholesterol Metabolism. Arteriosclerosis, thrombosis, and vascular biology *36*, 1305-1315.

Mahley, R.W., Weisgraber, K.H., and Huang, Y. (2009). Apolipoprotein E: structure determines function, from atherosclerosis to Alzheimer's disease to AIDS. J Lipid Res *50 Suppl*, S183-188.

Mahoney-Sanchez, L., Belaidi, A.A., Bush, A.I., and Ayton, S. (2016). The Complex Role of Apolipoprotein E in Alzheimer's Disease: an Overview and Update. Journal of molecular neuroscience : MN *60*, 325-335.

Mandrekar-Colucci, S., Karlo, J.C., and Landreth, G.E. (2012). Mechanisms underlying the rapid peroxisome proliferator-activated receptor-gamma-mediated amyloid clearance and reversal of cognitive deficits in a murine model of Alzheimer's disease. The Journal of neuroscience : the official journal of the Society for Neuroscience *32*, 10117-10128.

Manelli, A.M., Stine, W.B., Van Eldik, L.J., and LaDu, M.J. (2004). ApoE and Abeta1-42 interactions: effects of isoform and conformation on structure and function. Journal of molecular neuroscience : MN *23*, 235-246.

Martinez, F.O., Gordon, S., Locati, M., and Mantovani, A. (2006). Transcriptional profiling of the human monocyte-to-macrophage differentiation and polarization: new molecules and patterns of gene expression. Journal of immunology (Baltimore, Md : 1950) *177*, 7303-7311.

Masliah, E., Mallory, M., Alford, M., DeTeresa, R., Hansen, L.A., McKeel, D.W., Jr., and Morris, J.C. (2001). Altered expression of synaptic proteins occurs early during progression of Alzheimer's disease. Neurology *56*, 127-129.

Mauch, D.H., Nagler, K., Schumacher, S., Goritz, C., Muller, E.C., Otto, A., and Pfrieger, F.W. (2001). CNS synaptogenesis promoted by glia-derived cholesterol. Science (New York, NY) *294*, 1354-1357.

May, P., Rohlmann, A., Bock, H.H., Zurhove, K., Marth, J.D., Schomburg, E.D., Noebels, J.L., Beffert, U., Sweatt, J.D., Weeber, E.J.*, et al.* (2004). Neuronal LRP1 functionally associates with postsynaptic proteins and is required for normal motor function in mice. Molecular and cellular biology *24*, 8872-8883.

Mazaheri, F., Snaidero, N., Kleinberger, G., Madore, C., Daria, A., Werner, G., Krasemann, S., Capell, A., Trumbach, D., Wurst, W.*, et al.* (2017). TREM2 deficiency impairs chemotaxis and microglial responses to neuronal injury. EMBO reports *18*, 1186-1198.

Minett, T., Classey, J., Matthews, F.E., Fahrenhold, M., Taga, M., Brayne, C., Ince, P.G., Nicoll, J.A.R., Boche, D., and Mrc, C. (2016). Microglial immunophenotype in dementia with Alzheimer's pathology. Journal of neuroinflammation *13*, 135.

Mitrasinovic, O.M., Vincent, V.A., Simsek, D., and Murphy, G.M., Jr. (2003). Macrophage colony stimulating factor promotes phagocytosis by murine microglia. Neuroscience letters *344*, 185-188.

Mounier, A., Georgiev, D., Nam, K.N., Fitz, N.F., Castranio, E., Wolfe, C., Cronican, A.A., Schug, J., Lefterov, I., and Koldamova, R. (2015). Bexarotene-Activated Retinoid X Receptors

Regulate Neuronal Differentiation and Dendritic Complexity. Journal of Neuroscience *35*, 11862-11876.

Mucke, L., Masliah, E., Yu, G.Q., Mallory, M., Rockenstein, E.M., Tatsuno, G., Hu, K., Kholodenko, D., Johnson-Wood, K., and McConlogue, L. (2000). High-level neuronal expression of abeta 1-42 in wild-type human amyloid protein precursor transgenic mice: synaptotoxicity without plaque formation. The Journal of neuroscience : the official journal of the Society for Neuroscience *20*, 4050-4058.

Nagata, K.O., Nakada, C., Kasai, R.S., Kusumi, A., and Ueda, K. (2013). ABCA1 dimer-monomer interconversion during HDL generation revealed by single-molecule imaging. Proceedings of the National Academy of Sciences of the United States of America *110*, 5034-5039.

Naj, A.C., Jun, G., Beecham, G.W., Wang, L.S., Vardarajan, B.N., Buros, J., Gallins, P.J., Buxbaum, J.D., Jarvik, G.P., Crane, P.K.*, et al.* (2011). Common variants at MS4A4/MS4A6E, CD2AP, CD33 and EPHA1 are associated with late-onset Alzheimer's disease. Nature genetics *43*, 436-441.

Nam, K.N., Wolfe, C.M., Fitz, N.F., Letronne, F., Castranio, E.L., Mounier, A., Schug, J., Lefterov, I., and Koldamova, R. (2018). Integrated approach reveals diet, APOE genotype and sex affect immune response in APP mice. Biochimica et biophysica acta Molecular basis of disease *1864*, 152-161.

Neu, S.C., Pa, J., Kukull, W., Beekly, D., Kuzma, A., Gangadharan, P., Wang, L.S., Romero, K., Arneric, S.P., Redolfi, A.*, et al.* (2017). Apolipoprotein E Genotype and Sex Risk Factors for Alzheimer Disease: A Meta-analysis. JAMA Neurol *74*, 1178-1189.

Ni, C.L., Shi, H.P., Yu, H.M., Chang, Y.C., and Chen, Y.R. (2011). Folding stability of amyloid-beta 40 monomer is an important determinant of the nucleation kinetics in fibrillization. FASEB journal : official publication of the Federation of American Societies for Experimental Biology *25*, 1390-1401.

Nixon, R.A. (2017). Amyloid precursor protein and endosomal-lysosomal dysfunction in Alzheimer's disease: inseparable partners in a multifactorial disease. FASEB journal : official publication of the Federation of American Societies for Experimental Biology *31*, 2729-2743.

Numasawa, Y., Yamaura, C., Ishihara, S., Shintani, S., Yamazaki, M., Tabunoki, H., and Satoh, J.I. (2011). Nasu-Hakola disease with a splicing mutation of TREM2 in a Japanese family. European journal of neurology *18*, 1179-1183.

O'Donoghue, M.C., Murphy, S.E., Zamboni, G., Nobre, A.C., and Mackay, C.E. (2018). APOE genotype and cognition in healthy individuals at risk of Alzheimer's disease: A review. Cortex; a journal devoted to the study of the nervous system and behavior *104*, 103-123.

Otero, K., Turnbull, I.R., Poliani, P.L., Vermi, W., Cerutti, E., Aoshi, T., Tassi, I., Takai, T., Stanley, S.L., Miller, M.*, et al.* (2009). Macrophage colony-stimulating factor induces the proliferation and survival of macrophages via a pathway involving DAP12 and beta-catenin. Nat Immunol *10*, 734-743.

Painter, M.M., Atagi, Y., Liu, C.C., Rademakers, R., Xu, H., Fryer, J.D., and Bu, G. (2015). TREM2 in CNS homeostasis and neurodegenerative disease. Molecular neurodegeneration *10*, 43.

Paloneva, J., Mandelin, J., Kiialainen, A., Bohling, T., Prudlo, J., Hakola, P., Haltia, M., Konttinen, Y.T., and Peltonen, L. (2003). DAP12/TREM2 deficiency results in impaired osteoclast differentiation and osteoporotic features. J Exp Med *198*, 669-675.

Paloneva, J., Manninen, T., Christman, G., Hovanes, K., Mandelin, J., Adolfsson, R., Bianchin, M., Bird, T., Miranda, R., Salmaggi, A., *et al.* (2002). Mutations in two genes encoding different subunits of a receptor signaling complex result in an identical disease phenotype. American journal of human genetics *71*, 656-662.

Pankiewicz, J.E., Guridi, M., Kim, J., Asuni, A.A., Sanchez, S., Sullivan, P.M., Holtzman, D.M., and Sadowski, M.J. (2014). Blocking the apoE/Abeta interaction ameliorates Abeta-related pathology in APOE epsilon2 and epsilon4 targeted replacement Alzheimer model mice. Acta Neuropathol Commun *2*, 75.

Parhizkar, S., Arzberger, T., Brendel, M., Kleinberger, G., Deussing, M., Focke, C., Nuscher, B., Xiong, M., Ghasemigharagoz, A., Katzmarski, N., *et al.* (2019). Loss of TREM2 function increases amyloid seeding but reduces plaque-associated ApoE. Nature neuroscience *22*, 191-204.

Passer, B., Pellegrini, L., Russo, C., Siegel, R.M., Lenardo, M.J., Schettini, G., Bachmann, M., Tabaton, M., and D'Adamio, L. (2000). Generation of an apoptotic intracellular peptide by gamma-secretase cleavage of Alzheimer's amyloid beta protein precursor. Journal of Alzheimer's disease : JAD *2*, 289-301.

Peng, Q., Malhotra, S., Torchia, J.A., Kerr, W.G., Coggeshall, K.M., and Humphrey, M.B. (2010). TREM2- and DAP12-dependent activation of PI3K requires DAP10 and is inhibited by SHIP1. Sci Signal *3*, ra38.

Piccio, L., Deming, Y., Del-Aguila, J.L., Ghezzi, L., Holtzman, D.M., Fagan, A.M., Fenoglio, C., Galimberti, D., Borroni, B., and Cruchaga, C. (2016). Cerebrospinal fluid soluble TREM2 is higher in Alzheimer disease and associated with mutation status. Acta Neuropathol *131*, 925-933.

Pimenova, A.A., Raj, T., and Goate, A.M. (2018). Untangling Genetic Risk for Alzheimer's Disease. Biological psychiatry *83*, 300-310.

Poliani, P.L., Wang, Y., Fontana, E., Robinette, M.L., Yamanishi, Y., Gilfillan, S., and Colonna, M. (2015). TREM2 sustains microglial expansion during aging and response to demyelination. J Clin Invest *125*, 2161-2170.

Price, A.R., Xu, G., Siemienski, Z.B., Smithson, L.A., Borchelt, D.R., Golde, T.E., and Felsenstein, K.M. (2013). Comment on "ApoE-directed therapeutics rapidly clear beta-amyloid and reverse deficits in AD mouse models". Science (New York, NY) *340*, 924-d.

Rauchmann, B.S., Schneider-Axmann, T., Alexopoulos, P., Perneczky, R., and Alzheimer's Disease Neuroimaging, I. (2018). CSF soluble TREM2 as a measure of immune response along the Alzheimer's disease continuum. Neurobiol Aging *74*, 182-190.

Rayaprolu, S., Mullen, B., Baker, M., Lynch, T., Finger, E., Seeley, W.W., Hatanpaa, K.J., Lomen-Hoerth, C., Kertesz, A., Bigio, E.H., *et al.* (2013). TREM2 in neurodegeneration: evidence for association of the p.R47H variant with frontotemporal dementia and Parkinson's disease. Molecular neurodegeneration *8*, 19.

Robinson, M.D., McCarthy, D.J., and Smyth, G.K. (2009). edgeR: a Bioconductor package for differential expression analysis of digital gene expression data. Bioinformatics *26*, 139-140.

Ruiz, J., Kouiavskaia, D., Migliorini, M., Robinson, S., Saenko, E.L., Gorlatova, N., Li, D., Lawrence, D., Hyman, B.T., Weisgraber, K.H., *et al.* (2005). The apoE isoform binding properties of the VLDL receptor reveal marked differences from LRP and the LDL receptor. J Lipid Res *46*, 1721-1731.

Saber, M., Kokiko-Cochran, O., Puntambekar, S.S., Lathia, J.D., and Lamb, B.T. (2017). Triggering Receptor Expressed on Myeloid Cells 2 Deficiency Alters Acute Macrophage Distribution and Improves Recovery after Traumatic Brain Injury. Journal of neurotrauma *34*, 423-435.

Sasaki, A., Kakita, A., Yoshida, K., Konno, T., Ikeuchi, T., Hayashi, S., Matsuo, H., and Shioda, K. (2015). Variable expression of microglial DAP12 and TREM2 genes in Nasu-Hakola disease. Neurogenetics *16*, 265-276.

Satoh, J., Tabunoki, H., Ishida, T., Yagishita, S., Jinnai, K., Futamura, N., Kobayashi, M., Toyoshima, I., Yoshioka, T., Enomoto, K.*, et al.* (2011). Immunohistochemical characterization of microglia in Nasu-Hakola disease brains. Neuropathology : official journal of the Japanese Society of Neuropathology *31*, 363-375.

Saunders, A.M., Strittmatter, W.J., Schmechel, D., George-Hyslop, P.H., Pericak-Vance, M.A., Joo, S.H., Rosi, B.L., Gusella, J.F., Crapper-MacLachlan, D.R., Alberts, M.J.*, et al.* (1993). Association of apolipoprotein E allele epsilon 4 with late-onset familial and sporadic Alzheimer's disease. Neurology *43*, 1467-1472.

Schmechel, D.E., Saunders, A.M., Strittmatter, W.J., Crain, B.J., Hulette, C.M., Joo, S.H., Pericak-Vance, M.A., Goldgaber, D., and Roses, A.D. (1993). Increased amyloid beta-peptide deposition in cerebral cortex as a consequence of apolipoprotein E genotype in late-onset Alzheimer disease. Proceedings of the National Academy of Sciences of the United States of America *90*, 9649-9653.

Schmidt, M., Sachse, C., Richter, W., Xu, C., Fandrich, M., and Grigorieff, N. (2009). Comparison of Alzheimer Abeta(1-40) and Abeta(1-42) amyloid fibrils reveals similar protofilament structures. Proceedings of the National Academy of Sciences of the United States of America *106*, 19813-19818.

Selkoe, D.J., and Hardy, J. (2016). The amyloid hypothesis of Alzheimer's disease at 25 years. EMBO molecular medicine *8*, 595-608.

Sheng, M., Sabatini, B.L., and Sudhof, T.C. (2012). Synapses and Alzheimer's disease. Cold Spring Harbor perspectives in biology *4*.

Shi, Y., and Holtzman, D.M. (2018). Interplay between innate immunity and Alzheimer disease: APOE and TREM2 in the spotlight. Nat Rev Immunol.

Shi, Y., Yamada, K., Liddelow, S.A., Smith, S.T., Zhao, L., Luo, W., Tsai, R.M., Spina, S., Grinberg, L.T., Rojas, J.C.*, et al.* (2017). ApoE4 markedly exacerbates tau-mediated neurodegeneration in a mouse model of tauopathy. Nature *549*, 523-527.

Shinohara, M., Tachibana, M., Kanekiyo, T., and Bu, G. (2017). Role of LRP1 in the pathogenesis of Alzheimer's disease: evidence from clinical and preclinical studies. J Lipid Res *58*, 1267-1281.

Sims, R., van der Lee, S.J., Naj, A.C., Bellenguez, C., Badarinarayan, N., Jakobsdottir, J., Kunkle, B.W., Boland, A., Raybould, R., Bis, J.C.*, et al.* (2017). Rare coding variants in PLCG2, ABI3, and TREM2 implicate microglial-mediated innate immunity in Alzheimer's disease. Nature genetics *49*, 1373-1384.

Sisodia, S.S. (1992). Beta-amyloid precursor protein cleavage by a membrane-bound protease. Proceedings of the National Academy of Sciences of the United States of America *89*, 6075-6079.

Skerrett, R., Malm, T., and Landreth, G. (2014). Nuclear receptors in neurodegenerative diseases. Neurobiology of disease *72 Pt A*, 104-116.

Slattery, C.F., Beck, J.A., Harper, L., Adamson, G., Abdi, Z., Uphill, J., Campbell, T., Druyeh, R., Mahoney, C.J., Rohrer, J.D.*, et al.* (2014). R47H TREM2 variant increases risk of typical early-onset Alzheimer's disease but not of prion or frontotemporal dementia. Alzheimer's & dementia : the journal of the Alzheimer's Association *10*, 602-608.e604.

Small, B.J., Rosnick, C.B., Fratiglioni, L., and Backman, L. (2004). Apolipoprotein E and cognitive performance: a meta-analysis. Psychology and aging *19*, 592-600.

Song, W.M., Joshita, S., Zhou, Y., Ulland, T.K., Gilfillan, S., and Colonna, M. (2018). Humanized TREM2 mice reveal microglia-intrinsic and -extrinsic effects of R47H polymorphism. J Exp Med *215*, 745-760.

Soragna, D., Papi, L., Ratti, M.T., Sestini, R., Tupler, R., and Montalbetti, L. (2003). An Italian family affected by Nasu-Hakola disease with a novel genetic mutation in the TREM2 gene. Journal of neurology, neurosurgery, and psychiatry *74*, 825-826.

Sperling, R.A., Aisen, P.S., Beckett, L.A., Bennett, D.A., Craft, S., Fagan, A.M., Iwatsubo, T., Jack, C.R., Jr., Kaye, J., Montine, T.J.*, et al.* (2011). Toward defining the preclinical stages of Alzheimer's disease: recommendations from the National Institute on Aging-Alzheimer's Association workgroups on diagnostic guidelines for Alzheimer's disease. Alzheimer's & dementia : the journal of the Alzheimer's Association *7*, 280-292.

Strittmatter, W.J., Saunders, A.M., Goedert, M., Weisgraber, K.H., Dong, L.M., Jakes, R., Huang, D.Y., Pericak-Vance, M., Schmechel, D., and Roses, A.D. (1994). Isoform-specific interactions of apolipoprotein E with microtubule-associated protein tau: implications for Alzheimer disease. Proceedings of the National Academy of Sciences of the United States of America *91*, 11183-11186.

Strittmatter, W.J., Saunders, A.M., Schmechel, D., Pericak-Vance, M., Enghild, J., Salvesen, G.S., and Roses, A.D. (1993). Apolipoprotein E: high-avidity binding to beta-amyloid and increased frequency of type 4 allele in late-onset familial Alzheimer disease. Proceedings of the National Academy of Sciences of the United States of America *90*, 1977-1981.

Suarez-Calvet, M., Kleinberger, G., Araque Caballero, M.A., Brendel, M., Rominger, A., Alcolea, D., Fortea, J., Lleo, A., Blesa, R., Gispert, J.D.*, et al.* (2016). sTREM2 cerebrospinal fluid levels are a potential biomarker for microglia activity in early-stage Alzheimer's disease and associate with neuronal injury markers. EMBO molecular medicine *8*, 466-476.

Sudom, A., Talreja, S., Danao, J., Bragg, E., Kegel, R., Min, X., Richardson, J., Zhang, Z., Sharkov, N., Marcora, E.*, et al.* (2018). Molecular basis for the loss-of-function effects of the Alzheimer's disease-associated R47H variant of the immune receptor TREM2. J Biol Chem *293*, 12634-12646.

Sullivan, P.M., Mezdour, H., Aratani, Y., Knouff, C., Najib, J., Reddick, R.L., Quarfordt, S.H., and Maeda, N. (1997). Targeted replacement of the mouse apolipoprotein E gene with the common human APOE3 allele enhances diet-induced hypercholesterolemia and atherosclerosis. J Biol Chem *272*, 17972-17980.

Szklarczyk, D., Gable, A.L., Lyon, D., Junge, A., Wyder, S., Huerta-Cepas, J., Simonovic, M., Doncheva, N.T., Morris, J.H., Bork, P.*, et al.* (2019). STRING v11: protein-protein association networks with increased coverage, supporting functional discovery in genome-wide experimental datasets. Nucleic Acids Res *47*, D607-D613.

Takahashi, K., Rochford, C.D., and Neumann, H. (2005). Clearance of apoptotic neurons without inflammation by microglial triggering receptor expressed on myeloid cells-2. J Exp Med *201*, 647-657.

Takeda, S., Hashimoto, T., Roe, A.D., Hori, Y., Spires-Jones, T.L., and Hyman, B.T. (2013). Brain interstitial oligomeric amyloid β increases with age and is resistant to clearance from brain in a mouse model of Alzheimer's disease. FASEB journal : official publication of the Federation of American Societies for Experimental Biology *27*, 3239-3248.

Tanaka, M., Saito, S., Inoue, T., Satoh-Asahara, N., and Ihara, M. (2020). Potential Therapeutic Approaches for Cerebral Amyloid Angiopathy and Alzheimer's Disease. International journal of molecular sciences *21*.

Tanzi, R.E. (2012). The genetics of Alzheimer disease. Cold Spring Harbor perspectives in medicine *2*.

Tanzi, R.E., Gusella, J.F., Watkins, P.C., Bruns, G.A., St George-Hyslop, P., Van Keuren, M.L., Patterson, D., Pagan, S., Kurnit, D.M., and Neve, R.L. (1987). Amyloid beta protein gene: cDNA, mRNA distribution, and genetic linkage near the Alzheimer locus. Science (New York, NY) *235*, 880-884.

Tesseur, I., Lo, A.C., Roberfroid, A., Dietvorst, S., Van Broeck, B., Borgers, M., Gijsen, H., Moechars, D., Mercken, M., Kemp, J*., et al.* (2013). Comment on "ApoE-directed therapeutics rapidly clear beta-amyloid and reverse deficits in AD mouse models". Science (New York, NY) *340*, 924-e.

Thelen, M., Razquin, C., Hernandez, I., Gorostidi, A., Sanchez-Valle, R., Ortega-Cubero, S., Wolfsgruber, S., Drichel, D., Fliessbach, K., Duenkel, T*., et al.* (2014). Investigation of the role of rare TREM2 variants in frontotemporal dementia subtypes. Neurobiol Aging *35*, 2657.e2613-2657.e2619.

Trommsdorff, M., Gotthardt, M., Hiesberger, T., Shelton, J., Stockinger, W., Nimpf, J., Hammer, R.E., Richardson, J.A., and Herz, J. (1999). Reeler/Disabled-like disruption of neuronal migration in knockout mice lacking the VLDL receptor and ApoE receptor 2. Cell *97*, 689-701.

Ulland, T.K., Song, W.M., Huang, S.C., Ulrich, J.D., Sergushichev, A., Beatty, W.L., Loboda, A.A., Zhou, Y., Cairns, N.J., Kambal, A*., et al.* (2017). TREM2 Maintains Microglial Metabolic Fitness in Alzheimer's Disease. Cell *170*, 649-663.e613.

Ulrich, J.D., Finn, M.B., Wang, Y., Shen, A., Mahan, T.E., Jiang, H., Stewart, F.R., Piccio, L., Colonna, M., and Holtzman, D.M. (2014). Altered microglial response to Abeta plaques in APPPS1-21 mice heterozygous for TREM2. Molecular neurodegeneration *9*, 20.

Ulrich, J.D., Ulland, T.K., Colonna, M., and Holtzman, D.M. (2017). Elucidating the Role of TREM2 in Alzheimer's Disease. Neuron *94*, 237-248.

Ulrich, J.D., Ulland, T.K., Mahan, T.E., Nystrom, S., Nilsson, K.P., Song, W.M., Zhou, Y., Reinartz, M., Choi, S., Jiang, H*., et al.* (2018). ApoE facilitates the microglial response to amyloid plaque pathology. J Exp Med *215*, 1047-1058.

Unger, M.S., Schernthaner, P., Marschallinger, J., Mrowetz, H., and Aigner, L. (2018). Microglia prevent peripheral immune cell invasion and promote an anti-inflammatory environment in the brain of APP-PS1 transgenic mice. Journal of neuroinflammation *15*, 274-274.

Vanmierlo, T., Rutten, K., Dederen, J., Bloks, V.W., van Vark-van der Zee, L.C., Kuipers, F., Kiliaan, A., Blokland, A., Sijbrands, E.J., Steinbusch, H*., et al.* (2011). Liver X receptor activation restores memory in aged AD mice without reducing amyloid. Neurobiol Aging *32*, 1262-1272.

Veeraraghavalu, K., Zhang, C., Miller, S., Hefendehl, J.K., Rajapaksha, T.W., Ulrich, J., Jucker, M., Holtzman, D.M., Tanzi, R.E., Vassar, R*., et al.* (2013). Comment on "ApoE-directed

therapeutics rapidly clear beta-amyloid and reverse deficits in AD mouse models". Science (New York, NY) *340*, 924-f.

Vermunt, L., Sikkes, S.A.M., van den Hout, A., Handels, R., Bos, I., van der Flier, W.M., Kern, S., Ousset, P.J., Maruff, P., Skoog, I.*, et al.* (2019). Duration of preclinical, prodromal, and dementia stages of Alzheimer's disease in relation to age, sex, and APOE genotype. Alzheimer's & dementia : the journal of the Alzheimer's Association *15*, 888-898.

Villegas-Llerena, C., Phillips, A., Garcia-Reitboeck, P., Hardy, J., and Pocock, J.M. (2016). Microglial genes regulating neuroinflammation in the progression of Alzheimer's disease. Curr Opin Neurobiol *36*, 74-81.

Wahrle, S.E., Jiang, H., Parsadanian, M., Hartman, R.E., Bales, K.R., Paul, S.M., and Holtzman, D.M. (2005). Deletion of Abca1 increases Abeta deposition in the PDAPP transgenic mouse model of Alzheimer disease. J Biol Chem *280*, 43236-43242.

Wahrle, S.E., Jiang, H., Parsadanian, M., Kim, J., Li, A., Knoten, A., Jain, S., Hirsch-Reinshagen, V., Wellington, C.L., Bales, K.R.*, et al.* (2008). Overexpression of ABCA1 reduces amyloid deposition in the PDAPP mouse model of Alzheimer disease. J Clin Invest *118*, 671-682.

Walton, R.L., Soto-Ortolaza, A.I., Murray, M.E., Lorenzo-Betancor, O., Ogaki, K., Heckman, M.G., Rayaprolu, S., Rademakers, R., Ertekin-Taner, N., Uitti, R.J.*, et al.* (2016). TREM2 p.R47H substitution is not associated with dementia with Lewy bodies. Neurology Genetics *2*, e85.

Wang, Y., Cella, M., Mallinson, K., Ulrich, J.D., Young, K.L., Robinette, M.L., Gilfillan, S., Krishnan, G.M., Sudhakar, S., Zinselmeyer, B.H.*, et al.* (2015). TREM2 lipid sensing sustains the microglial response in an Alzheimer's disease model. Cell *160*, 1061-1071.

Wang, Y., Ulland, T.K., Ulrich, J.D., Song, W., Tzaferis, J.A., Hole, J.T., Yuan, P., Mahan, T.E., Shi, Y., Gilfillan, S.*, et al.* (2016). TREM2-mediated early microglial response limits diffusion and toxicity of amyloid plaques. J Exp Med *213*, 667-675.

Weisgraber, K.H. (1990). Apolipoprotein E distribution among human plasma lipoproteins: role of the cysteine-arginine interchange at residue 112. J Lipid Res *31*, 1503-1511.

Weisgraber, K.H., Rall, S.C., Jr., and Mahley, R.W. (1981). Human E apoprotein heterogeneity. Cysteine-arginine interchanges in the amino acid sequence of the apo-E isoforms. J Biol Chem *256*, 9077-9083.

Weisgraber, K.H., and Shinto, L.H. (1991). Identification of the disulfide-linked homodimer of apolipoprotein E3 in plasma. Impact on receptor binding activity. J Biol Chem *266*, 12029-12034.

Wilson, C., Wardell, M.R., Weisgraber, K.H., Mahley, R.W., and Agard, D.A. (1991). Three-dimensional structure of the LDL receptor-binding domain of human apolipoprotein E. Science (New York, NY) *252*, 1817-1822.

Wisdom, N.M., Callahan, J.L., and Hawkins, K.A. (2011). The effects of apolipoprotein E on non-impaired cognitive functioning: a meta-analysis. Neurobiol Aging *32*, 63-74.

Wisniewski, T., Golabek, A., Matsubara, E., Ghiso, J., and Frangione, B. (1993). Apolipoprotein E: binding to soluble Alzheimer's beta-amyloid. Biochem Biophys Res Commun *192*, 359-365.

Wolfe, C.M., Fitz, N.F., Nam, K.N., Lefterov, I., and Koldamova, R. (2018). The Role of APOE and TREM2 in Alzheimer's Disease-Current Understanding and Perspectives. International journal of molecular sciences *20*.

Wu, K., Byers, D.E., Jin, X., Agapov, E., Alexander-Brett, J., Patel, A.C., Cella, M., Gilfilan, S., Colonna, M., Kober, D.L.*, et al.* (2015). TREM-2 promotes macrophage survival and lung disease after respiratory viral infection. J Exp Med *212*, 681-697.

Wunderlich, P., Glebov, K., Kemmerling, N., Tien, N.T., Neumann, H., and Walter, J. (2013). Sequential proteolytic processing of the triggering receptor expressed on myeloid cells-2 (TREM2) protein by ectodomain shedding and gamma-secretase-dependent intramembranous cleavage. J Biol Chem *288*, 33027-33036.

Xiang, X., Werner, G., Bohrmann, B., Liesz, A., Mazaheri, F., Capell, A., Feederle, R., Knuesel, I., Kleinberger, G., and Haass, C. (2016). TREM2 deficiency reduces the efficacy of immunotherapeutic amyloid clearance. EMBO molecular medicine *8*, 992-1004.

Yamazaki, Y., Painter, M.M., Bu, G., and Kanekiyo, T. (2016). Apolipoprotein E as a Therapeutic Target in Alzheimer's Disease: A Review of Basic Research and Clinical Evidence. CNS drugs *30*, 773-789.

Yeh, F.L., Wang, Y., Tom, I., Gonzalez, L.C., and Sheng, M. (2016). TREM2 Binds to Apolipoproteins, Including APOE and CLU/APOJ, and Thereby Facilitates Uptake of Amyloid-Beta by Microglia. Neuron *91*, 328-340.

Yong, S.M., Lim, M.L., Low, C.M., and Wong, B.S. (2014). Reduced neuronal signaling in the ageing apolipoprotein-E4 targeted replacement female mice. Sci Rep *4*, 6580.

Yu, J.T., Jiang, T., Wang, Y.L., Wang, H.F., Zhang, W., Hu, N., Tan, L., Sun, L., Tan, M.S., Zhu, X.C.*, et al.* (2014). Triggering receptor expressed on myeloid cells 2 variant is rare in late-onset Alzheimer's disease in Han Chinese individuals. Neurobiol Aging *35*, 937 e931-933.

Yuan, P., Condello, C., Keene, C.D., Wang, Y., Bird, T.D., Paul, S.M., Luo, W., Colonna, M., Baddeley, D., and Grutzendler, J. (2016). TREM2 Haplodeficiency in Mice and Humans Impairs the Microglia Barrier Function Leading to Decreased Amyloid Compaction and Severe Axonal Dystrophy. Neuron *90*, 724-739.

Yuksel, M., and Tacal, O. (2019). Trafficking and proteolytic processing of amyloid precursor protein and secretases in Alzheimer's disease development: An up-to-date review. European journal of pharmacology *856*, 172415.

Zanjani, H., Finch, C.E., Kemper, C., Atkinson, J., McKeel, D., Morris, J.C., and Price, J.L. (2005). Complement activation in very early Alzheimer disease. Alzheimer Dis Assoc Disord *19*, 55-66.

Zhang, B., Gaiteri, C., Bodea, L.-G., Wang, Z., McElwee, J., Podtelezhnikov, A.A., Zhang, C., Xie, T., Tran, L., Dobrin, R.*, et al.* (2013). Integrated systems approach identifies genetic nodes and networks in late-onset Alzheimer's disease. Cell *153*, 707-720.

Zhang, G., Assadi, A.H., McNeil, R.S., Beffert, U., Wynshaw-Boris, A., Herz, J., Clark, G.D., and D'Arcangelo, G. (2007). The Pafah1b complex interacts with the reelin receptor VLDLR. PloS one *2*, e252.

Zhang, J., and Liu, Q. (2015). Cholesterol metabolism and homeostasis in the brain. Protein & cell *6*, 254-264.

Zhao, N., Liu, C.-C., Qiao, W., and Bu, G. (2018a). Apolipoprotein E, Receptors, and Modulation of Alzheimer's Disease. Biological psychiatry *83*, 347-357.

Zhao, N., Ren, Y., Yamazaki, Y., Qiao, W., Li, F., Felton, L.M., Mahmoudiandehkordi, S., Kueider-Paisley, A., Sonoustoun, B., Arnold, M., *et al.* (2020). Alzheimer's Risk Factors Age, APOE Genotype, and Sex Drive Distinct Molecular Pathways. Neuron *106*, 727-742.e726.

Zhao, Y., Wu, X., Li, X., Jiang, L.L., Gui, X., Liu, Y., Sun, Y., Zhu, B., Pina-Crespo, J.C., Zhang, M.*, et al.* (2018b). TREM2 Is a Receptor for beta-Amyloid that Mediates Microglial Function. Neuron *97*, 1023-1031.e1027.

Zheng, H., Jia, L., Liu, C.C., Rong, Z., Zhong, L., Yang, L., Chen, X.F., Fryer, J.D., Wang, X., Zhang, Y.W.*, et al.* (2017). TREM2 Promotes Microglial Survival by Activating Wnt/beta-Catenin Pathway. The Journal of neuroscience : the official journal of the Society for Neuroscience *37*, 1772-1784.

Zheng, H., Liu, C.C., Atagi, Y., Chen, X.F., Jia, L., Yang, L., He, W., Zhang, X., Kang, S.S., Rosenberry, T.L.*, et al.* (2016). Opposing roles of the triggering receptor expressed on myeloid cells 2 and triggering receptor expressed on myeloid cells-like transcript 2 in microglia activation. Neurobiol Aging *42*, 132-141.

Zhong, L., Chen, X.F., Wang, T., Wang, Z., Liao, C., Wang, Z., Huang, R., Wang, D., Li, X., Wu, L.*, et al.* (2017). Soluble TREM2 induces inflammatory responses and enhances microglial survival. J Exp Med *214*, 597-607.

Zhou, Y., Song, W.M., Andhey, P.S., Swain, A., Levy, T., Miller, K.R., Poliani, P.L., Cominelli, M., Grover, S., Gilfillan, S.*, et al.* (2020). Human and mouse single-nucleus transcriptomics reveal TREM2-dependent and TREM2-independent cellular responses in Alzheimer's disease. Nature medicine *26*, 131-142.

Zhu, Y., Nwabuisi-Heath, E., Dumanis, S.B., Tai, L.M., Yu, C., Rebeck, G.W., and LaDu, M.J. (2012). APOE genotype alters glial activation and loss of synaptic markers in mice. Glia *60*, 559-569.